FEASIBILITY STUDY OF PROTON ACTIVATION OF GOLD IN SOIL

Arif Hasan Khan

A Thesis

in

The Department

of

Physics

Presented in Partial Fulfillment of the Requirement

for the Degree of Master of Science at

Concordia University

Montreal, Canada

March, 1975

TABLE OF CONTENTS

TABLE OF CONTENTS

ACKNOWLEDGEMENTS

The author is very grateful to Mr. G. Kennedy at the Foster Radiation Laboratory, McGill University, with whose help we carried out many time-consuming experiments. His thanks are also due to Mr. G. Ansuelos for his help in transferring the data.

The author is very greatly indebted to Mr. J. W. Marvin for his constant help through all the phases of this work.

Most importantly, the author expresses his special gratitude to Dr. N. Eddy for his valuable suggestions and patient guidance. Without his supervision and assistance this project could not have been completed.

ABSTRACT

ARIF HASAN KHAN

FEASIBILITY STUDY OF PROTON ACTIVATION OF GOLD IN SOIL

A pure sample of gold was irradiated with protons of 20 MeV. The gamma-ray decays of various radionuclides, following (p,2n), (p,n), (p, pn) and (p, 3n) nuclear reactions, were observed.

Similarly, a sample of quartz and a sample of soil were irradiated with protons. Many elements were found present in traces which have measurable half-lives.

A known amount of gold was added to soil in three different concentrations. All the samples were activated by bombarding with protons of 20 MeV energy. The gold was detected in all the three samples. The smallest concentration was less than 40 ppm (parts per million).

LIST OF DIAGRAMS

CHAPTER I

INTRODUCTION

The technique of activation analysis has become quite popular for the detection of minute quantities of elements.

Activation analysis is based on determining the weight of a particular element in a sample by measuring the activity induced by irradiation with neutrons, photons, or charged particles. Half-life studies and radiation energy determinations of the radionuclide give its identity and purity. Besides the elemental, also the isotopic content of a sample can be determined. The ultimate sensitivity attainable depends upon the ability to detect accurately and quantitatively the radiation emitted in the decay process.

Neutron activation is an old technique, used in 1936 by von Hevesy and Levi[1]. They tried to detect dysprosium and europium activities in rare earth mixtures without tedious chemical separations. Since then this technique has gone through many refinements. The major advances can be attributed to the reactors yielding very high neutron fluxes and to the development of the neutron generator, as far as neutron activation is considered. Also the use of transistorized multi-channel analyzers which provide more rapid and easy data interpretation, and the advances in the production of sophisticated semi-conductor detectors with very high resolution, have transformed the whole field of activation analysis into an accurate, specific, nondestructive, fast, econ-

omical, and universally-applicable analytical technique. Finally the application of computers has created a certain degree of automation in activation analysis.

A target nucleus can be transmuted by many particles. Usually neutrons are chosen due to the fact that most of the elements have a high probability of capturing slow neutrons. Fermi had realized the fact in 1934. Usually activation analysis is done in macro amounts of the sample, whereas charged particle analysis is done in small samples and relatively thin layers due to the fact that charged particles have a limited range in matter.

Proton reactions are highly endoergic[2]; to induce a simple reaction as (p,n) the kinetic energies of at least 5 MeV are required. Proton activation requires considerably more care and detailed attention than neutron activation. In certain cases neutron activation analysis is not applicable and one is forced to use charged particle[3].

With charged particles some of the difficulties encountered arise from sample inhomogeneity, surface contamination, decreasing particle energy with penetration into the sample, etc. Quite often one must resort to decay curve analysis because many of the product nuclides emit mainly positrons.

The work presented here is a forceful example of proton activation analysis. The purpose of the series of experiments was to irradiate

gold (Au^{197}) with protons of suitable energy from the (synchrotron) cyclotron and to observe all the reactions such as (p,n), (p,p'), (p, pn), (p,2n), (p,3n), etc. and finally to determine the sensitivity of the analytical system by diluting the gold sample with soil.

It has been mentioned earlier that activation analysis with charged particles requires a considerable amount of care in handling the sample and a deeper understanding of nuclear reactions. Also the fact that work of this nature has not been done before makes it harder to obtain the results and to reach a conclusion. There are no data for the cross-sections of gold and soil constituents for the protons and for the competing reactions. Owing to these facts quite a few trial runs were made and protons of suitable energy were chosen. The irradiation time was also determined.

In Chapter II some theoretical aspects are covered which are necessary for the understanding of the gamma-ray spectroscopy.

In Chapter III detailed procedures of sample preparations, determinations of optimum proton energy and irradiation timing are discussed. Also, the various samples necessary to aid understanding the spectra are treated in this chapter. There is a brief discussion of the synchrocyclotron. Chapter III contains a brief explanation of the counting system, data-acquiring system, data-handling procedures and the computer programs.

Chapter IV deals with all the preliminary and final runs which were made during the project.

In Chapter V the results are discussed. It was the most interesting and the most difficult part of the whole project: interesting because the research was based on detecting minute quantities of gold by observing the various decay processes of Hg, Au and Pt isotopes, and difficult because of the competing reactions and the choice of various pathways of the above-mentioned decay processes. Chapter V contains the identification of various elements as soil constituents and qualitative determinations of their decay processes. Also comparisons of spectra with different cooling periods are made in this chapter.

Finally the sensitivity of the system is discussed and conclusions are drawn from the results. A large number of the original plots of the spectra is included to aid in understanding of the reactions. The appendix contains various computer programs necessary for data-handling and data analysis.

CHAPTER II

THEORETICAL PRELIMINARIES

II.1 Intrinsic Variables I

Before discussing the variety of nuclear reactions which took place in the series of experiments, it would be appropriate to get acquainted with gamma-ray spectroscopy terminology.

There are many ways in which an excited nucleus may return to the ground state, such as spontaneous fission, neutron emission, isomeric transition, alpha emission, positron emission, electron capture, beta emission, gamma emission, and internal conversion. A decay scheme of excited nuclei includes all the modes of decay of the nuclide, the abundance, the energies of the radiations, and the sequence in which the radiations are emitted. There are many complete compilations of the decay schemes of the nuclides[4].

(i) Gamma emission and internal conversion.

Gamma emission is due to a de-excition of an excited nuclear state to a state of lower excitation but with the same A and Z. Gamma radiation is due to electromagnetic effects which can be considered as the changes in the charge and current distribution in the nuclei which give rise to electric and magnetic moments. These transitions are characterized according to the angular momentum (quantized in units of $h/2\pi$) which the gamma-rays carry away. The transitional probability decreases with increasing angular momentum change.

Gamma emission may be accompanied, or even replaced by the emission of internal conversion electrons. Internal conversion is the manifestation of the electromagnetic interaction between the nucleus and the orbital electrons. This process can be explained by the quantum theory of radiation as a direct coupling between the atomic electrons and a nuclear multipole field. The result of this interaction is the emission of an electron with kinetic energy equal to the energy of the nuclear transition involved minus the binding energy of the electron in the atom. The internal conversion coefficient α, which can have any value between 0 to ∞, is defined as the ratio of the number of internal conversion electrons to the number of gamma quanta emitted.

The internal conversion coefficients for any shell K, L, M, etc. increase with decreasing energy, increasing A, and increasing difference between the initial and the final state of spin. Tables of α for various shells are given by M. E. Rose(5).

As soon as the electron is emitted, a vacancy is created in one of the shells, which is most frequently filled by an electron from the next shell (higher). This atomic re-arrangement process can result in the emission of characteristic X-rays and internal electrons from the L or M shell, etc. This is called an Auger electron and its kinetic energy is equal to the characteristic X-ray energy minus its own binding energy. (See figure 5 for Au^{196} X-rays)

Isomeric transitions

This term is used for both gamma-ray emissions and internal conversion processes. An isomeric state differs only in that it implies an

independent existence of an excited state. The nuclear isomers are those whose half-lives are not too short to be measured. The important effect of these transitions is the sometime summing of two peaks if they are not delayed. (See figure 5 .)

(ii) The atoms can be ionized by four primary processes. Internal conversion and orbital electron capture are the two nuclear decay processes. The other two result from the interaction of the atomic electrons with external radiation, i.e. gamma-ray absorption by the photoelectric effect and the absorption of beta-rays. These are the four methods of characteristic X-ray excitation which are important in applied gamma-ray spectroscopy.

In a particular atom the primary excitation probabilities of the K, L, etc. shells may vary in each of the four processes. They may be summarized briefly for each process.

(a) For electron capture, the ratio of L- to K- electron capture is approximately 0.1 and increases slowly with Z. At Z=80, the ratio is approximately 0.15.

(b) For internal conversion, the L/K values vary in a complex way with the gamma transition energy and the atomic number.

(c) The ratio of photoelectric interactions with the L and K shells is constant, 0.25.

(d) The production of characteristic X-rays by beta-ray absorption has not been described adequately in theory.

After an excitation, characteristic X-rays are emitted as the atom reorganizes. Sometimes, instead of X-ray emission the excess energy may be transferred to another outer electron which is ejected from the atom (Auger electron).

(iii) Beta Transitions (EC, B^+ and B^-)

Beta Transition may be considered as the conversion of nucleons (protons to neutrons or vice-versa) in the nucleus. The mass number of the nucleus remains the same, but the atomic number changes. The following are the conversion processes:

$$n \longrightarrow p + e^- + \bar{\nu}$$

$$p \longrightarrow n + e^+ + \nu$$

$$p + e^- \longrightarrow n + \nu$$

n and p represent the nucleous, $e^{\pm}$, the positrons or negatrons, ν and $\bar{\nu}$, the neutrino and anti-neutrino.

Electron capture decay to the ground state is the most difficult to observe. The atom is left in an excited state, and is now the product nucleus Z - 1. It emits its characteristic radiation or Auger electrons in the manner analogous to the atoms excited by the internal conversion process.

The undetected neutrino carries off all the energy of the nuclear transition, except the binding energy of the captured electron. Since very little energy is imparted to the nucleus as it recoils, therefore, the energy of the nuclear transition is unknown if it is only due to electron capture process.

Electron capture and positron emission may be considered as competing processes, both resulting in the capture of an electron by the nucleus. In the case of positron emission, the "captured electron" joins a proton to become a neutron.

The energy equation for positron emission is:

$$M_z = M_{z-1} + 2m_e + Q.$$

The corresponding condition for electron capture is:

$$M_z = M_{z-1} + Q$$

given in mass units.

Nuclear transitions which involve less energy than 2 mc^2 (1.022 MeV) required by pair formation cannot decay by positron emission..

II.2 Intrinsic Variables II

Interaction Processes of Radiation with Matter.

Interaction of gamma-rays with matter leads to a complete absorption or scattering in a single event.

Photons can interact with the following:

(I) With bound atomic electrons.

(II) With free electrons.

(III) With Coulomb fields (of nuclei or electrons).

(IV) With nucleons (individual nucleons or a whole nucleus).

These interactions may lead to one of the three effects which are as follows:

(a) complete absorption of a photon;

(b) elastic scattering;

(c) inelastic scattering.

Therefore, there are twelve processes for gamma-ray absorption or scattering. But between the energy range from about 10 KeV to about 10 MeV (we are considering) most of the interactions result in one of the following processes:

(1) The photoelectric effect predominates at low energies. A photon gives up all of its energy to the bound electron, which uses part of the energy to overcome the binding force and takes off with the rest.

(2) The photon may be scattered by atomic or individual electrons, in another direction with or without loss of energy. When the binding energy of the electron is much smaller than the photon energy, the photon gets scattered as if the electron were free and at rest. This is called the Compton effect, and it is the dominant mode of interaction around 1 MeV.

The Compton effect can be seen in all the spectra in conjunction with the 0.511 MeV or 0.662 MeV peaks.

(3) If the energy of the interacting photon exceeds 1.022 MeV pair production becomes possible. In the Coulomb field of a charged particle an electron pair is created with total kinetic energy equal to the difference of the photon energy and the rest mass energy of the two particles ($2mc^2$ = 1.022 MeV).[10]

For example, in the gold spectrum there are quite a few single escape peaks. These are due to the photons of energies more than 1.022 MeV interacting with the material of the detector and producing an electron pair. In the positron annihilation, one or both .511 MeV X-rays will escape.

A. Photoelectric Effect

An electromagnetic quantum of energy $h\nu$ ejects a bound electron from an atom or molecule and imparts to it an energy $h\nu - be$, where be is the electron binding energy. In this process (photoelectric effect) the electrons must be initially bound in the atom, because a third body, the nucleus is necessary for conserving momentum.

The energy, be, subsequently appears as characteristic X-rays and Auger electrons from the filling of the vacancy created by the ejection of the electron. The Auger electrons have short tracks in a detector medium, and usually they are easily absorbed. They are never detected in a gamma detector.

B. Compton Scattering

Compton scattering is different from the photoelectric effect in the sense that it is a collision between a gamma-ray and an electron, which can either be bound or free. Usually the electrons are bound, though it is not a necessary condition for the Compton effect. The photoelectric effect takes place almost entirely with the K or L electrons and it is a relatively intense source of characteristic X-ray. Compton scattering usually involves the outer electrons and does not

produce a significant amount of K or L X-rays except in very light elements.

The photon gives part of its energy to the electron and is deflected from its original path. As shown in the figure, the photon makes an angle ϕ with its original direction, while the electron recoils making an angle θ.

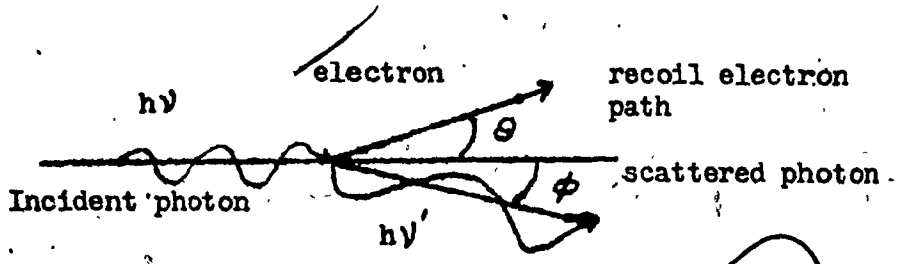

The trajectories of the incident photon, the Compton scattered photon and the recoil electron occur always in one plane. The angles and are correlated thus:

$$\cot \theta = (1 + \alpha) \tan \frac{\phi}{2}, \qquad 2.1$$

where $\alpha = E/mc^2$.

From relativistic conditions for conservation of momentum and energy:

$$h\nu' = \frac{h\nu}{1 + (h\nu/mc^2)\ (1 - \cos\phi)}, \qquad 2.2$$

where m is the rest mass and mc^2 (0.511 MeV) is the rest mass energy of the electron.

The energy E' of the scattered photon is given by:

$$E' = \frac{E}{1 + \alpha(1 - \cos\phi)} \qquad 2.3$$

The energy T of the scattered electron equals the difference between the original photon energy E and the scattered photon energy E'

$$T = \frac{\alpha E (1 - \cos\phi)}{1 + \alpha (1 - \cos\phi)} \qquad 2.4$$

From equations 2.3 and 2.4 it can be seen that the energies of the scattered electron lie between zero ($\phi = 0^\circ$, $\theta = 90^\circ$) up to a maximum value ($\phi = 180^\circ$, $\theta = 0^\circ$). This maximum value is called the Compton edge:

$$T_m = \frac{E}{1 + 1/2\alpha} \qquad 2.5$$

The minimum energy due to the backwards scattered photon is given by:

$$E' = \frac{E}{1 + 2\alpha} = \frac{mc^2}{2} \cdot \frac{1}{1 + (mc^2/2E)}$$

For large incident gamma-ray energies ($2 E_\gamma > mc^2$) the minimum energy of the scattered gamma-rays approaches $1/2\ mc^2 = 250$ KeV. For this reason, spectra of highly energetic gamma-rays often show a back-scattering in surrounding material.

C. Pair Production

Pair production becomes possible if the incident photon energy is above $2mc^2$ (1.022 MeV).

The energy $2mc^2$ is a threshold for the process and provides the rest mass energy necessary to create the positron-negatron pair. The interaction of an incident photon with a negatron converts it from a negative to a positive energy state and creates a hole (positron) and an electron.

Shown in the figure:

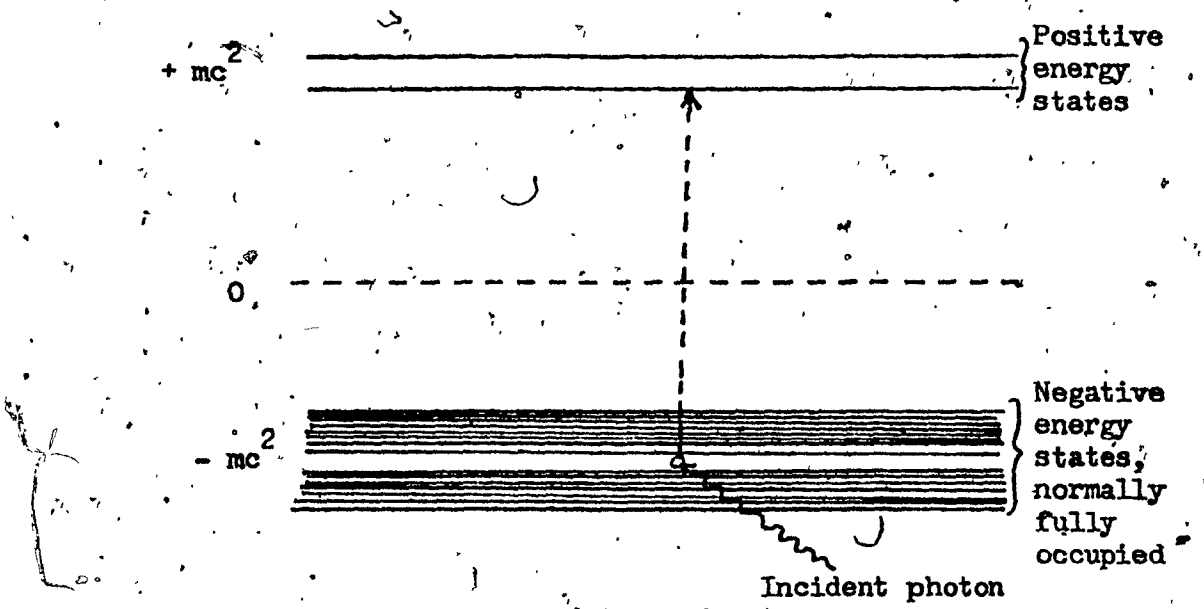

Pair production.

According to Dirac Theory; the relativistic wave equation for a free electron suggests that both positive and negative states $|mc^2|$ exist. It is assumed that all the negative energy states are occupied by a sea of electrons and the exclusion principle forbids the transitions to the fully occupied negative energy states.

Passing through the electric field of a nucleus, a photon may be absorbed by an electron in the sea of fully occupied negative energy states. The electrons can be raised into the positive energy states and observed as a negatron, if it absorbs energy greater than $2mc^2$. A hole is created in the negative energy states which is called a positron, it has the same mass and opposite but equal charge as an electron.

When a negatron in the positive energy states fills the hole in the negative energy states, the annihilation of a pair of electrons occurs. When all the positron kinetic energy has been dissipated by ionization or radiative (bremsstrahlung) process then the annihilation occurs. Two annihilation photons, each with 0.511 MeV energy, are emitted at approximately 180° with respect to each other, but nevertheless, random with respect to the photon direction.

The annihilation radiation can produce two escape peaks in the detector response at 0.511 MeV intervals.

All the spectra presented here show peaks at 0.511 MeV which are the results of positron annihilation.

II.3 Theoretical estimation of cross sections for charged-particle reaction

The radioactivity induced in an element by the charged-particle activation is directly proportional to the amount of element present in the sample. The main difference between charged-particle activation analysis and other activation methods stems from the characteristically strong interaction of protons or energetic ions with electrons in matter. A wide variety of sizes of the sample can be chosen when photons or neutrons are used for nuclear reactions; as they can penetrate matter easily and the variations in flux and energy are negligible. But the charged particles are quickly slowed down and stopped. See figure II.1.

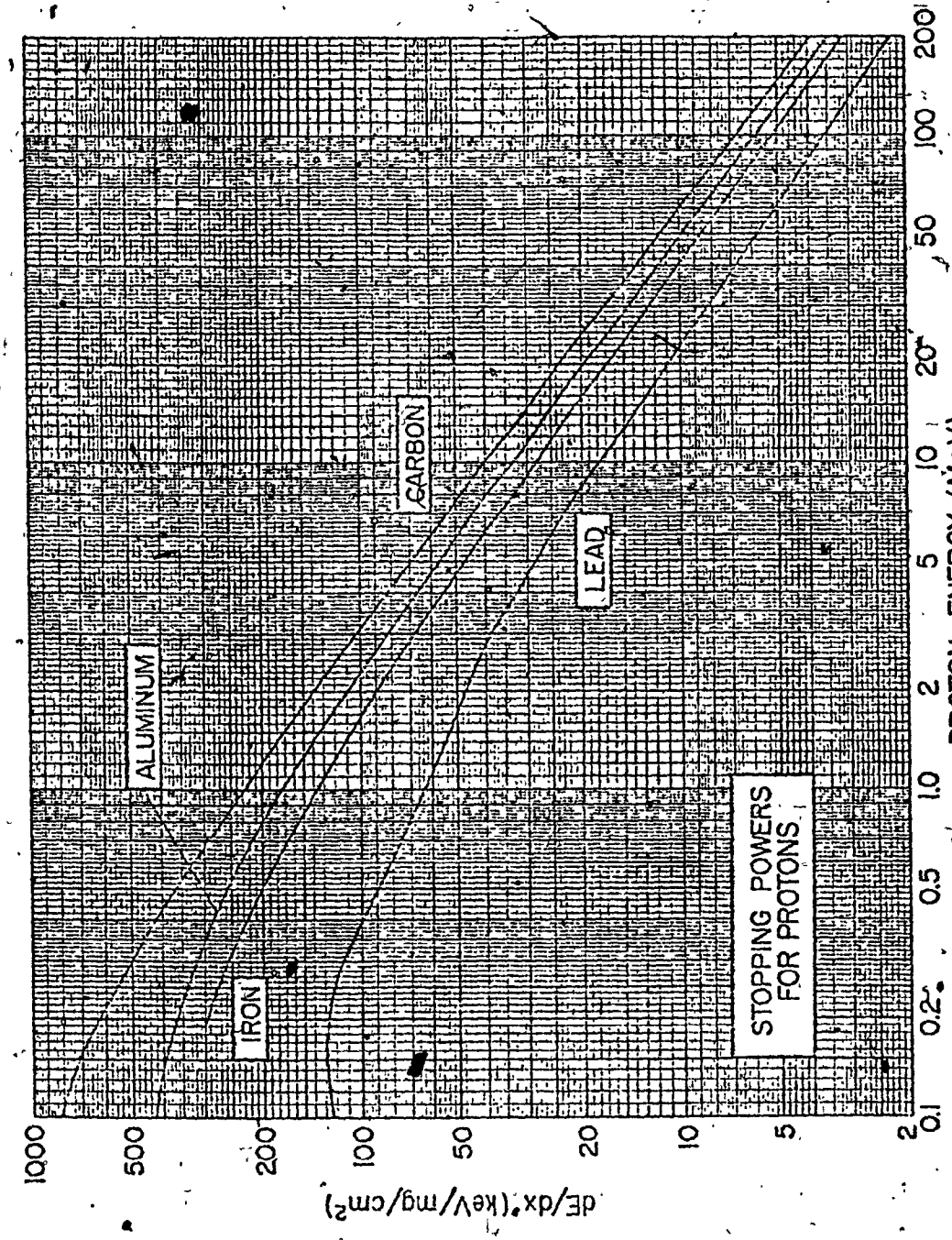

Figure II.1 Stopping powers of carbon, aluminum, iron and lead for protons.

In typical activation analysis maximum particle penetrations (ranges) are usually of the order of 10-100μ. While for photons and neutrons the nuclear-reaction cross-section may be considered constant throughout the sample.

The stopping power, i.e. the rate of energy loss per unit length inside the sample, is given by the relation (Friedlander et al)[8]

$$-\frac{dE}{dx} = \frac{4\pi Z^2 e^4 \nu}{mv^2} \ln \frac{2mv^2}{i} \qquad 2.6$$

Where E is the kinetic energy of the charged particle at depth x in a sample, z is the atomic number of the target, v is the velocity of the bombarding particle, while ν is the number of electrons per unit volume of the sample, and i is the ionization potential of its atoms, m is the electron mass.

In proton activation analysis the kinetic energies are always much smaller than the particle rest mass energy, therefore, this equation is valid for non-relativistic interactions.

Multiplying and dividing both fractions on the right by the charged-particle mass M, and putting $E = \frac{Mv^2}{2}$, we get:

$$-\frac{dE}{dx} = \frac{4\pi Z^2 e^4 \nu M}{mE} \ln \frac{4mE}{Mi} \qquad 2.7$$

Since $\frac{4\pi e^4}{m}$ is constant, we call it K. Thus,

$$-\frac{dE}{dx} = \nu K \frac{Z^2 M}{E} \ln \frac{4mE}{Mi} \qquad 2.8$$

The stopping power depends on the nature of the matrix (y, i), the kinetic energy (E) and the nature (Z,M) of the bombarding particle. The stopping power is the same for proton of energy E and deutron of energy 2E and triton of energy 3E or α-particle of energy 4E.

The Coulomb barrier of the nuclear reaction and its threshold energy are the two useful parameters in charged-particle activation analysis. An approximate value of the electrostatic Coulomb barrier V is given by (Ricci and Hahn):[9]

$$V\ (MeV) = \frac{0.959\ k\ Zp\ Zn}{A_p^{1/3} + A_n^{1/3}} \qquad 2.9$$

Where Zp, Zn and Ap, An are the atomic numbers and the mass numbers of the bombarding particle and the reacting nucleus, respectively. K is less than 1. The (p, xn) reactions are endoergic, i.e. Q is negative. Therefore, minimum kinetic energy necessary to produce the reaction--the threshold energy E_t - is slightly greater than Q, because the momentum must be conserved in the interaction,[8]

$$E_t = -Q\ (A_p + A_n)\ /A_n \qquad 2.10$$

Therefore, in endoergic reactions the minimum energy to induce a charged-particle reaction must be equal to either V, the Coulomb barrier, or to the threshold energy E_t, whichever is larger.

There is a method of mathematical treatment of charged-particle induced reactions in activation analysis developed at the Oak Ridge National Laboratory by Ricci and Hahn.[9] This method is similar to neutron

activation analysis in experimental and computing procedures. It is called the method of average cross-section.

To account for the variation of the reaction cross-section $\bar{\sigma}$ with depth x in a thick target (shown below), the "theorem of the averages" can be used to define an average cross-section $\bar{\sigma}$,

$$\bar{\sigma} = \frac{\int_0^R \sigma_x \, dx}{\int_0^R dx} \qquad 2.11$$

The integrals are to be calculated over the particle range R:

$$R = \int_0^R dx = \int_{E_0}^0 \frac{dE}{(dE/dx)} \qquad 2.12$$

because $\sigma_x = 0$ for $X \geq R > R'$. Because the particle energy E and depth X are interdependent, we change the variable in equation

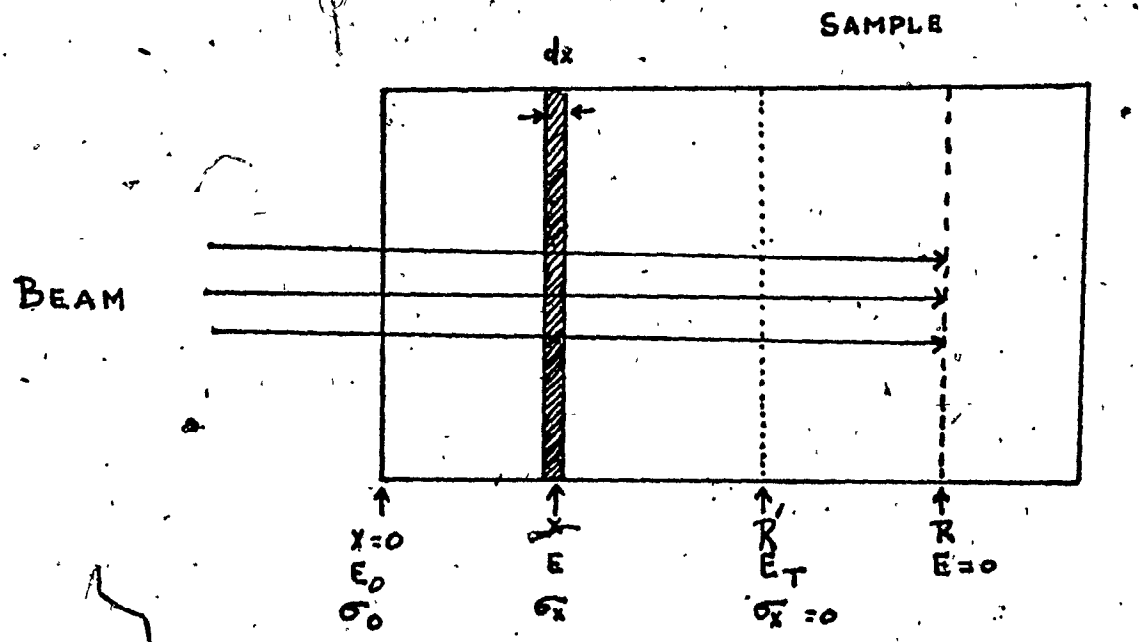

Where σ_E represents the variation of the cross-section with particle energy, i.e. the excitation function for the reaction, and $-\frac{dx}{dE}$ is the reciprocal of the stopping power of the given thick matrix for the bombarding particle. Hence, from Equation 2.12

$$\bar{\sigma} = \frac{\int_0^{E_0} \sigma_E \, E \left[\ln(4mE/Mi)\right]^{-1} dE}{\int_0^{E_0} E\left[\ln(4mE/Mi)\right]^{-1} dE} \qquad 2.12'$$

ν, K, Z, and M cancel out. It should be noted, however, that equation (2.12') is not valid for low energies (E below 0.5 - 1 MeV), but our energies are well above that.

Although the logarithm depends on the E for a given particle and target (4m/Mi = constant), it varies slowly with E. Thus, In (4mE/Mi) $\approx$ constant, and equation 2.12' reduces to:

$$\bar{\sigma} \approx \frac{\int_0^{E_0} \sigma_E \, E \, dE}{\int_0^{E_0} E \, dE} \qquad 2.12''$$

Therefore, the average cross-section, $\bar{\sigma}$, is approximately independent of the nature of the target material, and constant for a given nuclear reaction (σ_E) and particle energy E_0.

Ricci and Hahn calculated $\bar{\sigma}$, shown in the figure below:

Variation of average cross-section with atomic number Z.

$\bar{\sigma}$ varies 3% for Z from 4 to 57, while the total variation (Z = 4 to 95) is no larger than 8%.

CHAPTER III

EXPERIMENTAL PROCEDURES & APPARATUS

III.1 Sample Preparation

The samples irradiated during the experiments are the following:

(1) Pure quartz (SiO_2)

(2) Sand or soil

(3) Gold (Au^{197})

(4) Gold + sand; Au $\leq$ 4000 ppm.

(5) Gold + sand; Au $\leq$ 400 ppm.

(6) Gold + sand; Au $<$ 40 ppm.

Optically high grade quartz was obtained from Beckman Instruments, supplied as cells for a UV spectrophotometer. The quartz cell was soaked in chromic acid overnight and washed many times with distilled water. Sandy soil from the banks of the Ottawa River was chosen to be the diluent. Its composition is quite similar to ordinary soil (sandy loam). A sample of sandy loam has been found to contain (12):

	Percent by weight		
Oxygen	49	Ca	1.37
Si	33	Mg	0.60
Al	7.13	K	1.36
Na	0.63	Ti	0.46
Fe	3.80	C	2.00

There are 35 other elements which are found, most of them in traces only. Even quartz crystals contain Re, Mg, Al, Ti, Na, B, Ga, Ge, Mn and Zn in traces i.e. 10 ppm or less.

The gold was bought from: Reactor Experiments, Inc.
963 Terminal Way
San Carlos, California

It had a thickness of .002 inch and guaranteed purity was 99.99%. This is standard activation grade gold.

Also (AuCl) gold chloride solution (0.5%) was used to mix with the soil samples. 0.5% AuCl can be obtained from Fisher Scientific Company.

Three samples of sand were prepared with different concentrations of gold chloride. A known quantity of gold chloride was added as solution to the weighed quantities of sand and then the water was allowed to evaporate under a hot lamp. A simple calculation can give the concentration of gold in sand.

(a) Sample 1.

0.1 ml of AuCl in 10 gms of sand.

Atomic weight of gold is 197 amu.

Atomic weight of chlorine is 35.5 amu.

Molecular weight of gold chloride is 232.5 amu.

Hence, 232.5 gms of AuCl contains 197 gms Au.

Also, AuCl is 0.5%.

Therefore, 100 mls of AuCl solution contains 0.5 gms of AuCl or 0.1 ml of AuCl solution contains 5×10^{-4} gms of AuCl.

Now, 232.5 gms AuCl contains 197 gms of Au.

Therefore 5×10^{-4} gms of AuCl $\frac{197}{232.5} \times 5 \times 10^{-4}$ gms of Au,

which is 4.236×10^{-4} gm of Au.

Therefore we have 4.236×10^{-4} gms of Au in 10 gms of sand or 42.36 ppm.

(b) Sample 2.

0.1 ml of AuCl in 1.0 gm of sand would give the concentration of gold to be 423.5×10^{-6} gms.

(c) Sample 3.

1.0 ml of AuCl in 1.0 gm of sand gives 4235×10^{-6} gms of gold.

Each sample (of sand and AuCl) was crushed in the mortar with a pestle to obtain a homogeneous districution of gold chloride molecules. But since gold chloride is a strong yellow colored substance, it was seen that some of the gold chloride stained the mortar and the concentrations were obbiously less than 40, 400, 4000 ppm in samples numbers 1, 2, 3, respectively. It is estimated that about 5% of the AuCl was adhering to the mortar.

III.2 The Sample Holder

The penetration of protons into matter is severely limited by Coulomb repulsion. Hence at moderate proton energies most of the activation takes place on the surface or in a thin film of the target sample. However, mixtures and pulverized samples etc. have to be enclosed in an aluminium tubing, as there is a high vacuum (less than 5×10^{-6} torr) in the cyclotron.

This aluminum tubing has an outer diameter of 0.0625 inches and the wall thickness is 0.003 inches. A tube about 1 inch long is used to contain the sample during irradiation. The ends of the tubes are closed with tweezers and it is mounted on a sample holder. The sample holder in turn is mounted on a shaft which is capable of inserting the sample into the proton beam of desired energy with reasonable accuracy. Proton energy loss in the Al tubing is about 1 MeV. In choosing the radius (energy) of the proton beam, allowance must be made for this.

It was realized very quickly that a speck of dirt on the aluminum tubing could cause great problems in analyzing the spectra. Therefore, all the tubes were cleaned with 95% alcohol and this did help.

III.3 The Foster Radiation Laboratory Synchrocyclotron

The Synchrocyclotron:

The cyclotron was invented by E. C. Lawrence at the University of California in 1930. Since then it has been a very successful particle accelerater. Its success is due to the fact that relatively low potentials (electronic) are required for its operation, and, therefore, it is possible to reach particle kinetic energies much higher than those obtained by Van de Graaff generators.

The acceleration chamber of a cyclotron resembles a pillbox, like two D's back to back with a gap between them. These "dees" are located between the poles of an electromagnet which creates a continuous, strong field through them. In addition, the two "dees" are connected to alternating radiofrequency potentials.

Positive ions are released by a source near the center of the gap, and are immediately drawn into one of the "dees" which is charged negatively at that instant. Once inside the "dee", the ion keeps its speed constant, since the electric field vanishes there, but its path is bent into a circle by the continuous magnetic field. As a consequence, the ion is driven around the center of the cyclotron and back to the gap. The radiofrequency energy source has charged negatively the opposite "dee" by now. Thus, this "dee" attracts the ion and increases its kinetic energy as it crosses the gap. The ion's speed remains constant inside this "dee", while its circular path takes back to the gap, around the center.

The kinematics may be quickly derived from the cyclotron's equation of motion. A particle of mass m and charge q, circling with linear velocity v at a distance r from the center of a cyclotron of magnetic field B. The centripetal magnetic force Bqv and the centrifugal force $\frac{mv^2}{r}$ balance each other.

$$Bqv = \frac{mv^2}{r};$$

The radius of the particle path is then,

$$r = \frac{mv}{Bq},$$

Squaring the above equation, we get the non-relativistic kinetic energy of the particle,

$$E = 1/2\ mv^2 = \frac{B^2q^2r^2}{2m},$$

Hence, $$E_{max} \propto r^2.$$

Small machines can produce high energies and the final kinetic energy is independent of the potential difference between the "dees".

One difficulty of the standard cyclotron is the energy limitation the relativistic effects impose on the validity of the equation;

$$E = \frac{1}{2} mv^2 = \frac{B^2 q^2 r^2}{2m} .$$

The relativistic mass increase is already 1.0% for a 10 -MeV proton and it grows with increasing energy.

From equation $\frac{v}{r} = \omega = \frac{Bq}{m}$ if m increases, then B must be increased to keep ω constant.

To overcome the above mentioned difficulty, i.e. the relativistic energy limitation, a much more efficient method was found in 1945. It consists in modulating the oscillator radiofrequency to syncronize it with the frequency of revolution which decreases as the velocity and mass of the particle increases. These frequency-modulated cyclotrons are called synchrocyclotrons and the largest machines are capable of producing protons of energy 33 Gev (Brookhaven AGS). But synchrocyclotrons cannot produce a continuous particle beam. It must accelerate one ion cluster at a time to synchronize with its reduction frequency. Thus, though pulse rates of 100 sec^{-1} are common, beam currents are no greater than 10 microamperes. See figures III.1 and III.2.

The synchrocyclotron at the Foster Radiation Laboratory can accelerate protons to 100 MeV. The figure III.3 shows the relation between the proton energy in MeV and the target radius in inches for the relative proton beam intensity in μA.

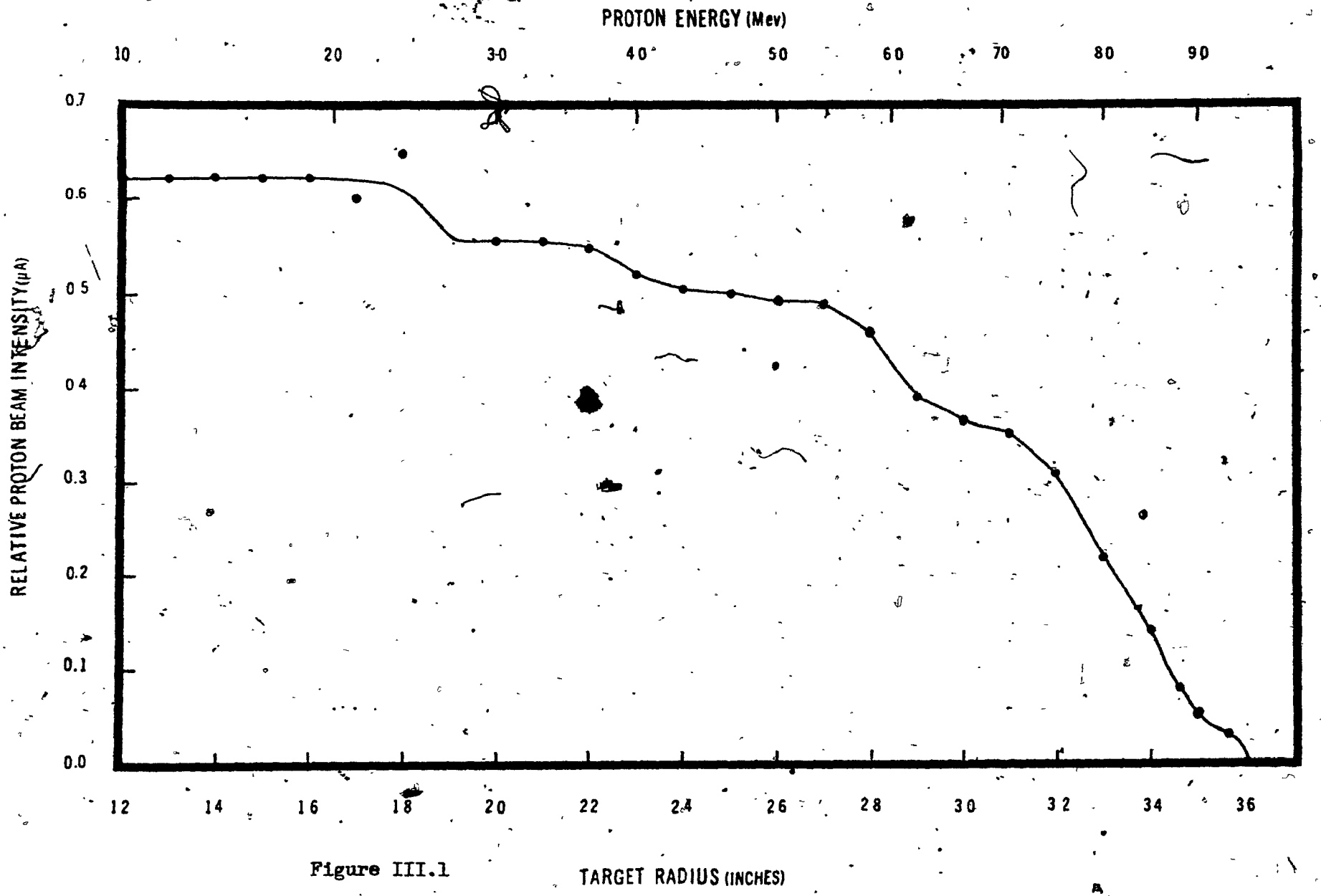
PROTON ENERGY (Mev)
10
20
30
40
50
60
70
80
90
RELATIVE PROTON BEAM INTENSITY (μA)
0.7
0.6
0.5
0.4
0.3
0.2
0.1
0.0
12
14
16
18
20
22
24
26
28
30
32
34
36
TARGET RADIUS (INCHES)

Figure III.1

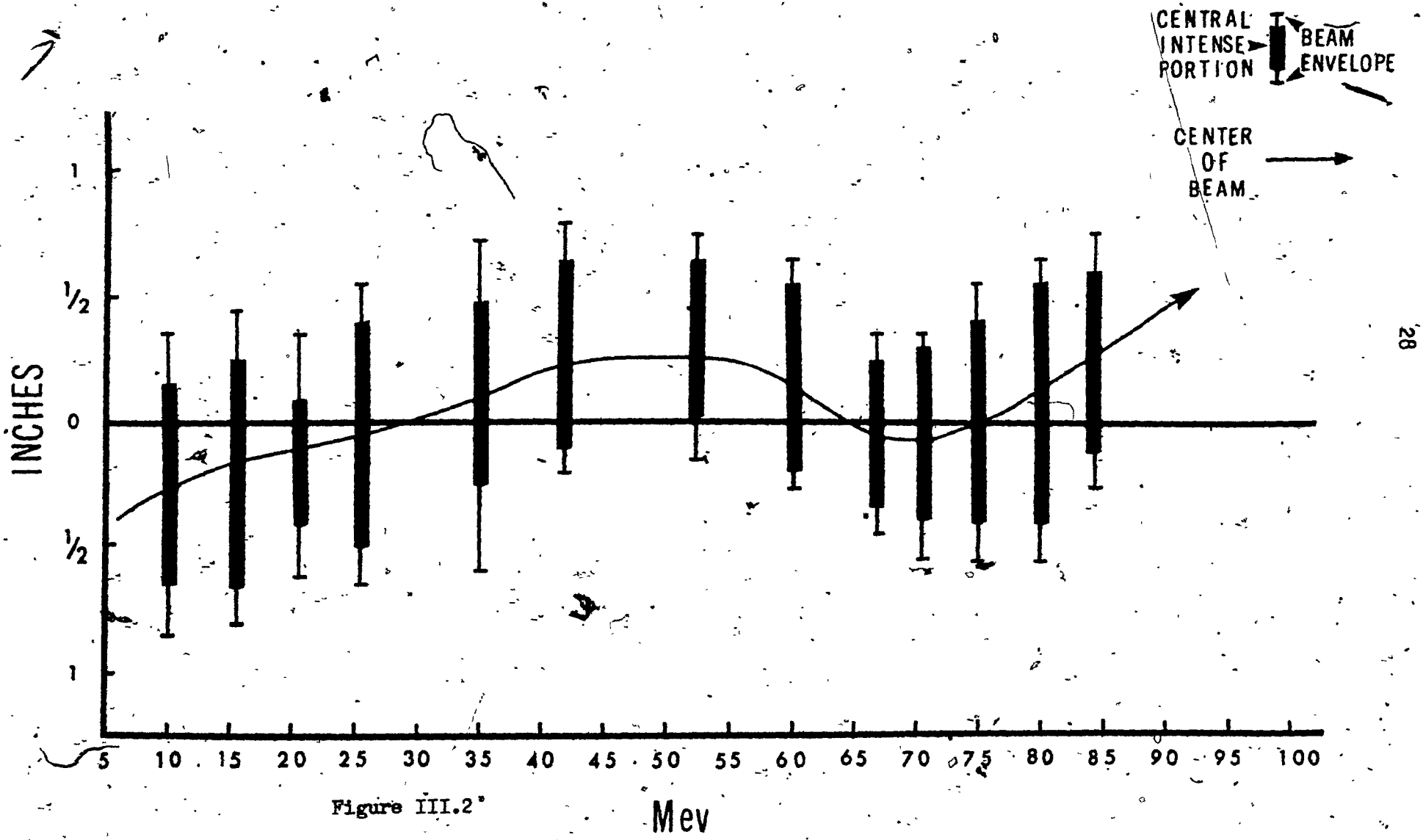
CENTRAL INTENSE PORTION
BEAM ENVELOPE
CENTER OF BEAM
INCHES
1
½
0
½
1
5
10
15
20
25
30
35
40
45
50
55
60
65
70
75
80
85
90
95
100
Mev

Figure III.2

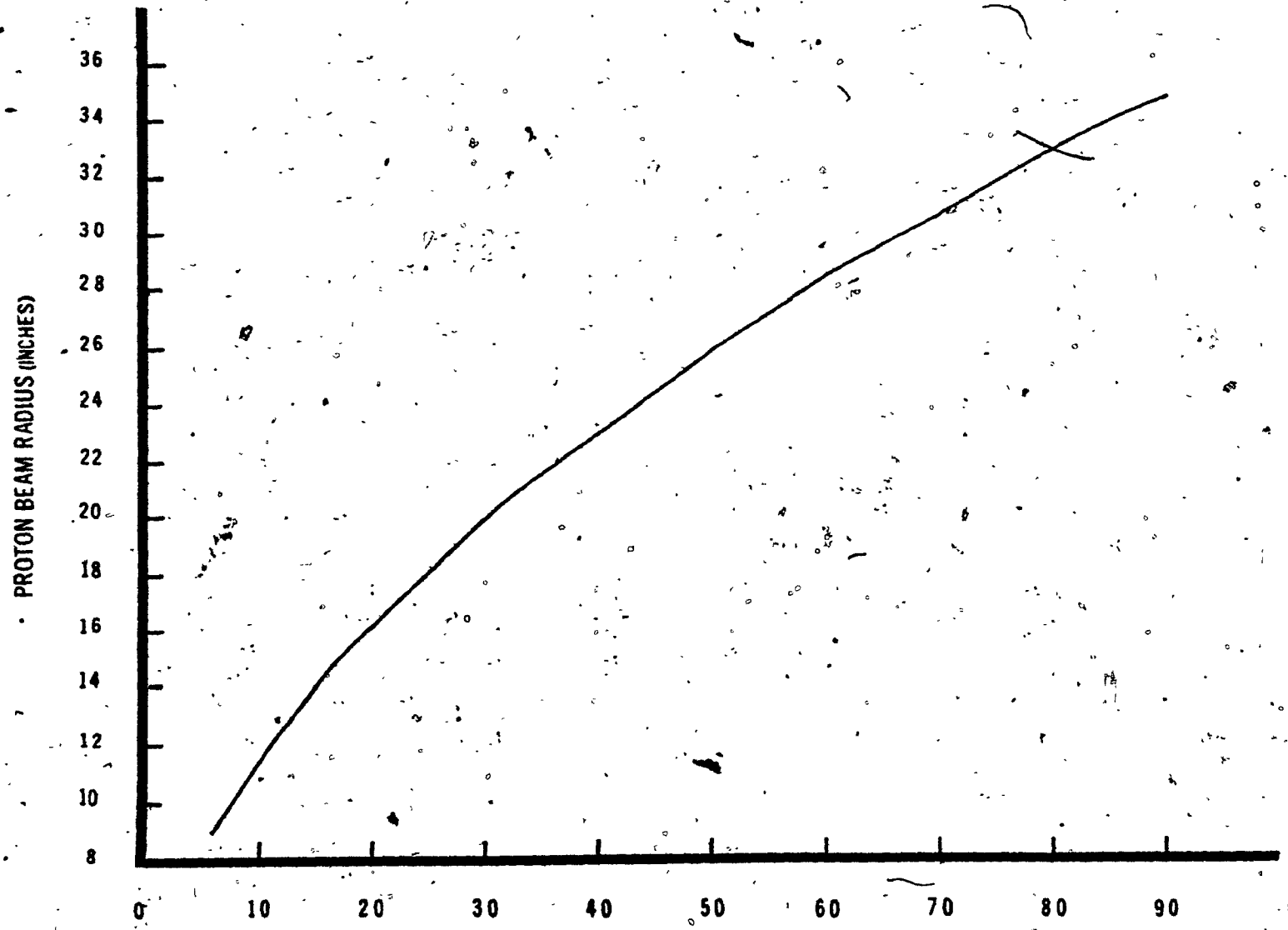
PROTON BEAM RADIUS (INCHES)
36
34
32
30
28
26
24
22
20
18
16
14
12
10
8
0
10
20
30
40
50
60
70
80
90
PROTON ENERGY (Mev)

Figure III.3

III.4 The Counting Apparatus

The block diagram in figure III.4 shows the solid state detector which is biased with high voltage. Soon after the dectector follows the preamplifier, linear amplifier, and the usual counting and storing systems.

It would be appropriate to discuss the semiconductor gamma dectector in brief.

Gamma radiation or charged particles lose energy through interaction with the detector material. These interactions cause the electrons of valence bands to be raised to conductance bands. A strong electrical field can sweep these charges to an electrical pulse. Semiconductors became popular because of the greater energy resolution they produce. The number of charge carriers produced in a solid-state detector depends only on the energy deposited by the radiation, and is independent of the type of radiation. Therefore, germanium detectors used for gamma-ray spectroscopy will readily detect electrons and other charged particles if these are not absorbed before reaching sensitive volume of the detector. Hence, conversion electrons and gamma-rays can be determined simultaneously. The Ge(Li) detector used for gold assay shows very good energy resolution and due to its large sensitive volume, higher numbers of peaks can be seen in figure 5 .

The most important characteristics of Germanium-Lithium drifted detectors can be summarized as follows:

(a) High resolving power

(b) Complete charge collection

III.4 The Counting Apparatus

The block diagram in figure III-4 shows the solid state detector which is biased with high voltage. Soon after the dectector follows the preamplifier, linear amplifier, and the usual counting and storing systems.

It would be appropriate to discuss the semiconductor gamma dectector in brief.

Gamma radiation or charged particles lose energy through interaction with the detector material. These interactions cause the electrons of valence bands to be raised to conductance bands. A strong electrical field can sweep these charges to an electrical pulse. Semiconductors became popular because of the greater energy resolution they produce. The number of charge carriers produced in a solid-state detector depends only on the energy deposited by the radiation, and is independent of the type of radiation. Therefore, germanium detectors used for gamma-ray spectroscopy will readily detect electrons and other charged particles if these are not absorbed before reaching sensitive volume of the detector. Hence, conversion electrons and gamma-rays can be determined simultaneously. The Ge(Li) detector used for gold assay shows very good energy resolution and due to its large sensitive volume, higher numbers of peaks can be seen in figure 5 .

The most important characteristics of Germanium-Lithium drifted detectors can be summarized as follows:

(a) High resolving power

(b) Complete charge collection

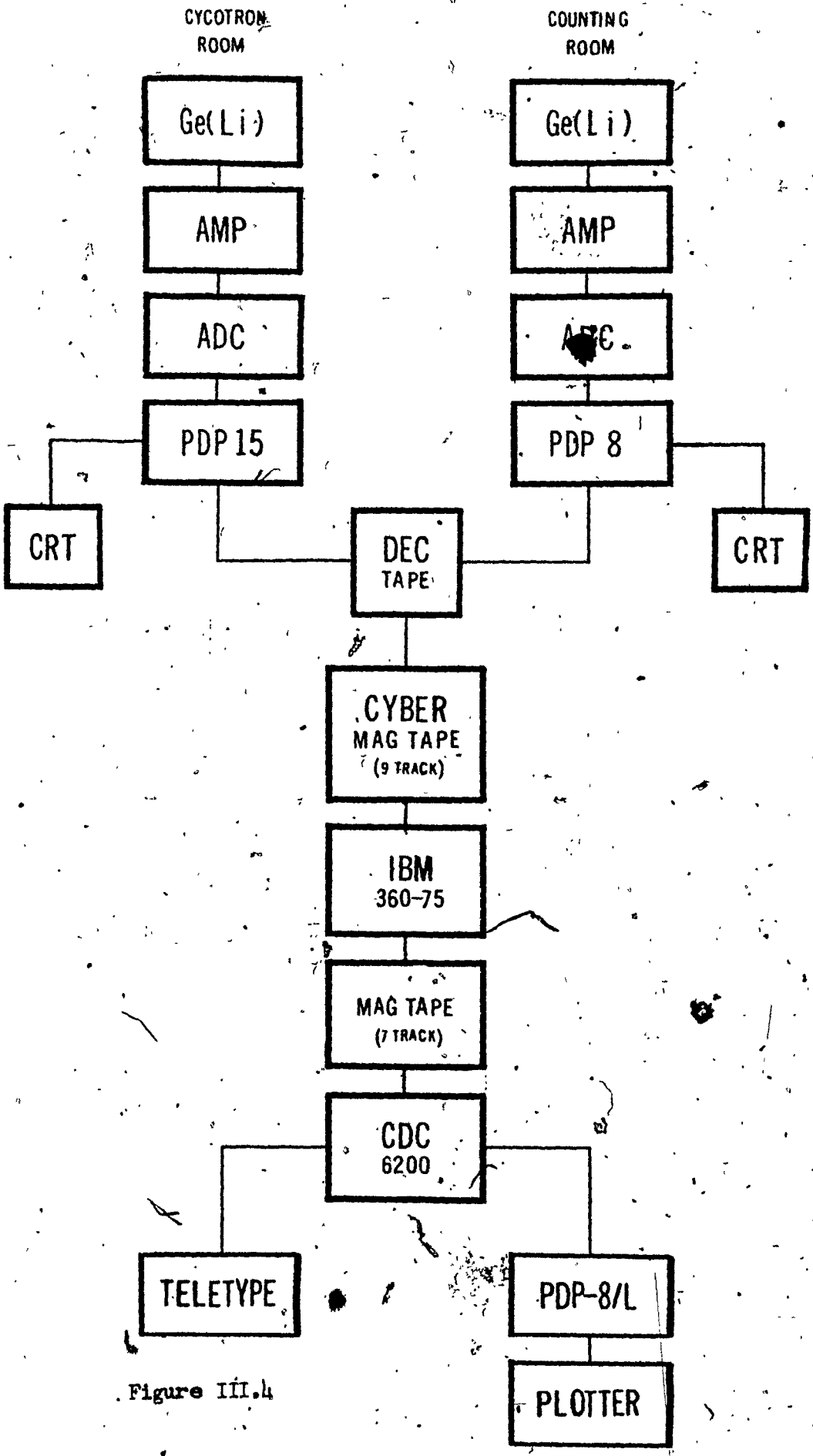
CYCOTRON ROOM
COUNTING ROOM
Ge(Li)
Ge(Li)
AMP
AMP
ADC
ADC
PDP 15
PDP 8
CRT
DEC TAPE
CRT
CYBER MAG TAPE (9 TRACK)
IBM 360-75
MAG TAPE (7 TRACK)
CDC 6200
TELETYPE
PDP-8/L
PLOTTER

Figure III.4

(c) A well designed detector can have constant resolution over large range of bias voltage.

(d) The operating temperature ranges over 5-77 degrees K.

(e) Excellent linear response. Milver[6] and Murray[7] have a linearity better than 0.2 KeV from 300 to 1300 KeV.

(f) Neutron radiation can damage Ge(Li).

The detectors we used were capable of fullfilling most of the above mentioned characteristics.

The random addition of detector signal and noise, which appears as a random fluctuation of the base line, adds to the depression of the detector signals and consequently affects the resolution. A charge sensitive or integrating preamplifier is used with the semiconductor line. It is highly desirable to have the signal as a step function for the input of the preamplifier. Otherwise, there would be pile-up effects which cause non-linearity problems in the linear amplifier. We have obtained very high linearity, better than 1 KeV over 1000 channels (see the gold spectrum figures). The efficiency of the detector is shown in Figure III.5.

III.5 The Data Handling

There were many technical problems in transferring the data from the Foster Radiation Laboratory to Concordia University. (See the block diagram in figure III.4).

At FRL the spectrum could be seen on the CRT (cathode-ray tube) and with the help of a light pen various visual operations can be performed without changing the raw data.

The efficiency of the ORTEC Detector

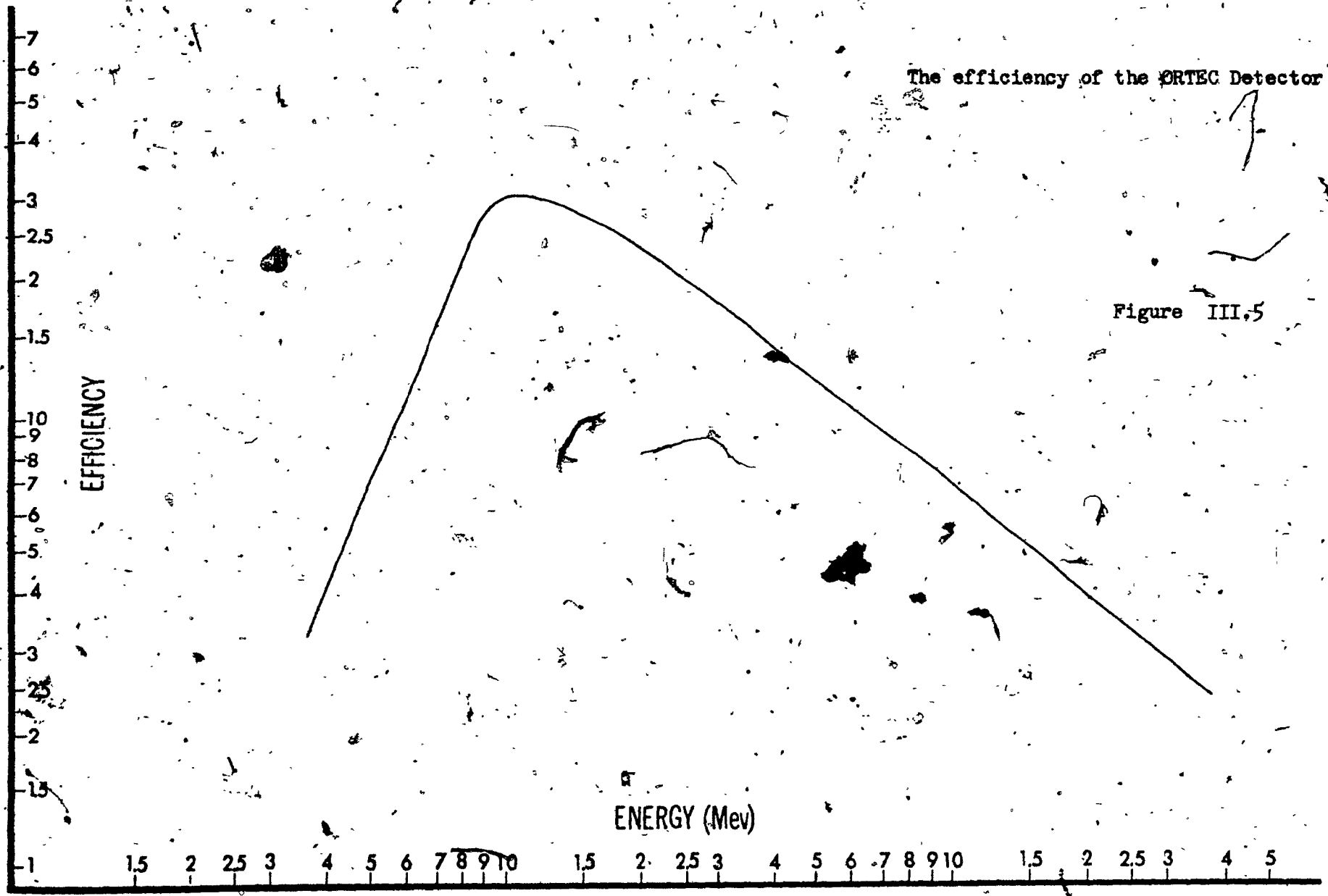

Figure III.5

From PDP memories the data are transferred onto a DEC (Digital Equipment Corporation) tape which can be stored until needed for analysis. DEC tape information can be transferred only onto a 9-track magnetic tape (called Cyber) through the PDP B or PDP 15. 9-track magnetic tape can be read by the I.B.M. 360-75 at McGill Computer Center.

The problems are twofold. The word sizes are 12 bit (PDP's), 32 bit (IBM), and 60 bit (CDC). So the program "PDP" transfers the 12 bit words into the IBM core (from the CYBER tape), re-arranges the bits to make an IBM word, and prints out the data on the line printer. Simultaneously, the data are put on a 7 track Concordia tape (in BDC) in blocks of 800 characters.

At Concordia University, the data is transferred into the CDC core (no program necessary--just a few commands), but Fortran cannot read the 800 character blocks. It can only handle 136 character blocks. Therefore MCGILL uses a newly developed command by the software department at Concordia University Computer Center which divides the 800 character blocks into 10 80-word character blocks. REFORM then reformats the data into 70 character records (which is the TTY line capacity) and the data is now in the form required by SPEC.

SPEC is a very powerful program: it can give the channel numbers and the energies (E in KeV) to three decimal places. After running SPEC on raw data, various other operations can be performed, such as obtaining energies of the peaks, which were determined by SPEC, using a cubic equation to fit the energy vs. channel number calibration curve and preparing the magnetic tape for plotting.

Without a program like SPEC, it would have been a tremendous task to locate the peaks of the various runs and determine their energies. In the activation analysis, we are concerned with many radiation energies with different half-lives of controlled activated samples. These determinations would become very tedious without handling them with the help of fast computers and sophisticated programs like SPEC.

Mathematically, SPEC advances through the spectrum one channel at a time looking for a valid spectral peak. In each fitting attempt, a straight line is drawn through the first and last few channels, forming a background line. The background is then subtracted from the data, channel by channel. SPEC then attempts to fit the gaussian expression

$$p(x) = C\,EXP - (x-\mu)^2/2\sigma^2$$

(C, μ, and σ are peak height, position and standard deviation, respectively) to a selected group of channels in the center of the fit. The validity of the fit is determined by a figure-of-merit (FOM) based upon a chi-squared formation.

$$FOM = \frac{1}{N} \sum_{i=1}^{N} (Y_i - P_i) / \bar{P}^2$$

where: N = number of channels per fit

y_i = corrected data (background subtracted) in channel i

p_i = computed value in channel i from gaussian curve

$\bar{p} = C/\sqrt{2}$ = average value of p(x)

If the FOM $\leq$ 0.1, the fit is deemed successful and output is generated.

The fitting procedure "linearizes" the gaussian expression by expanding it in terms of a Taylor series and dropping all but the linear terms. SPEC then performs a linear least squares fit, and using some initial estimates of the three parameters C, μ, and σ, arrives at a better values than the initial estimates. It then takes these better values and uses them to achieve still better values. This iteration continues until further improvement is far beyond experimental expression. At this time the FOM formation is invoked to accept or reject the fit.

III.6 Plotting of the spectra

In activation analysis, it is very important to have a visual display of the various reactions which took place so that one can compare the results later on. This is specially helpful when reactions of different half-lives have to be compared. For this reason, a computer program was written called PLOTAK (see appendix), which was able to plot the spectra on the plotter COMPLOT, manufactured by Houston Instrument, a Division of Bausch & Lomb.

PLOTAK has the property that it can pick the tallest peak and make it 100%, list the channel number, and the number of counts. It is flexible enough to expand any part of the spectrum and give the correct peak location and counts per channel.

The raw data cannot be plotted directly. First, it has to be operated on by SPEC and then PLOTAK can accept it.

It can be seen in a few of the spectra that a certain portion of them were expanded or certain peaks were brought to the maximum height. Again PLOTAK would overlap a peak if the counts per channel are very large, such as X-rays of Au^{196} in figure 5, or the Cs^{137} 661.64 peak in figure 24.

Another interesting feature of the plotting of spectra can be noticed in figures 21, 22, and 23 where the Cs^{137} peak gradually increases as .511 MeV (annihilation radiation) decreases.

CHAPTER IV

EXPERIMENTS

IV.1 Preliminary Investigations

All the activations of the samples were carried out at Foster Radiation Laboratory. The first seven spectra were counted in the counting room and the cyclotron room of FRL. The remaining four spectra were obtained at Concordia University. Finally all the raw data ended up in the core memory of the C.D.C. 6200 computer at the computer center of Concordia University.

The initial runs were done with various proton energi[redacted] as 12 MeV, 15 MeV and 20 MeV and the machine time varied, also, [redacted]inutes to 25 minutes. These trial and error runs had to be carried out in order to determine the optimum proton energy and irradiation time.

Figure 1 shows the pure quartz (SiO_2) spectrum. Quartz was irradiated for 18 minutes with protons of energy of 13 MeV corresponding to the radius 14.4 inches, with beam intensity 0.6 - 0.7 μA. The sample was allowed to "cool off" for 3 minutes. The counting was performed in the counting room. The Ge(Li) detector, LGTC, 4.8β-2.5, was used with a Tennelec 205 Linear Amplifier. A Nuclear Data ADC and Multichannel Analyzer were used. The whole spectrum was in the first portion of the memory i.e. 1024 channels. After accumulating the counts for 10 minutes, a DEC (Digital Equipment Corp.) tape was used to store the data.

It can be seen from Figure 1 that there is a very strong peak of 0.511 MeV energy in channel number $\approx$190. This is annihilation radiation. It is due to electron (megatron) and positron annihilation, following positron emission by protron-rich nuclides formed in the (p, xn) reactions. This phenomenon will be discussed later. For the time being it is sufficient to know that from pure quartz a "clean" spectrum was obtained. It was interesting to notice that if the irradiation time was decreased then the 0.511 MeV intensity decreased correspondingly.

Another run was made with quartz, but this time the proton energy was 25 MeV instead of 13 MeV as in the previous case. Again, 0.511 MeV annihilation energy was the most dominating peak and the spectrum remained very similar to the first one. Compare Figure 1 with Figure 2.

Another run was made with protons of 25 MeV energy and an irradiation time of 20 minutes, but this time soil (sand) was the target instead of pure quartz. After three minutes of cooling time the "hot" (high activity) source was brought to the counting room. This source was counted with a standard calibrated source of Eu^{154} whose decay scheme is very well known. Eu^{154} was used in order to be able to draw a very accurate energy calibration curve to determine the exact energies which arise from (p,n), (p,pn) etc. reactions of the soil and its constituents. This spectrum is shown in Figure 3. Again it can be seen that the 0.511 MeV peak due to positron annihilation dominates this spectrum and serves as a calibration energy.

In this experiment the irradiated sand sample was kept at a distance of 8 cm from the Ge(Li) detector whereas the standard Eu^{154} source was 35 cm from the detector. This gave a better counting rate and also the peaks from Eu^{154} source were of reasonable height. In the first few minutes the counting rate was higher than 3000 counts per second, but after 10 minutes it dropped to 900 counts per second.

The next spectrum shown in Figure 4 is of two standard sources: one is Eu^{154} and the other Co^{60}. The total accumulation time was 14 minutes with a counting rate of 1500 counts per second while the dead time losses were kept less than 5%. The same Ge(Li) detector was used as in previous experiments so that its efficiency could be determined and used in other cases.

Figures 5, 6, 7, 8 and 9 belong to the gold spectrum. Au^{197} was irradiated with protons of 20 MeV for 5 minutes. An Ortec Ge(Li) detector (positive Bias, Serial No. 14-1125) capable of producing very high resolution and efficiency was used in this and in the subsequent two experiments. Full memory was used i.e. 4096 channels. The Multichannel Analyzer was calibrated in such a manner that 1 KeV corresponded to one channel i.e. 1 KeV per channel. This makes it very easy to recognize the undnown energies. These 4096 channels had to be divided into four spectra of 1024 channels in order to run through the plotter, hence all the four spectra (Figures 5, 6, 7 and 8) constitute one spectrum.

At the high-energy end of the spectrum (see figure 8) there is a sharp peak; this is due to an electronic pulser which was kept on during all three experiments (this and the two subsequent ones) to determine the deviation of the calibration from 1 KeV per channel, and to provide timing information.

Since figure 8 has a very high count from the pulser, therefore, no other peak can be seen. Because of this, this part of the spectrum (figure 8) was replotted, just missing the pulser peak. This new spectrum is shown in figure 9. It is interesting to notice the statistical fluctuations which were suppressed when they were normalized to the pulser peak. Note, however, that several peaks are significantly above the "background" level and are obviously not due to statistical fluctuations.

The next logical step was to dope soil with a known quantity of gold and make an attempt to detect it. A sample of sand and gold was irradiated with protons of 20 MeV for a period of 10 minutes. Cooling off time was 3 minutes.

Again 4096 channels were used to accumulate the data and these channels were divided into four parts for plotting purposes. The last portion of the spectrum was replotted without the pulser peak.
These spectra are shown in figures 10, 11, 12, 13 and 14.
The source was counted only for a short period of 5 minutes.

It should be noted from figure 10 that the positron annihilation peak (0.511 MeV) has overlapped; that is to say that the counts per channel are many more than shown in figure 10. This is because of the finite size of the memory of the computer accumulating the data.

The next sample of sand with gold chloride was activated in a similar way as the last sample. But this time it was allowed to cool for 25 minutes and for the next 25 minutes it was counted. The counts due to 0.511 MeV peak have gone down and new peaks have appeared. This was the first time that gold was detected due to Au^{197} (p,n) Hg^{197} reaction which gives a peak of 0.134 MeV.

All the sections of the spectrum are shown in figures 15, 16, 17, 18 and 19. Again, the last part of the spectrum was plotted twice, the second time without the pulser peak.

It was realized that if this sample were allowed to cool off for a longer period and if counting time were increased considerable, then the gold could be detected easily. Hence, after four hours of cooling off period, the sample was brought to the Physics Laboratory at Concordia University and was counted for eight hours. This improved the statistics and made it easier to detect the presence of gold. Figures 20 and 20a show the details.

IV.2. Final Runs

Equipped with the above information (concerning proton energies, cooling time, etc.) and all associated data, the last set of runs was made.

Three samples of soil were prepared with varying amounts of gold, i.e. 4000, 400 and 40 ppm. All the samples were activated with protons of 20 MeV for 10 minutes. Also, a sample of quartz was activated as a control. After a few hours they were counted at Concordia University. See figures 21, 22, 23 and 24.

A Cs^{137} calibrated source was present throughout the counting. This helped in determining KeV per Channel. There was another interesting feature: as the time went by the activated samples were not so much radioactive as they were initially. As a consequence, 0.511 MeV peak decreased in height compared to 0.662 MeV Cs^{137} peak. In the spectrum shown in figure 23 the peak due to annihilation radiation has become smaller than the peak from the standard source. In fact, some of the peaks have completely vanished from the spectrum. This has been of great help in determining the elements present in the sandy loam as it gave an estimation of half-lives of these elements.

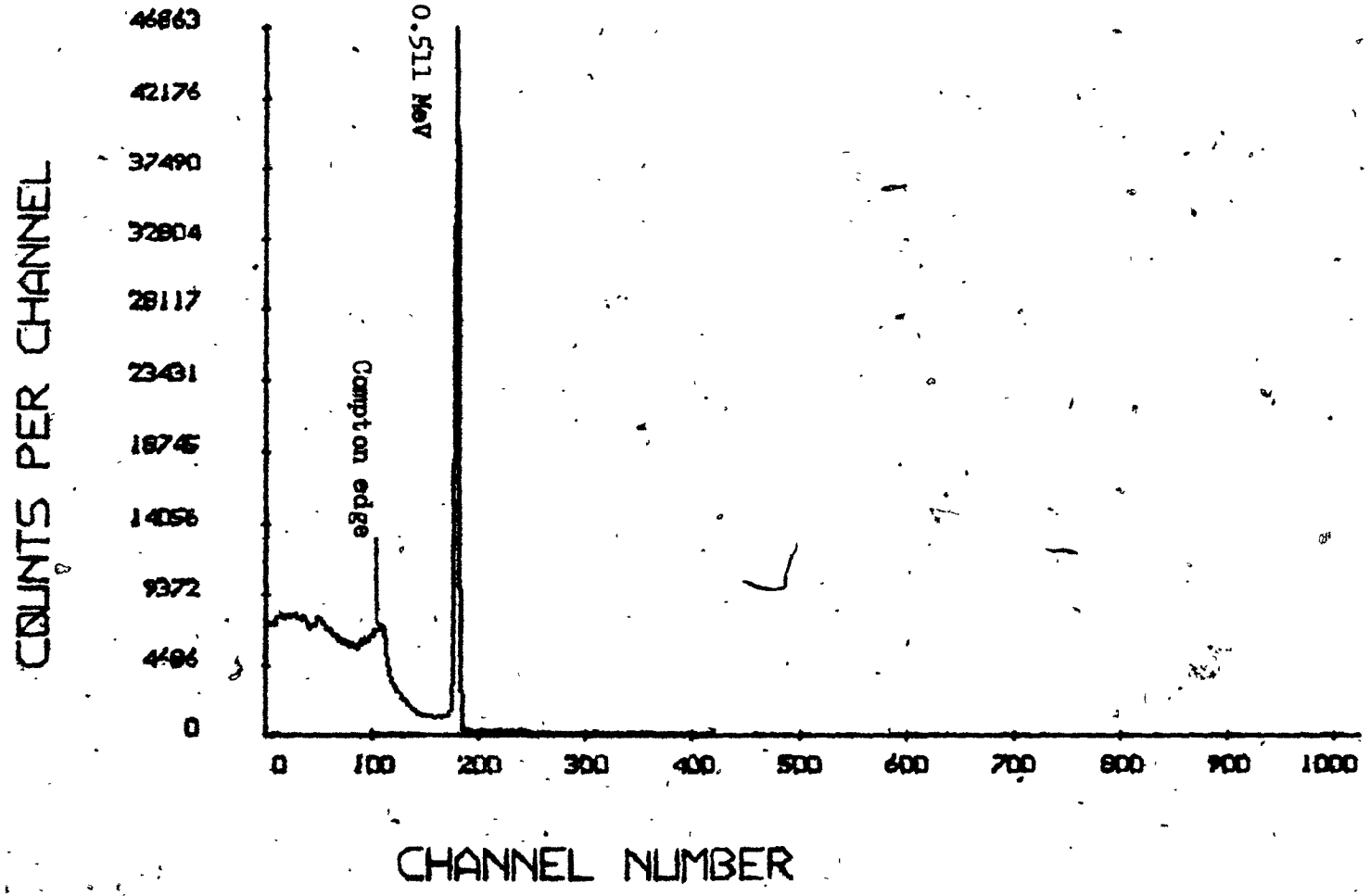

Figure 1. Quartz spectrum, irradiation energy 13 MeV.

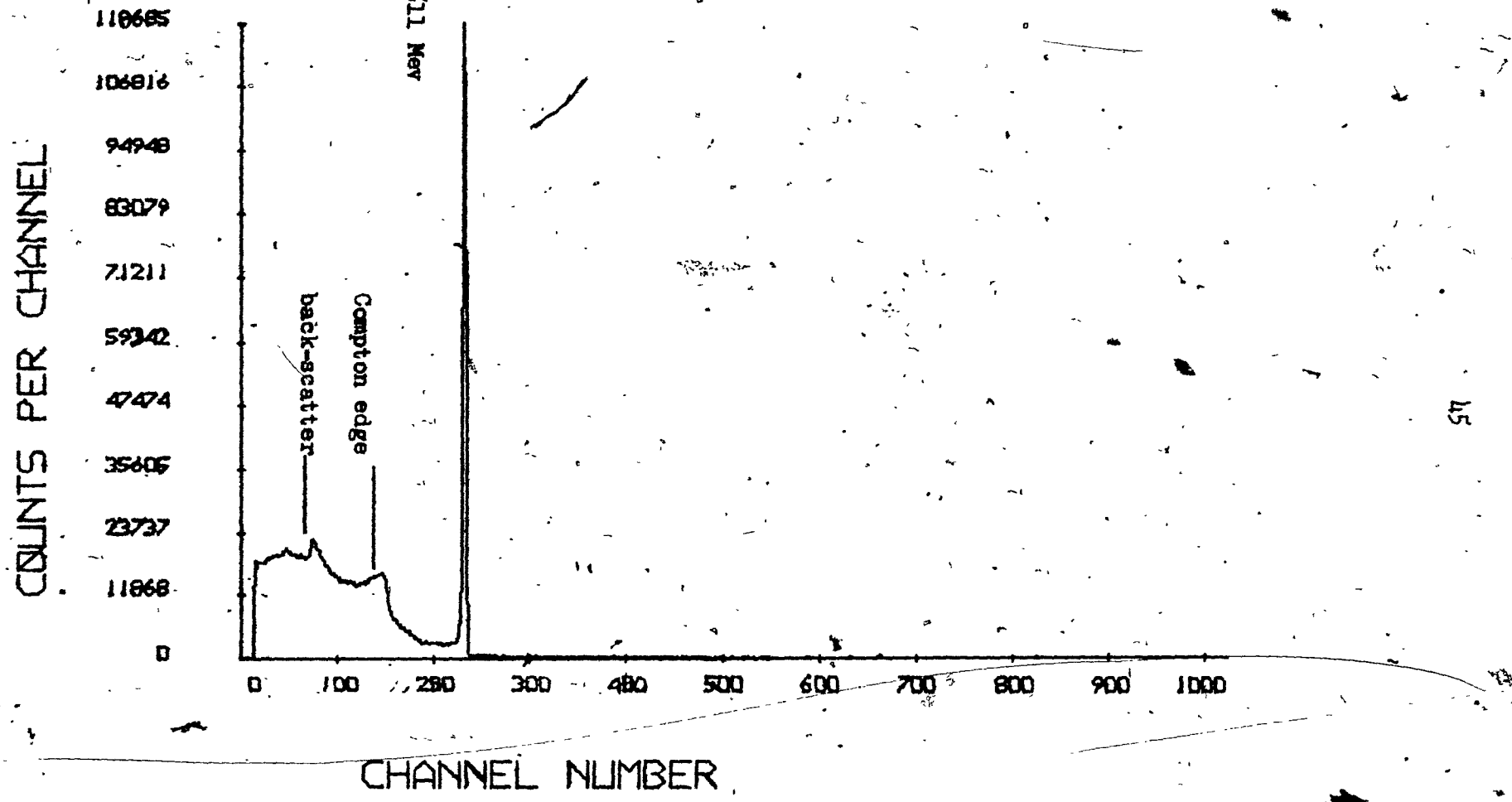

Figure 2. Quartz spectrum, protons of energy 25 MeV.

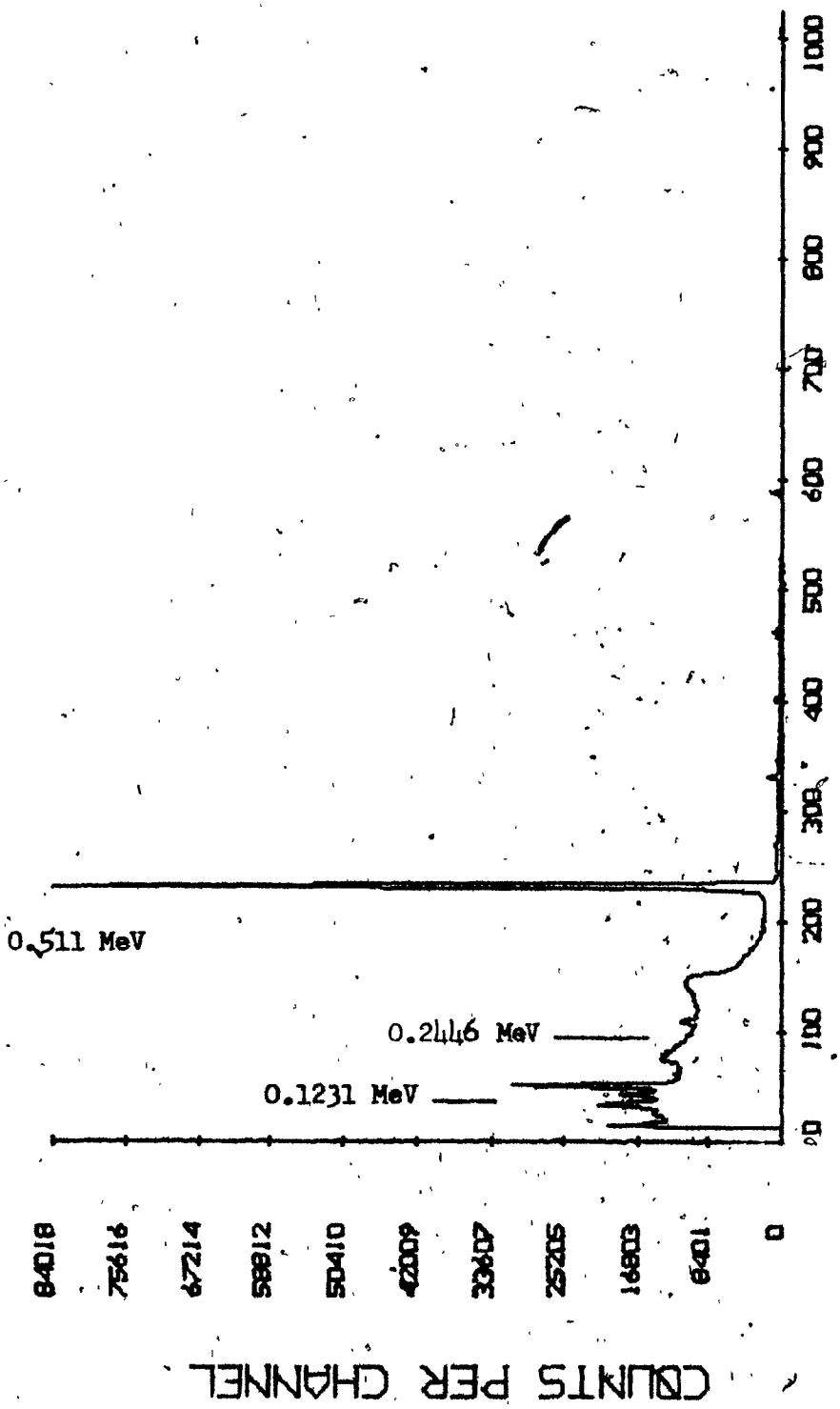

Figure 3. Sand spectrum, and the standard Eu^{154} spectrum.

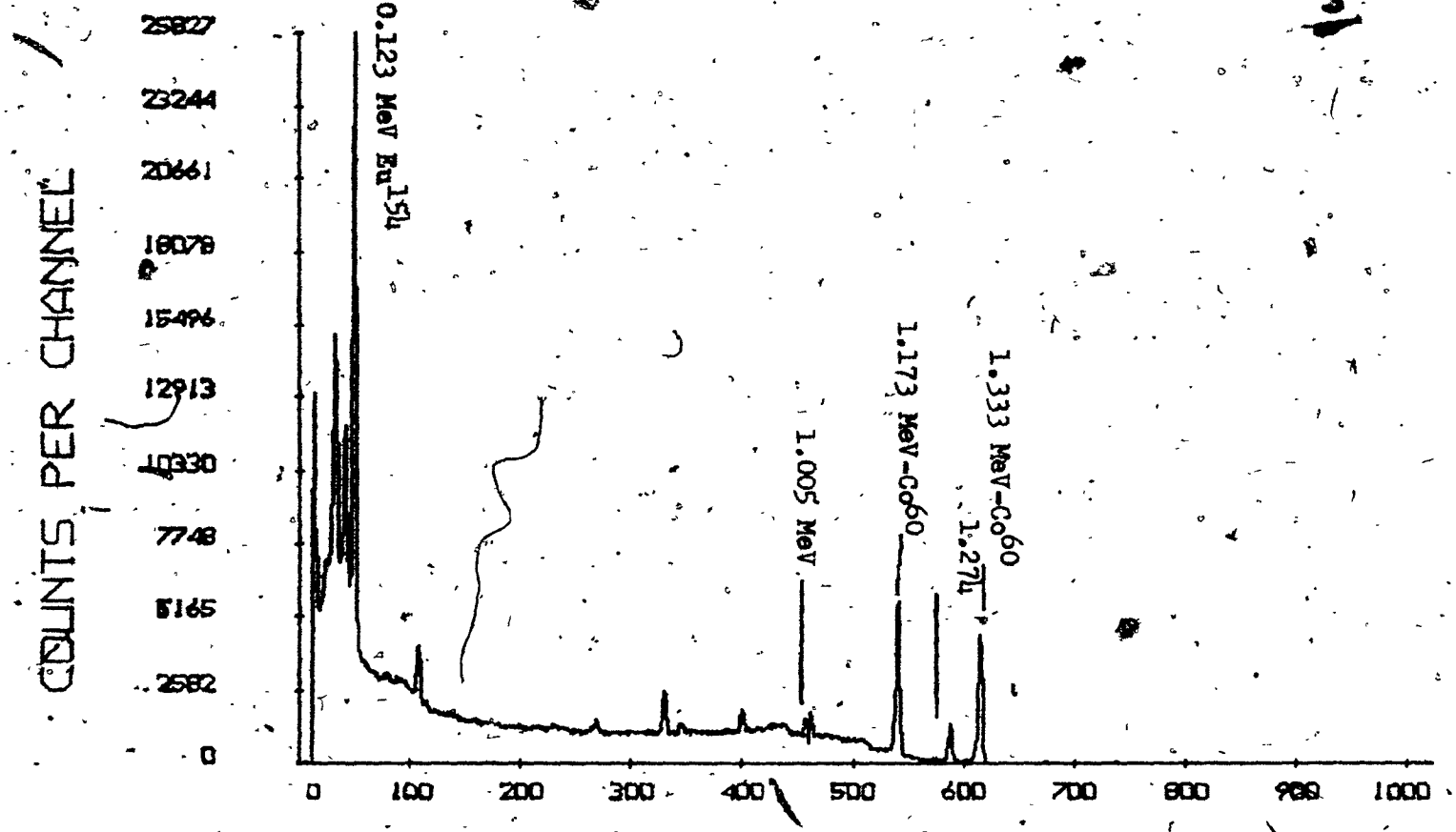

Figure 4. Standards; Eu^{154} + Co^{60}, spectrum.

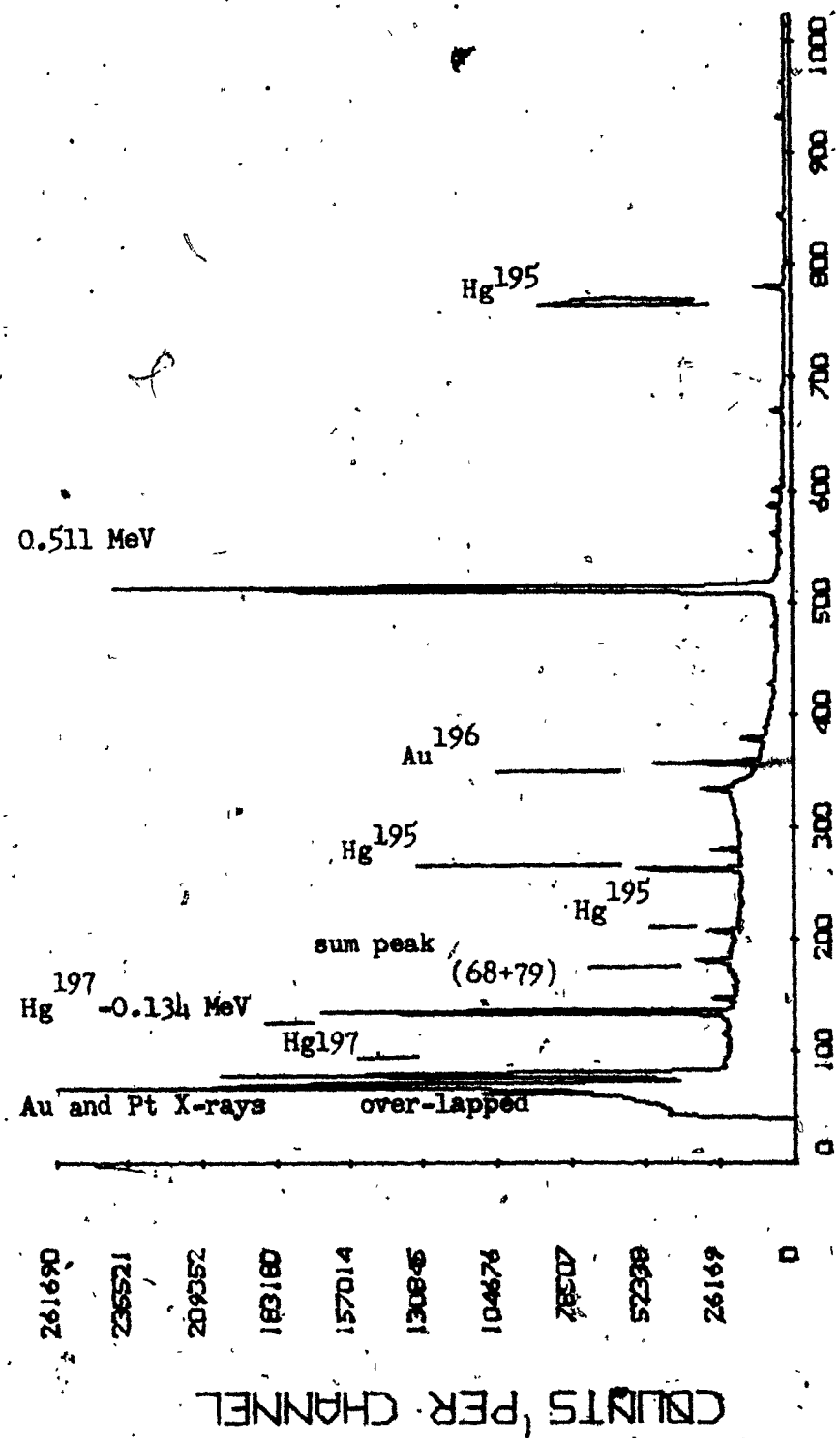

Figure 5. Gold spectrum, protons of energy 20 Mev.

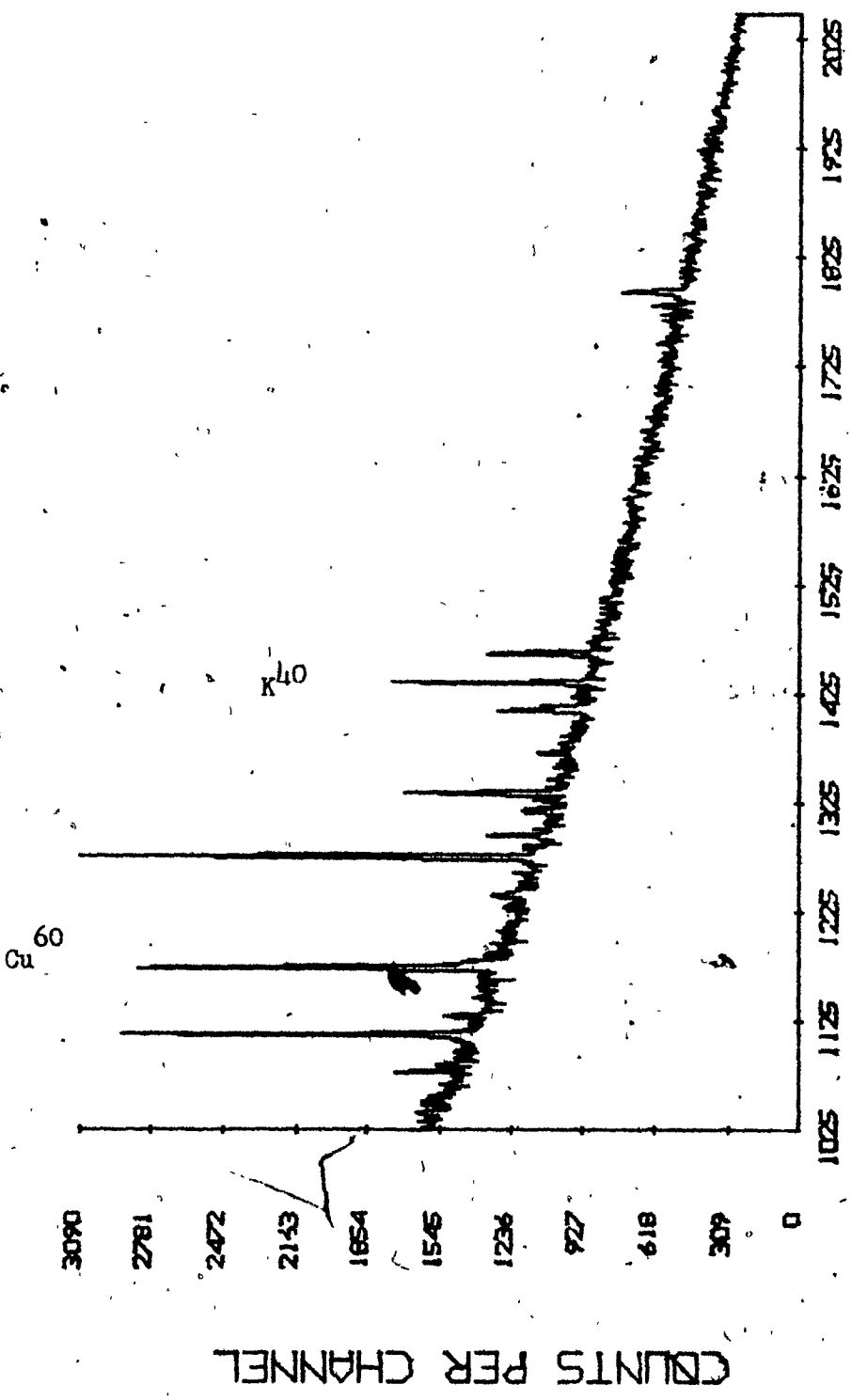

Figure 6. Au spectrum.

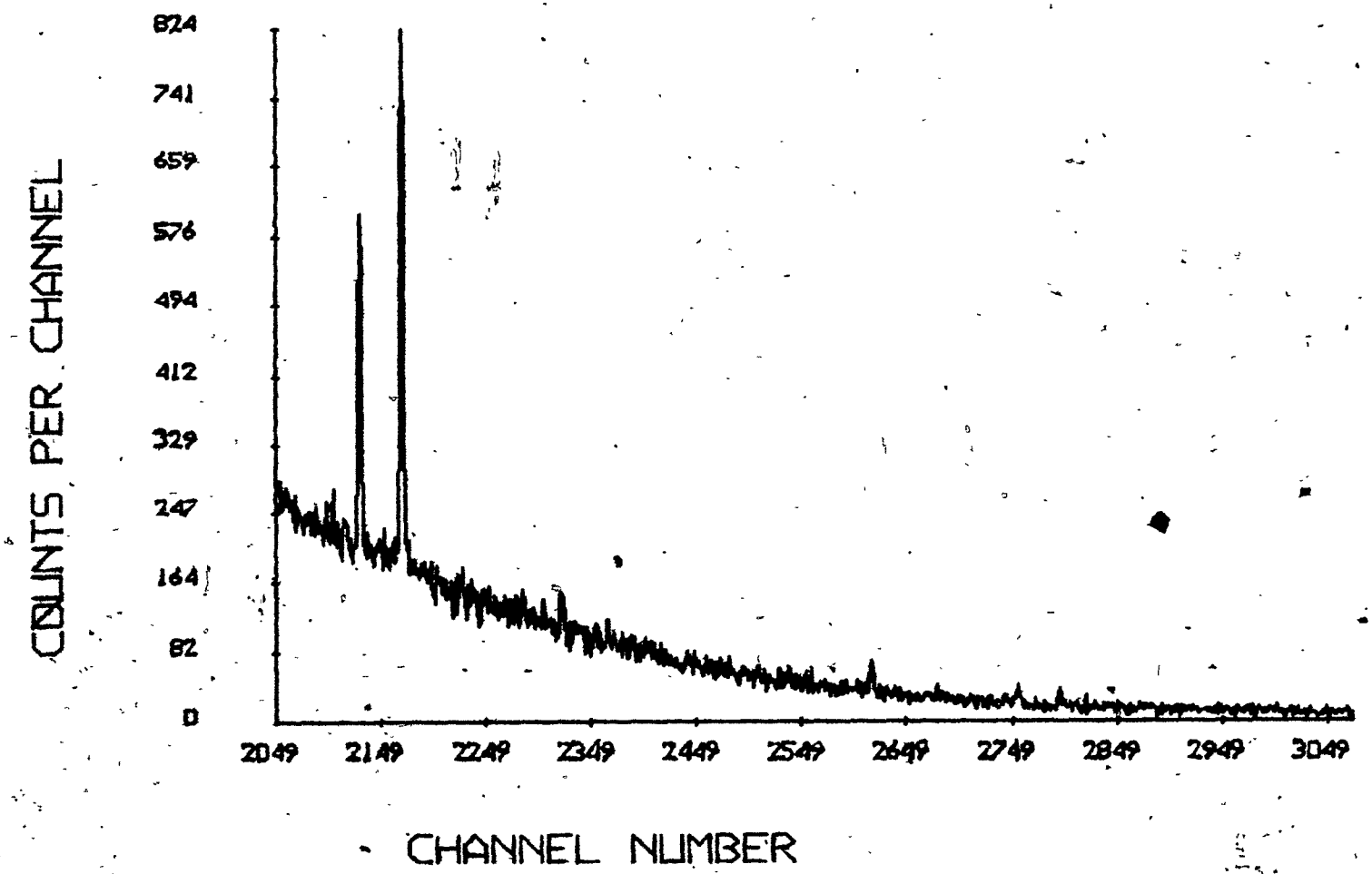

Figure 7. Au-spectrum.

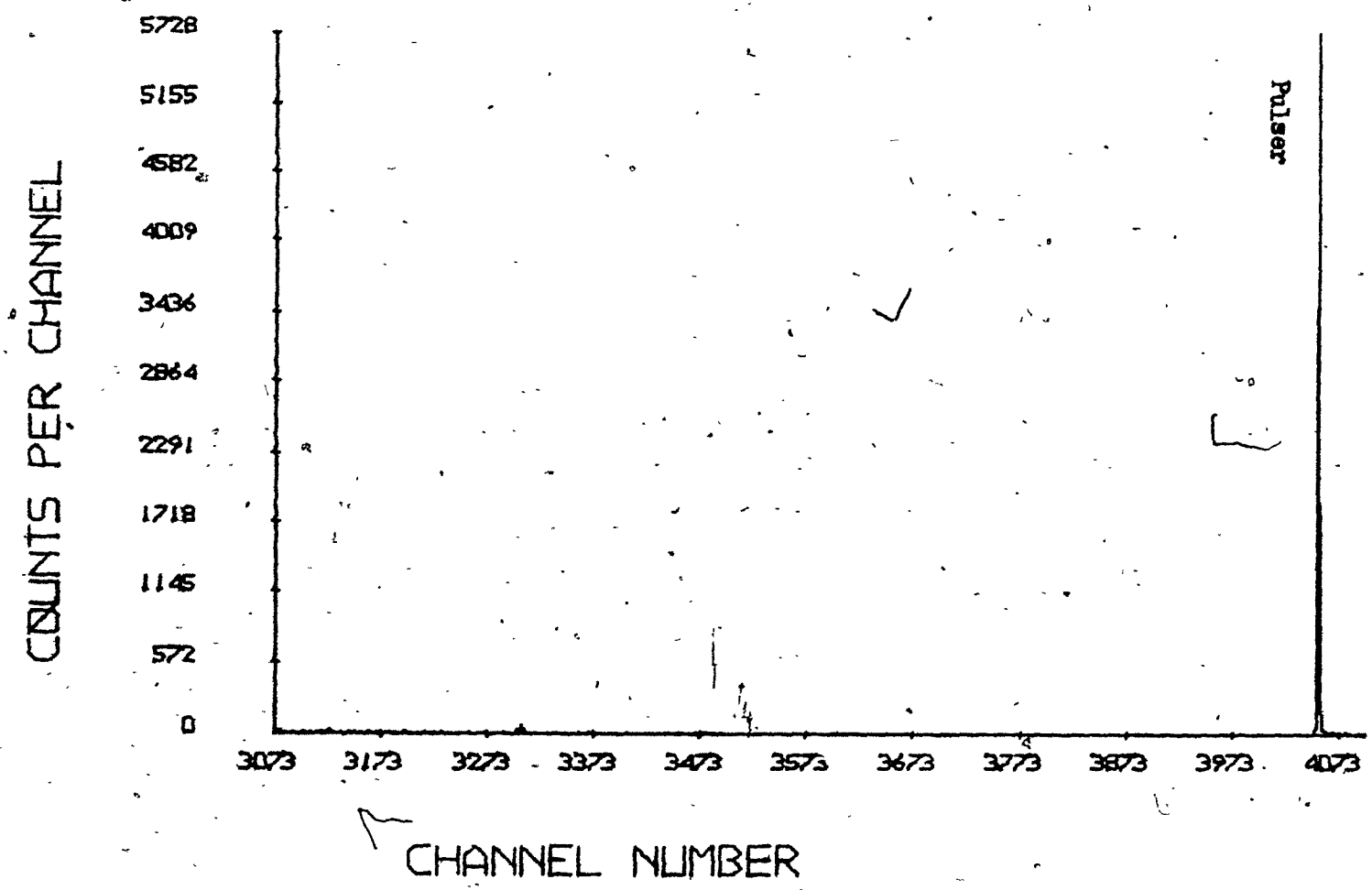

Figure 8. Au-spectrum.

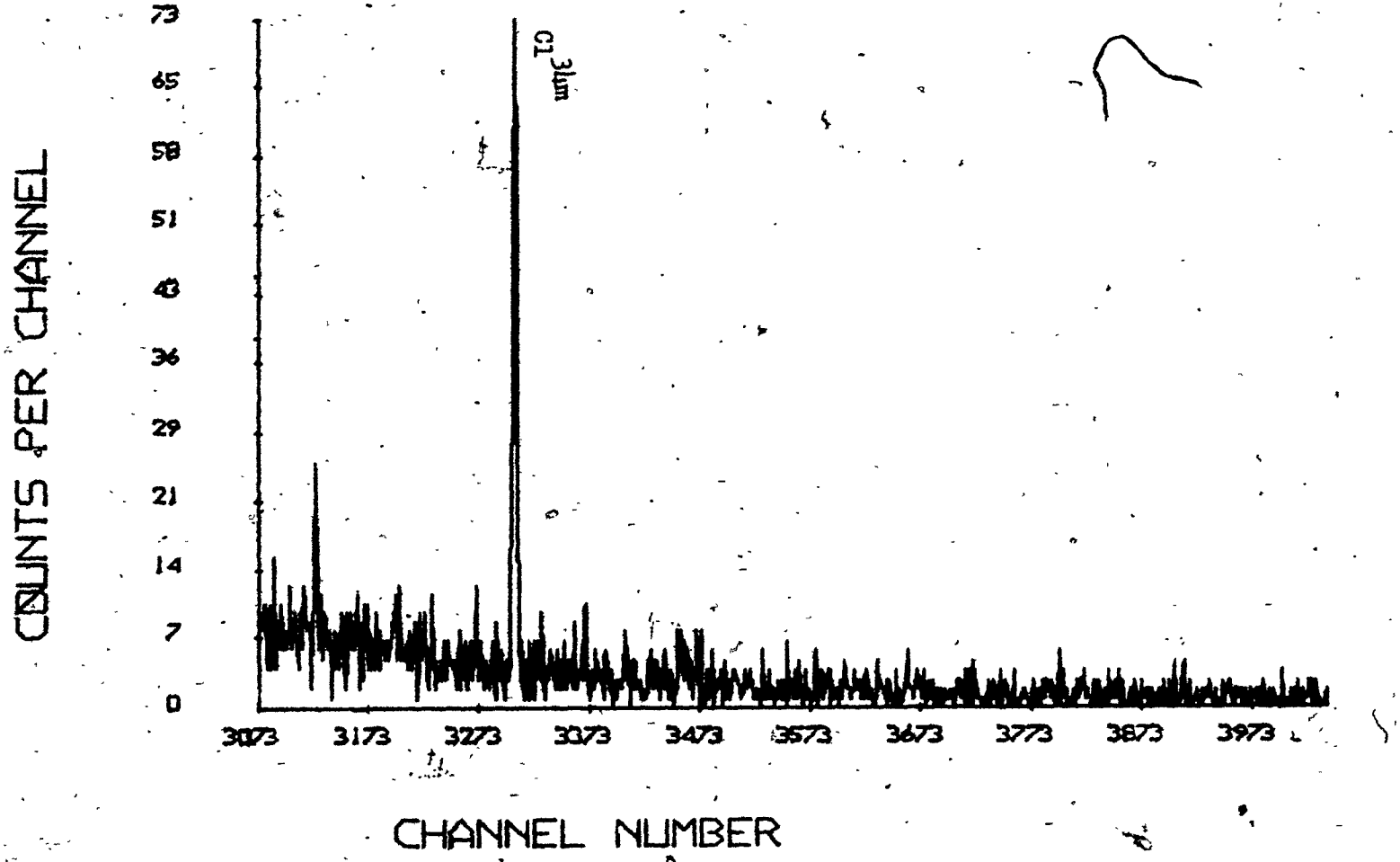

Figure 9. Au-spectrum without pulser.

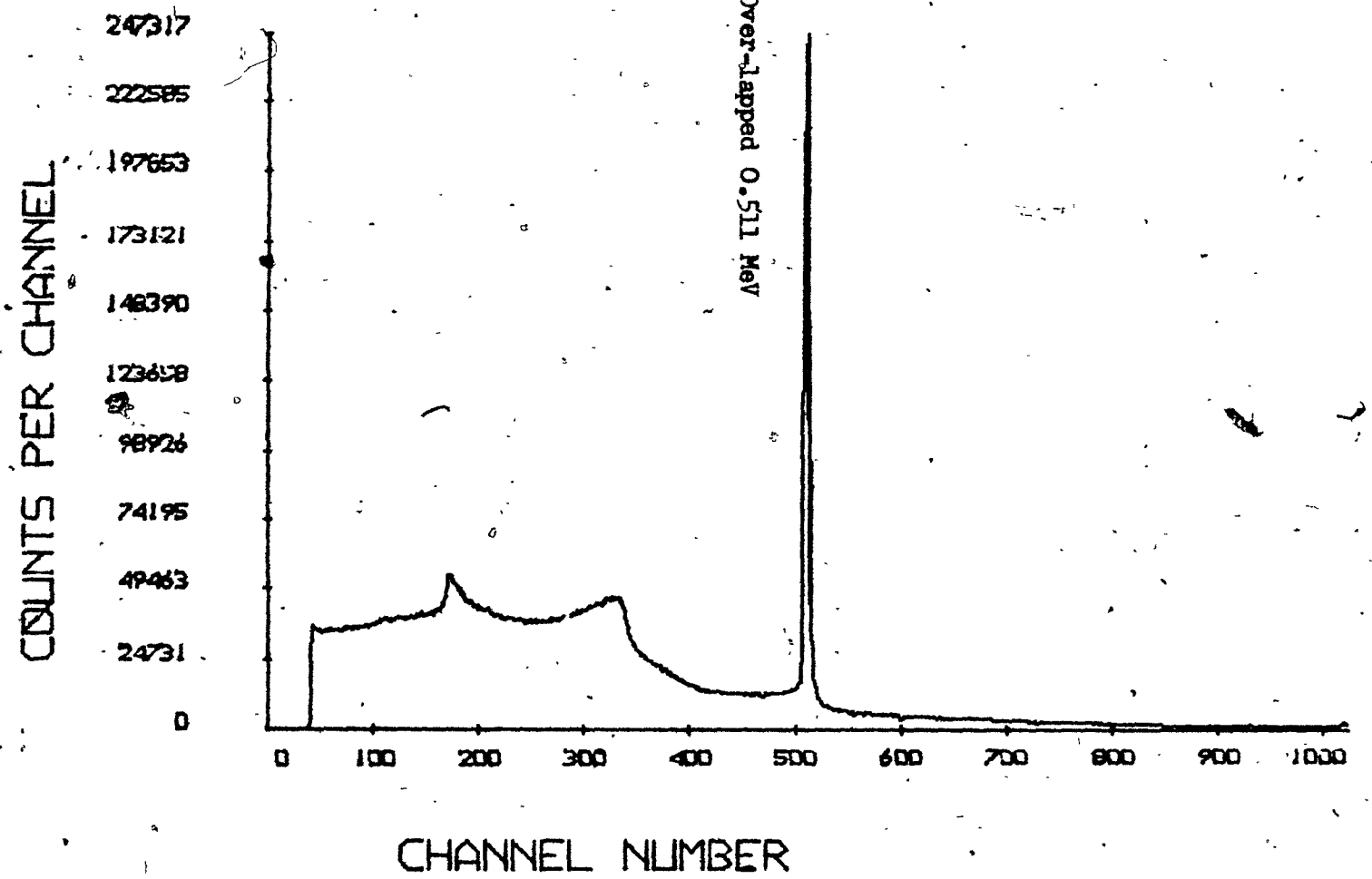

Figure 10,11,12,13,and14. (Sand + Gold) spectrum, irradiated with protons of 20 MeV for 10 minutes.

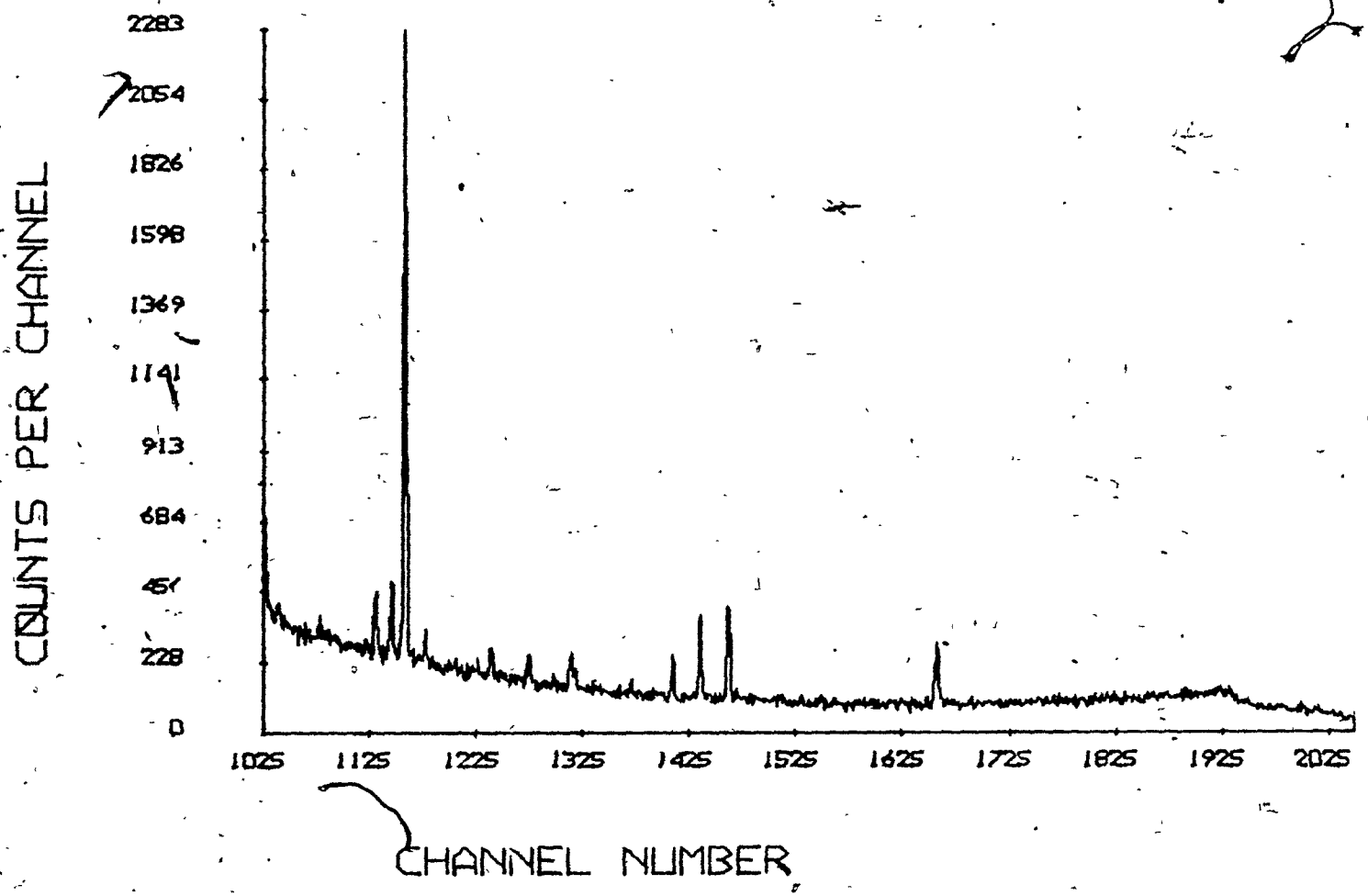
COUNTS PER CHANNEL
2283
2054
1826
1598
1369
1141
913
684
457
228
0
1025
1125
1225
1325
1425
1525
1625
1725
1825
1925
2025
CHANNEL NUMBER

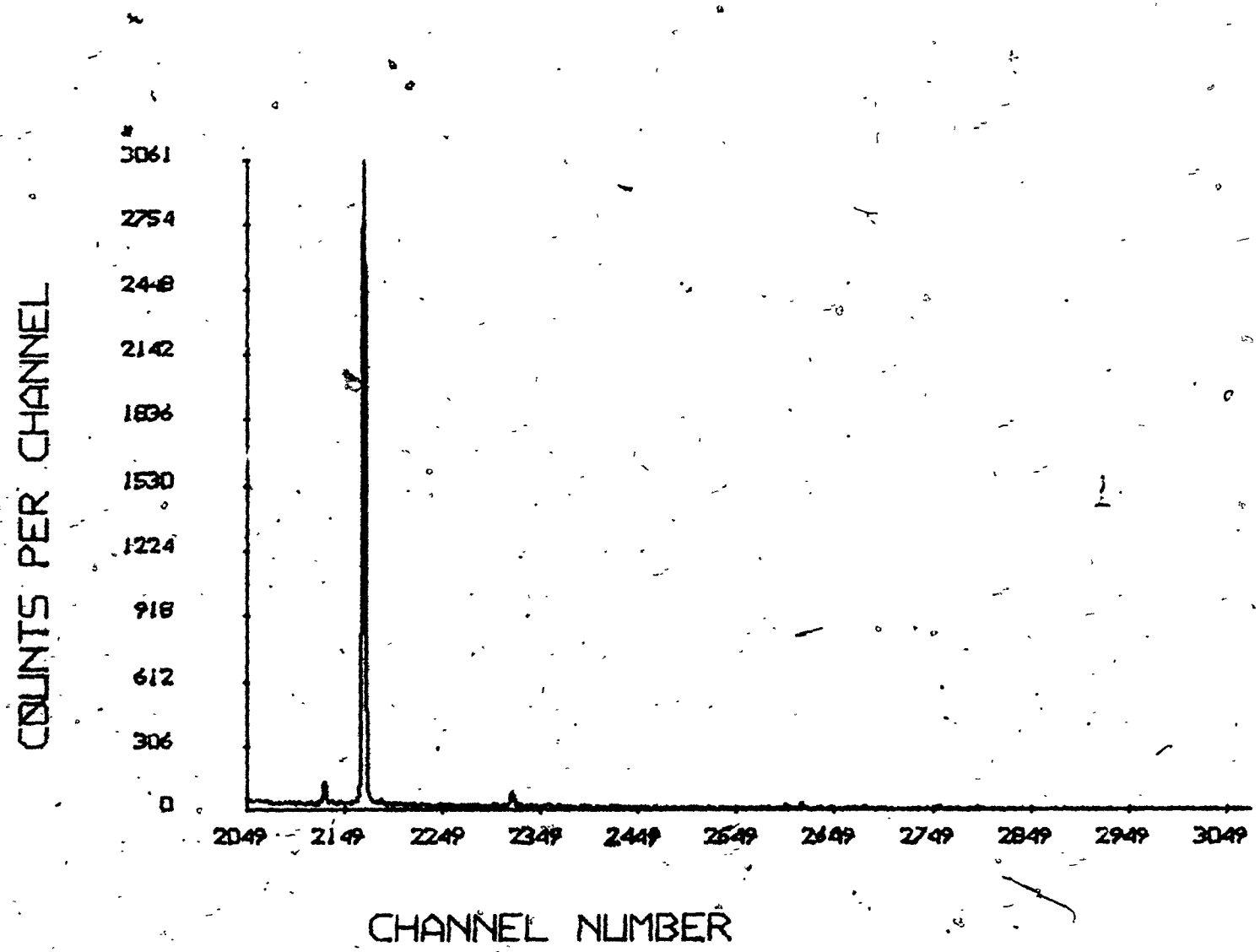
COUNTS PER CHANNEL
3061
2754
2448
2142
1836
1530
1224
918
612
306
0
2049
2149
2249
2349
2449
2549
2649
2749
2849
2949
3049
CHANNEL NUMBER

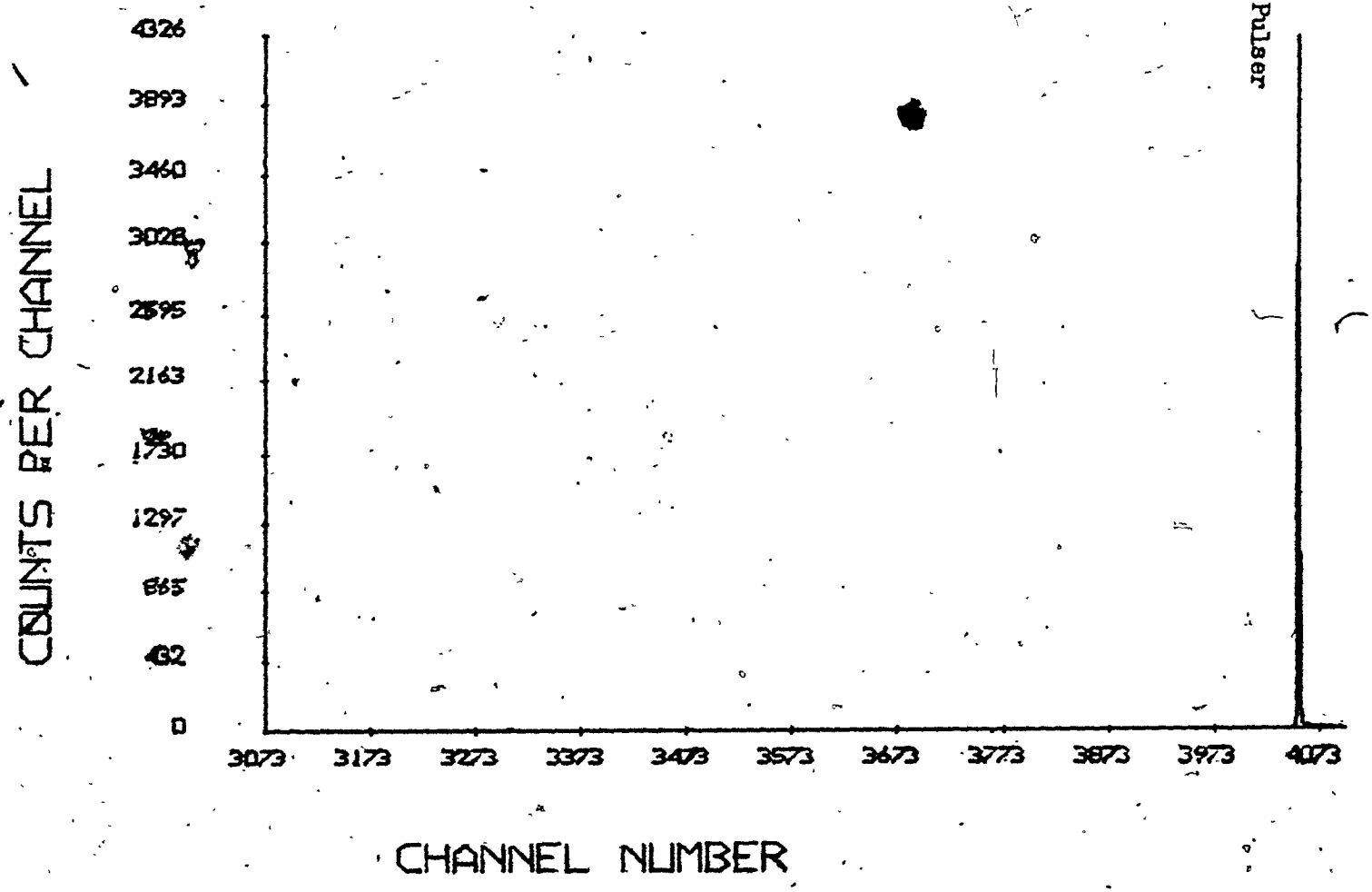
COUNTS PER CHANNEL
4326
3893
3460
3028
2595
2163
1730
1297
865
432
0
3073
3173
3273
3373
3473
3573
3673
3773
3873
3973
4073
CHANNEL NUMBER
Pulser

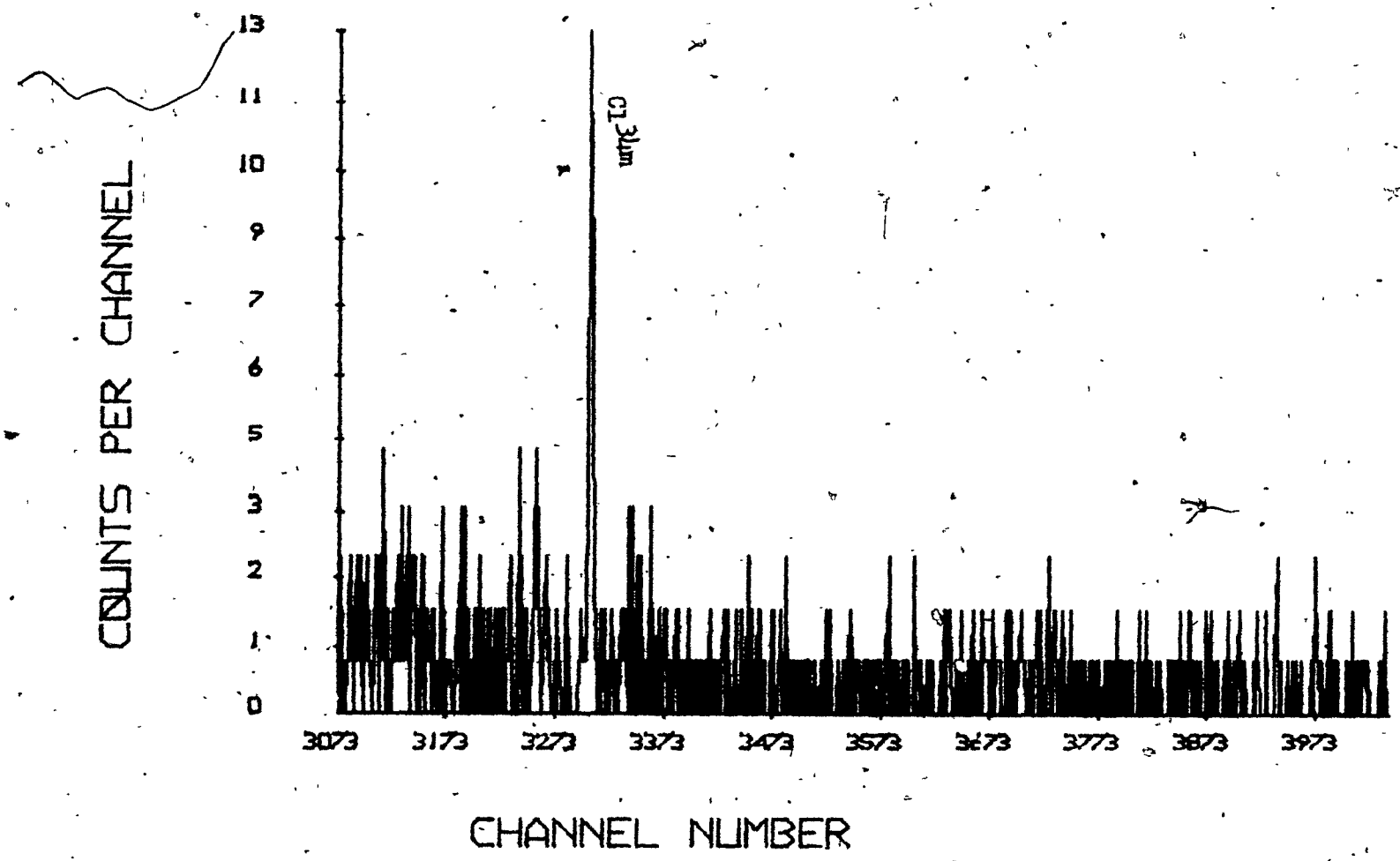
COUNTS PER CHANNEL
13
11
10
9
7
6
5
3
2
1
0
Cl 34m
3073
3173
3273
3373
3473
3573
3673
3773
3873
3973
CHANNEL NUMBER

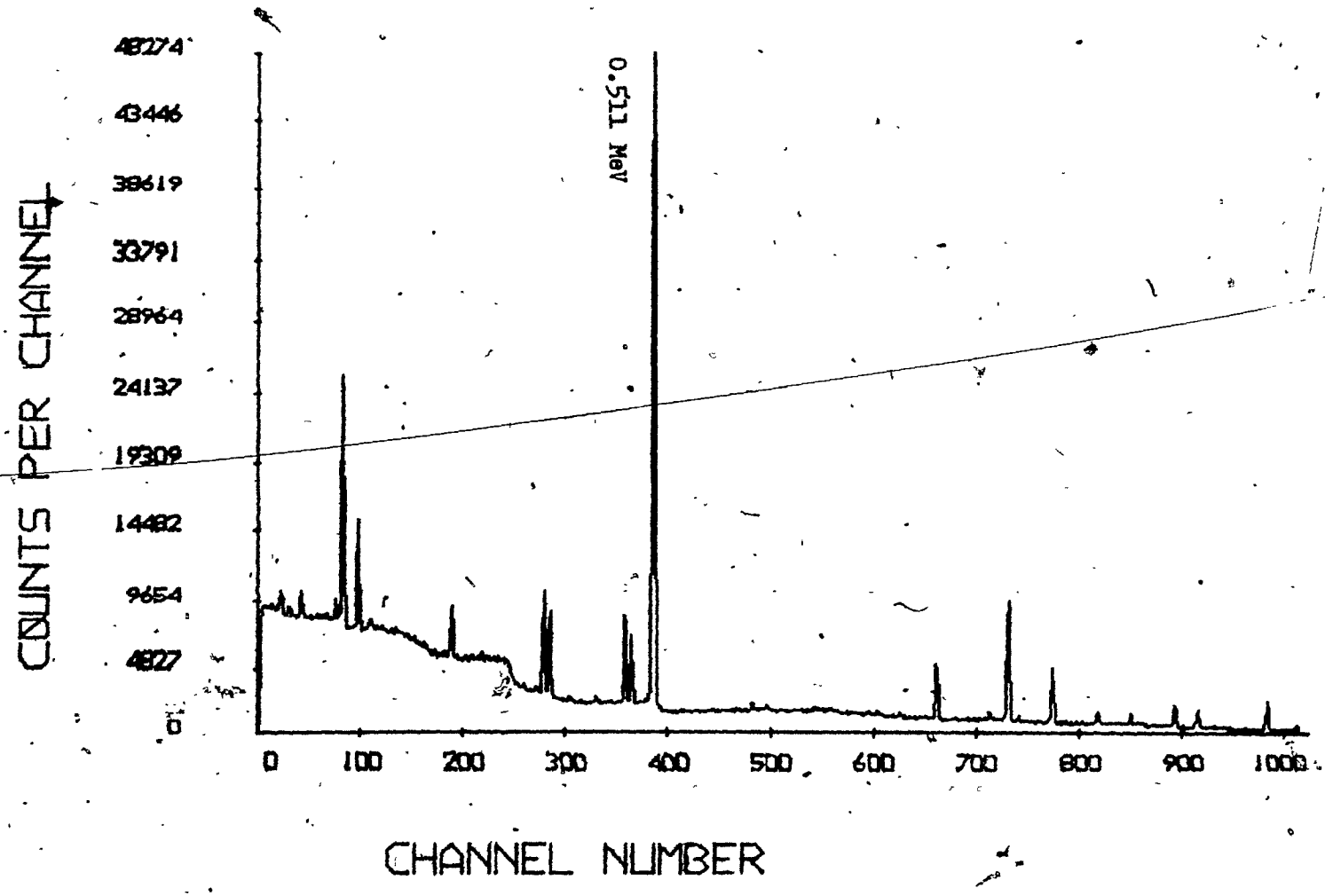

Figure 10a. Same spectrum as the last one but counted after a cooling-off period of 26 hours. The rest of the spectrum is shown in figure 12a.

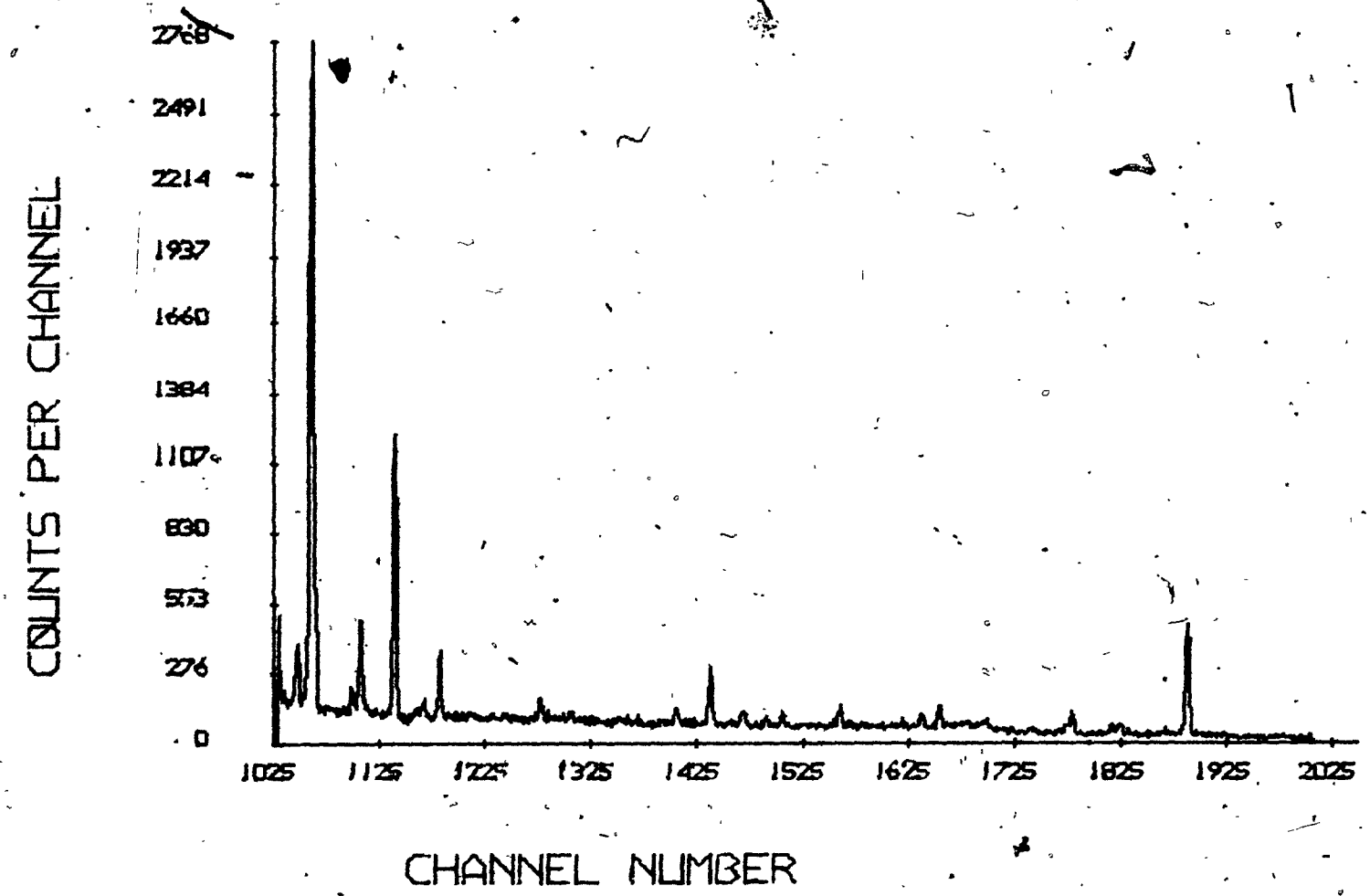
COUNTS PER CHANNEL
2768
2491
2214
1937
1660
1384
1107
830
553
276
0
1025
1125
1225
1325
1425
1525
1625
1725
1825
1925
2025
CHANNEL NUMBER

Figure 12a.

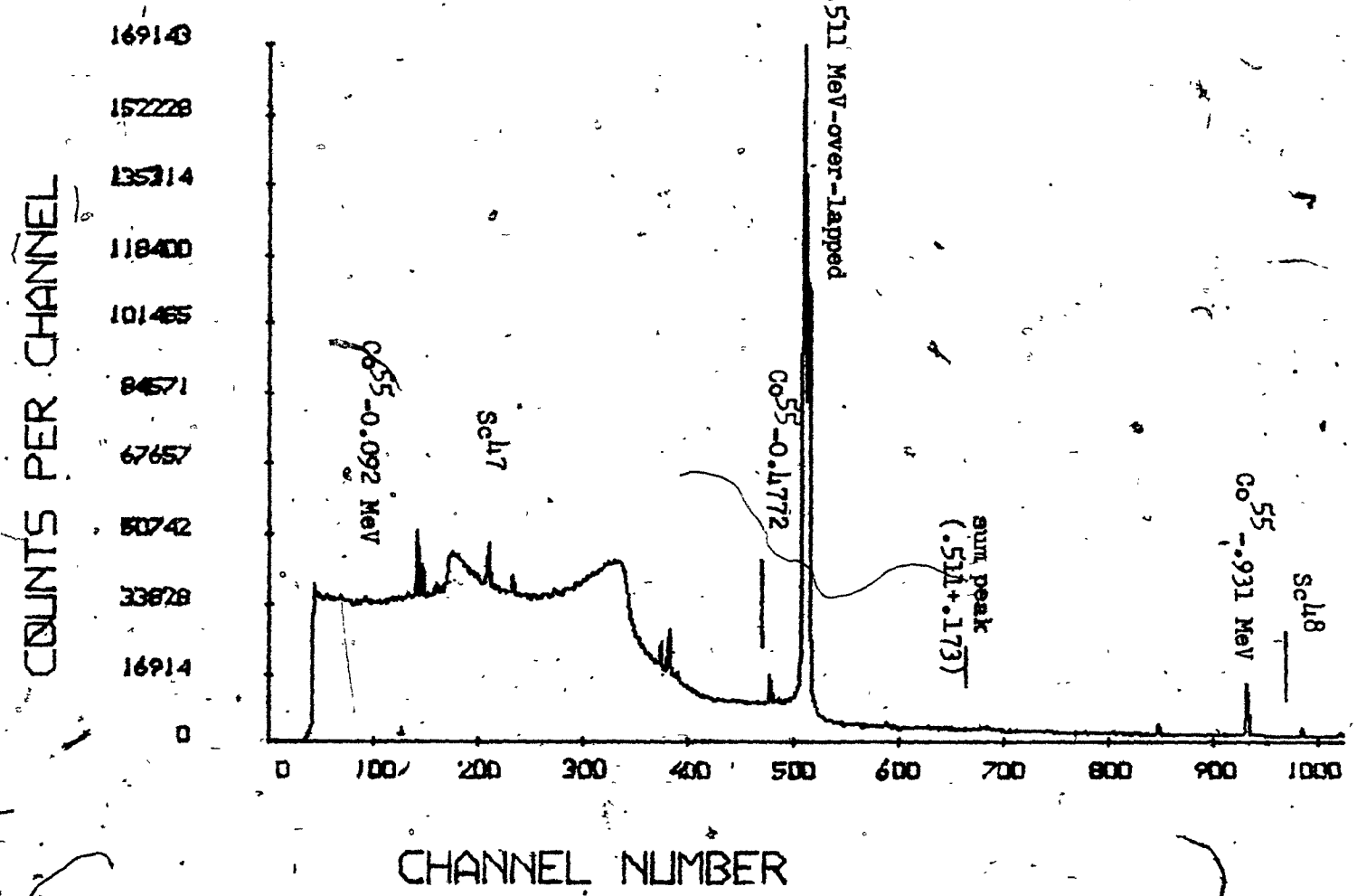

Figures 15,16,17,18,and19. All these spectra are from the sample of (sand+gold), but it was allowed to cool-off for 25 minutes. This set of spectra should be compared with the last one.

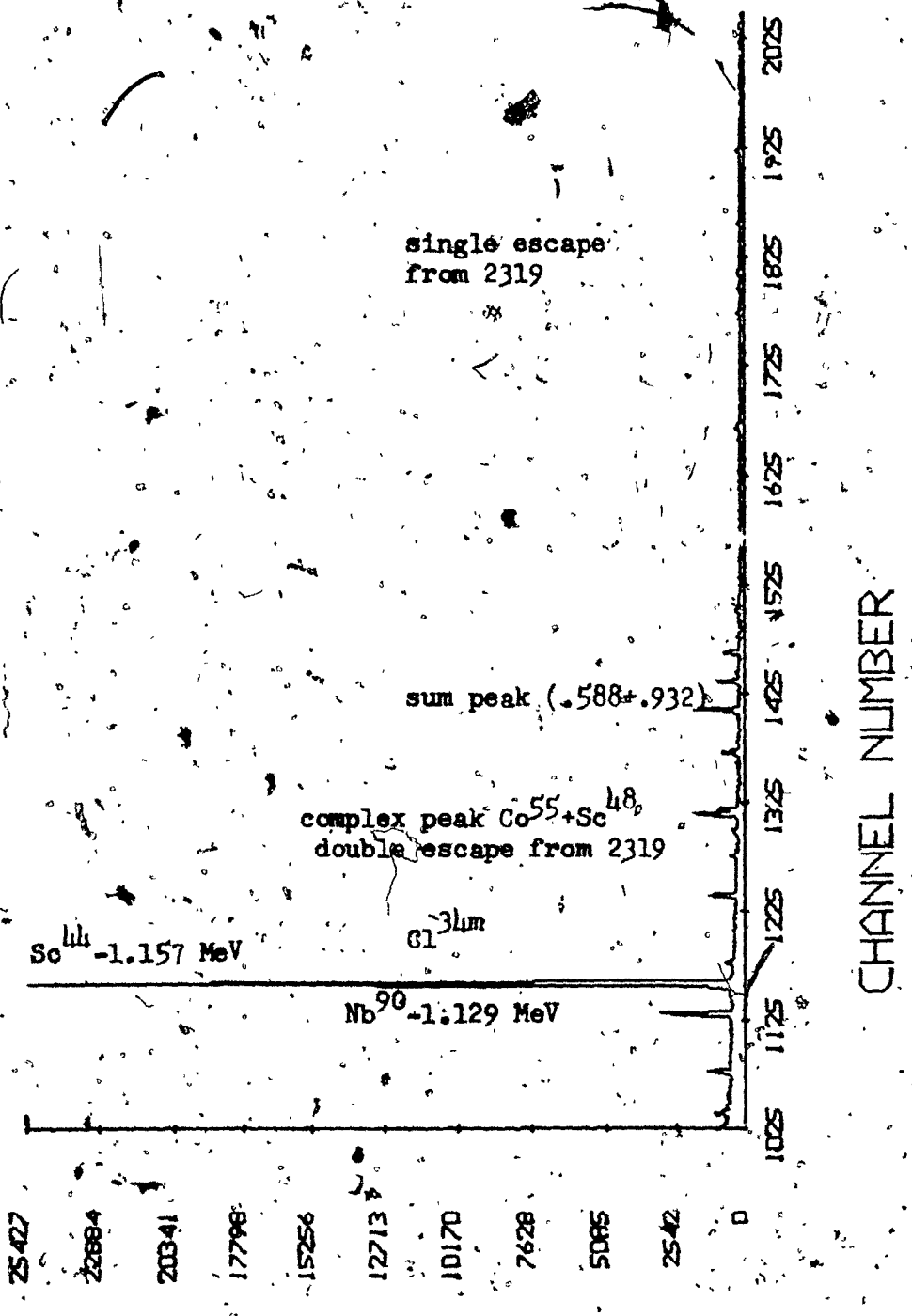
single escape from 2319
sum peak (.588+.932)
complex peak Co^{55}+Sc^{48}
double escape from 2319
Cl^{34m}
Sc^{44}-1.157 MeV
Nb^{90}-1.129 MeV
CHANNEL NUMBER
COUNTS PER CHANNEL

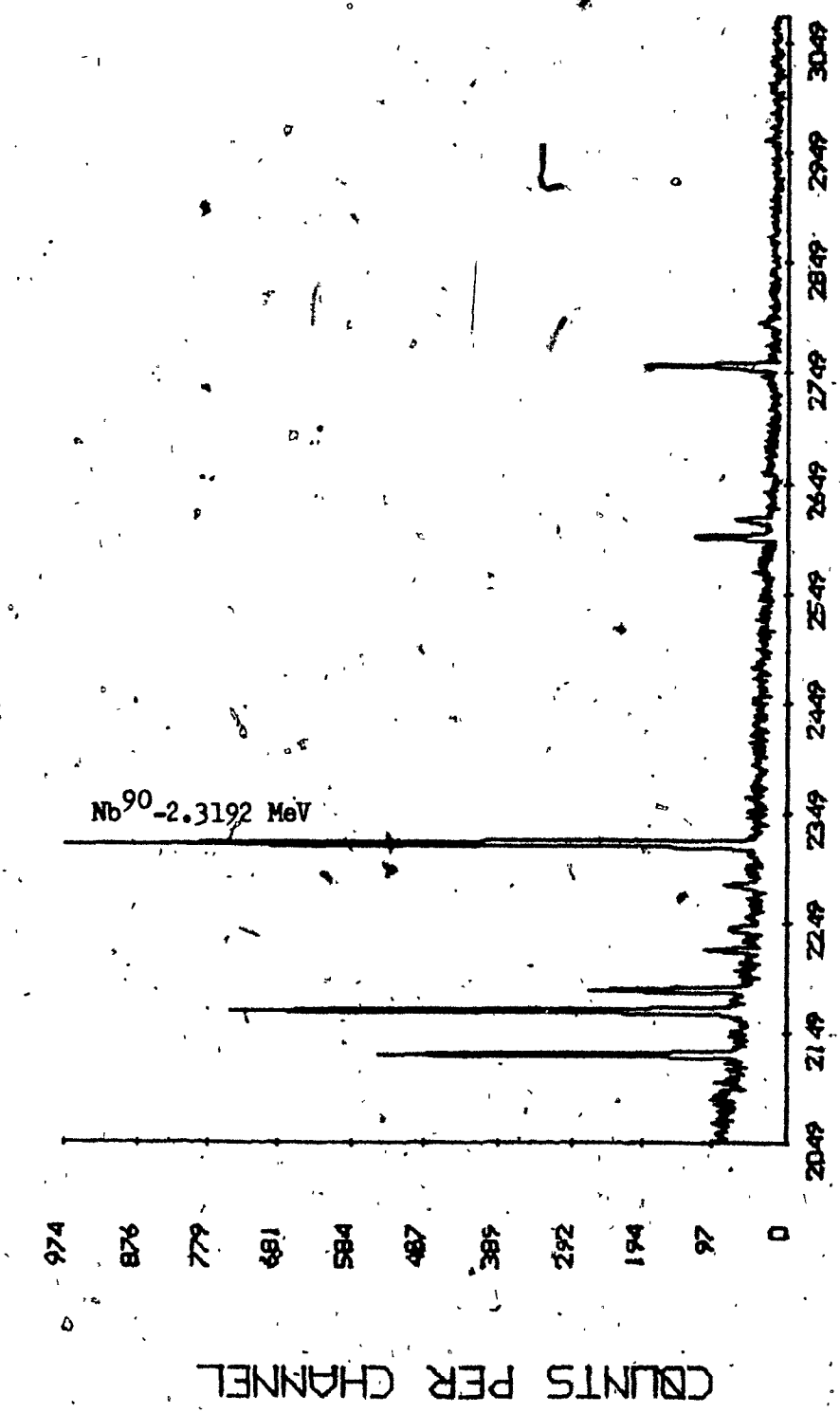
Nb^{90}-2.3192 MeV
COUNTS PER CHANNEL
974
876
779
681
584
487
389
292
194
97
0
2049
2149
2249
2349
2449
2549
2649
2749
2849
2949
3049
CHANNEL NUMBER

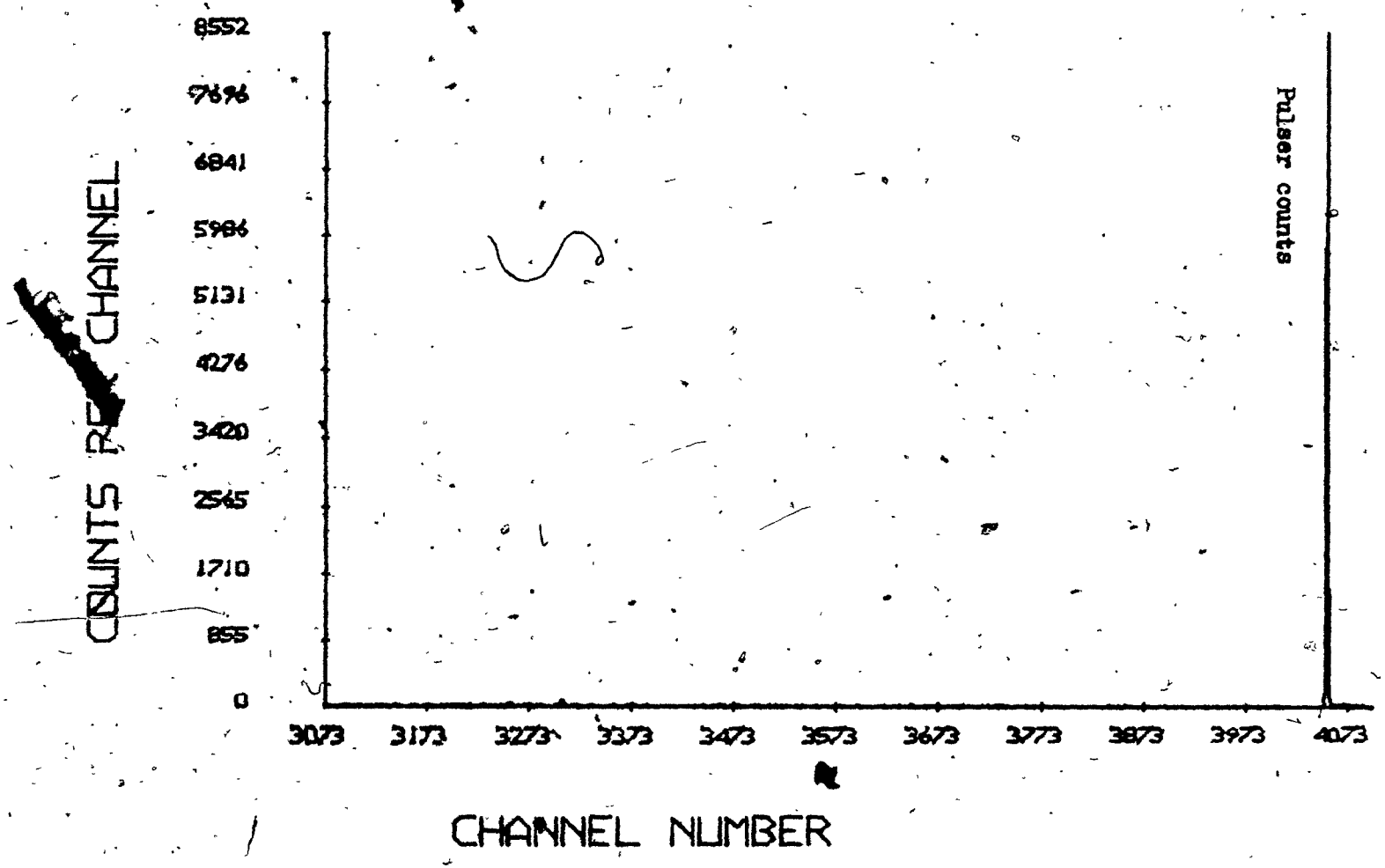
8552
7696
6841
5986
5131
4276
3420
2565
1710
855
0
COUNTS PER CHANNEL
3073
3173
3273
3373
3473
3573
3673
3773
3873
3973
4073
CHANNEL NUMBER
Pulser counts

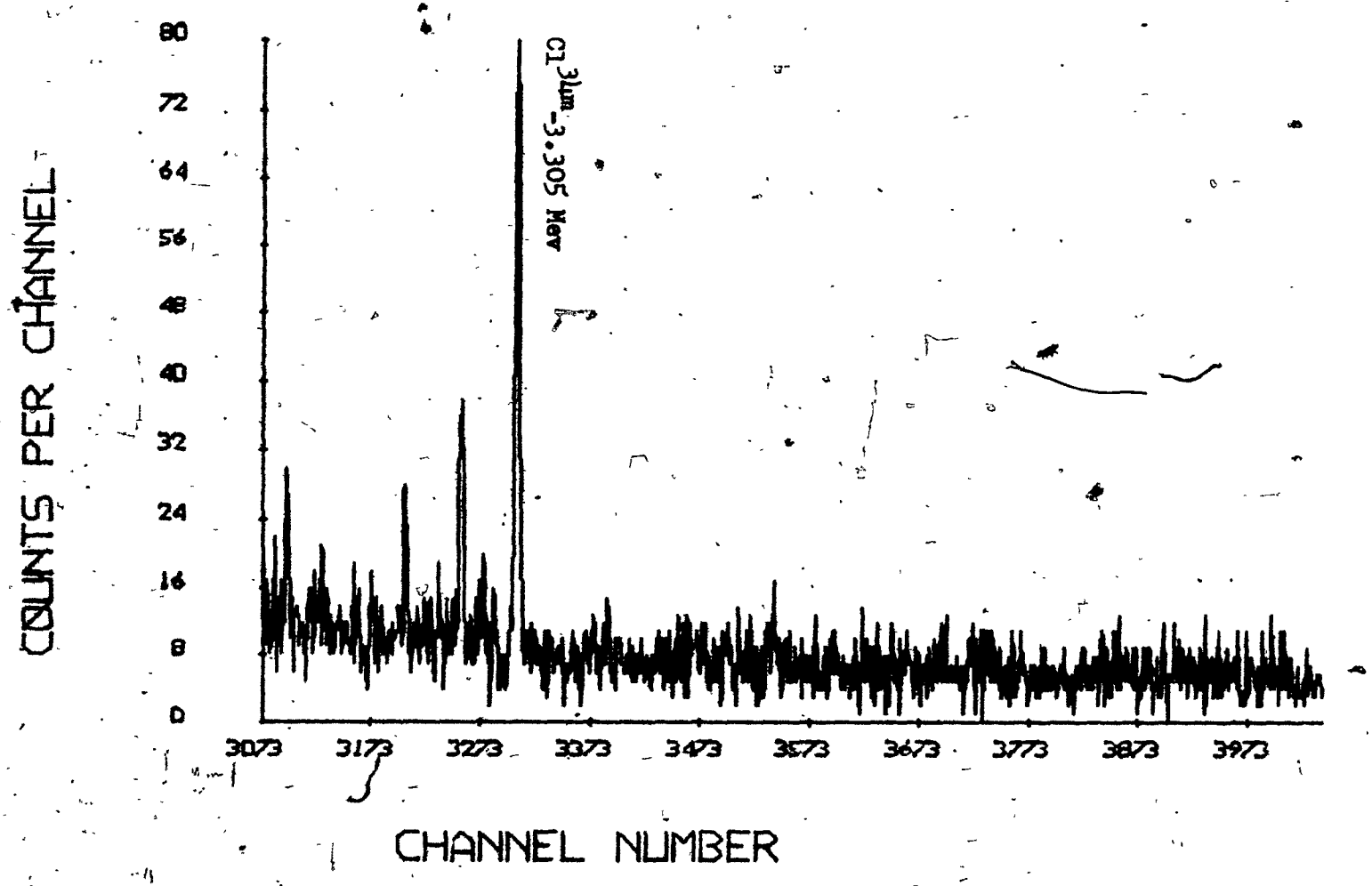
COUNTS PER CHANNEL
80
72
64
56
48
40
32
24
16
8
0
Cl^{34m} -3.305 Mev
3073
3173
3273
3373
3473
3573
3673
3773
3873
3973
CHANNEL NUMBER

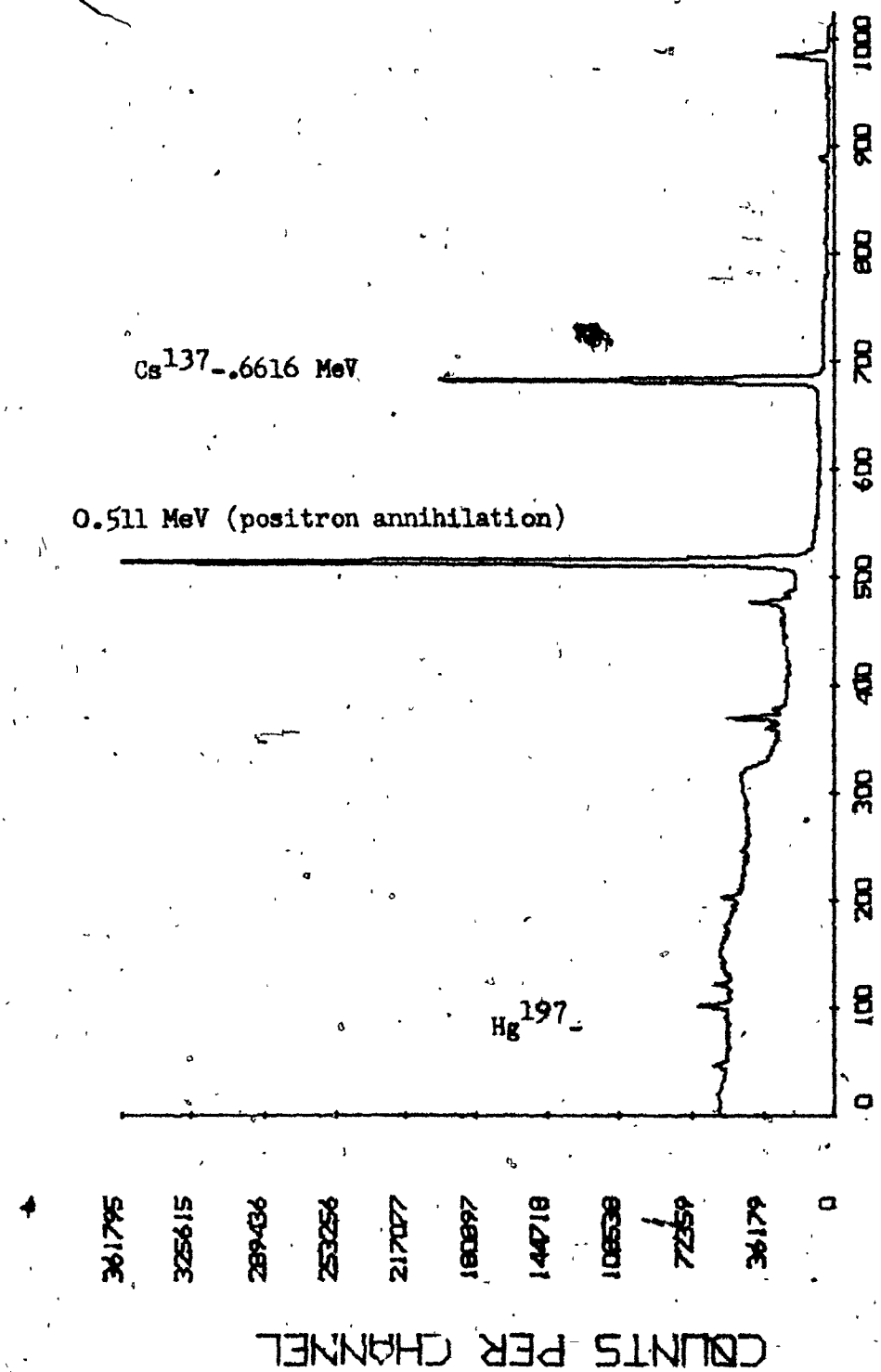

Figure 20. (sand+gold) spectrum.

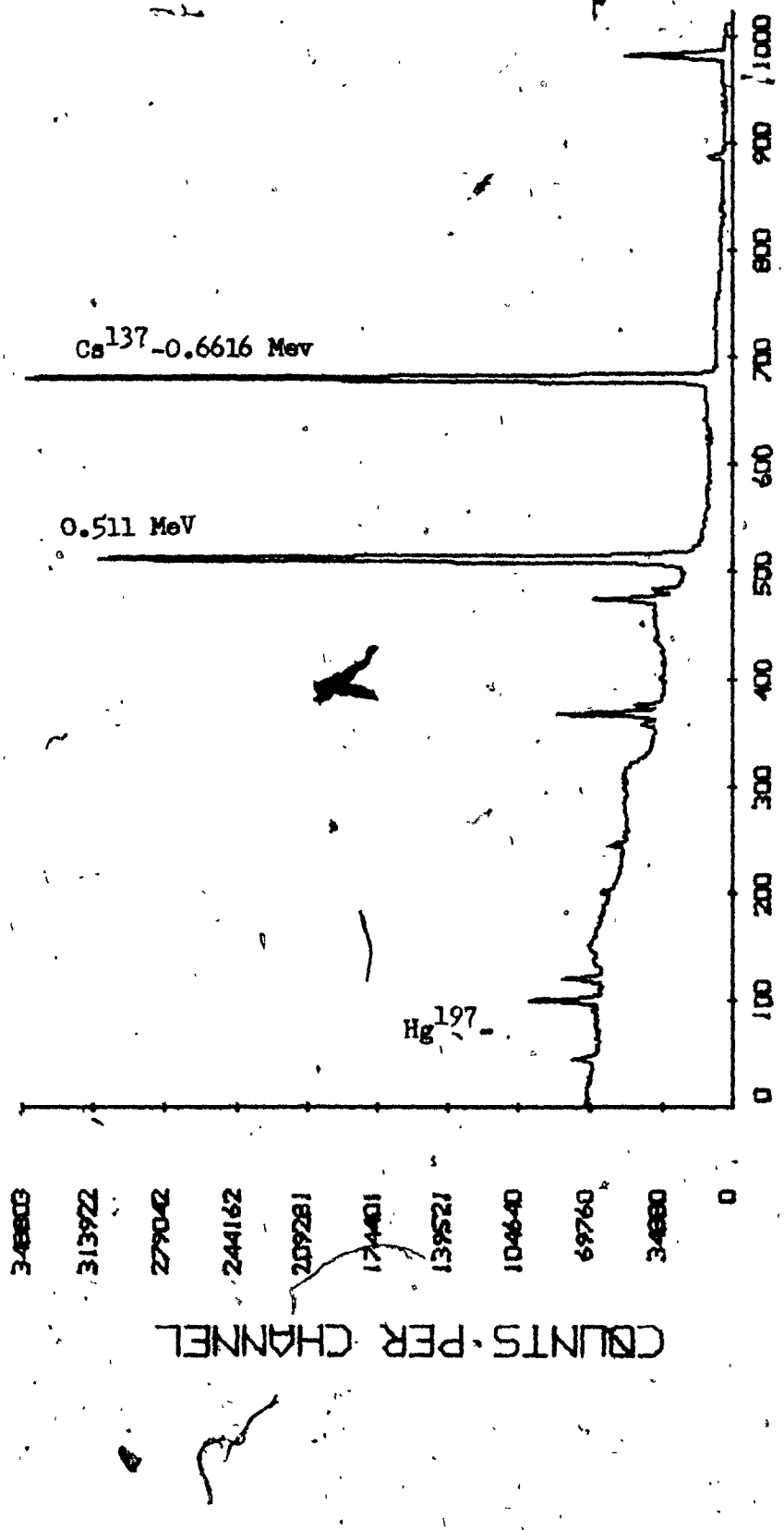

Figure 21. (sand+gold) spectrum.

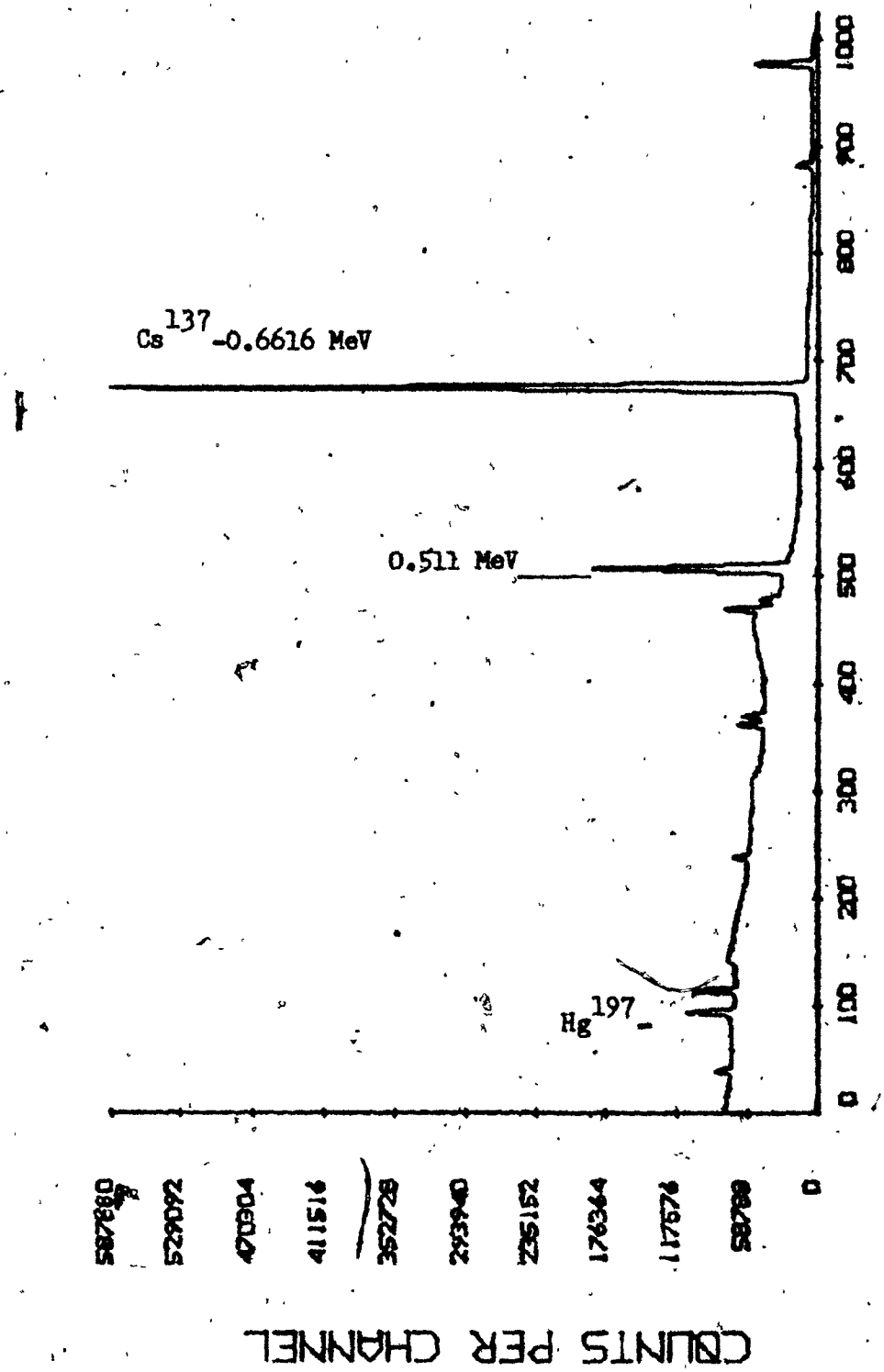

Figure 28. (sand+gold) spectrum.

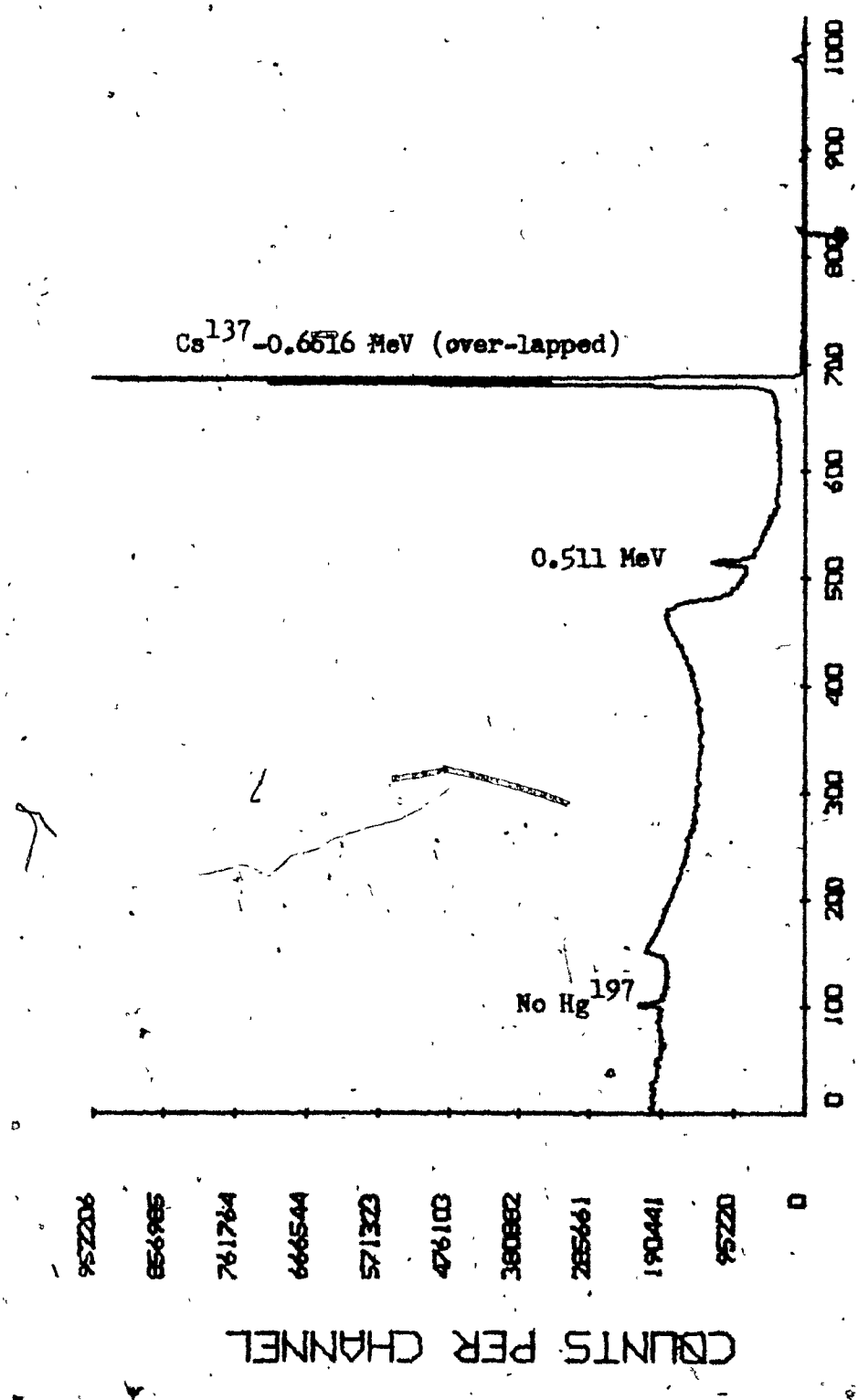

Figure 23. Quartz spectrum (no gold peak).

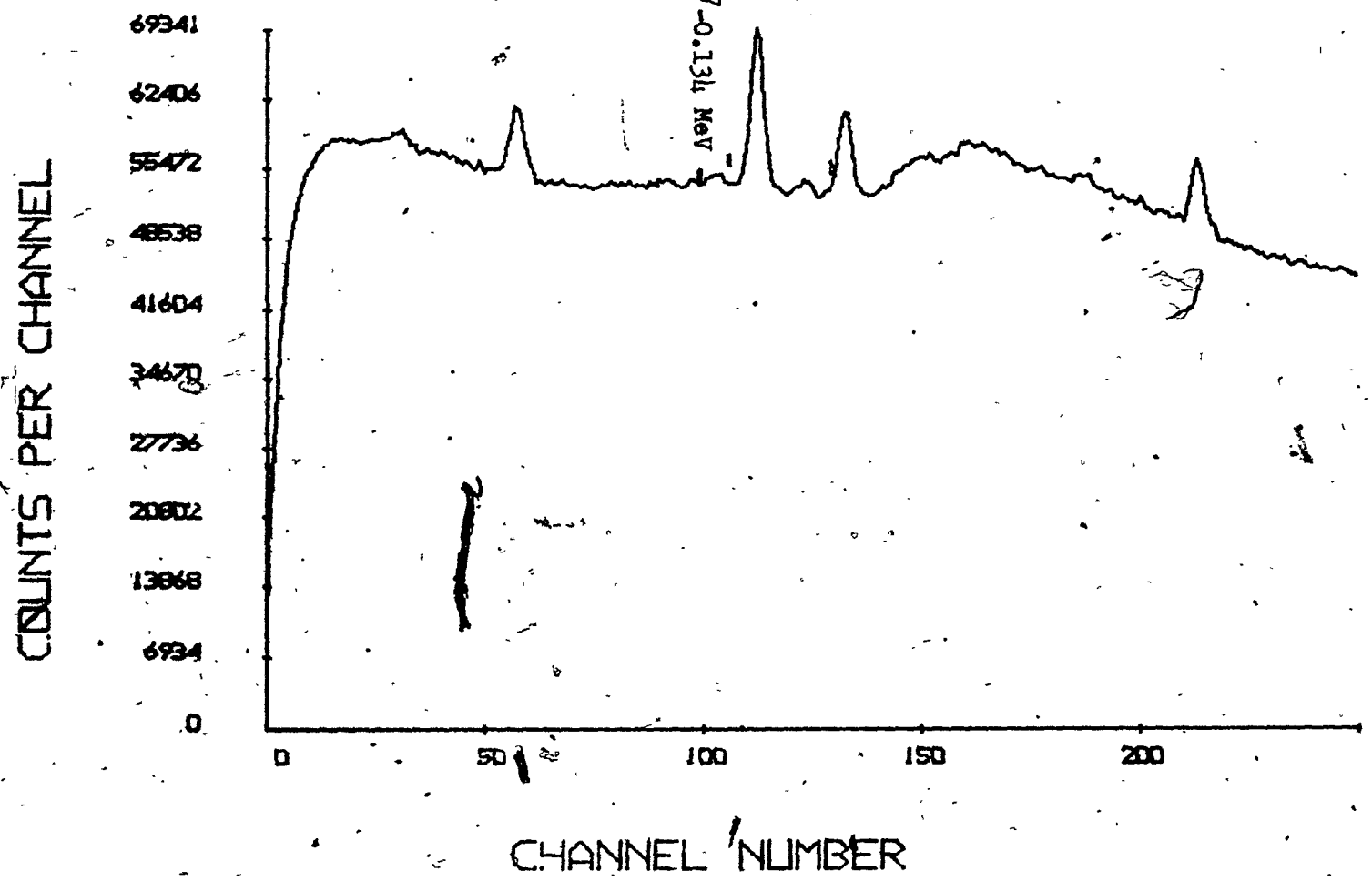

Figure 20a. (figure 20, expanded).

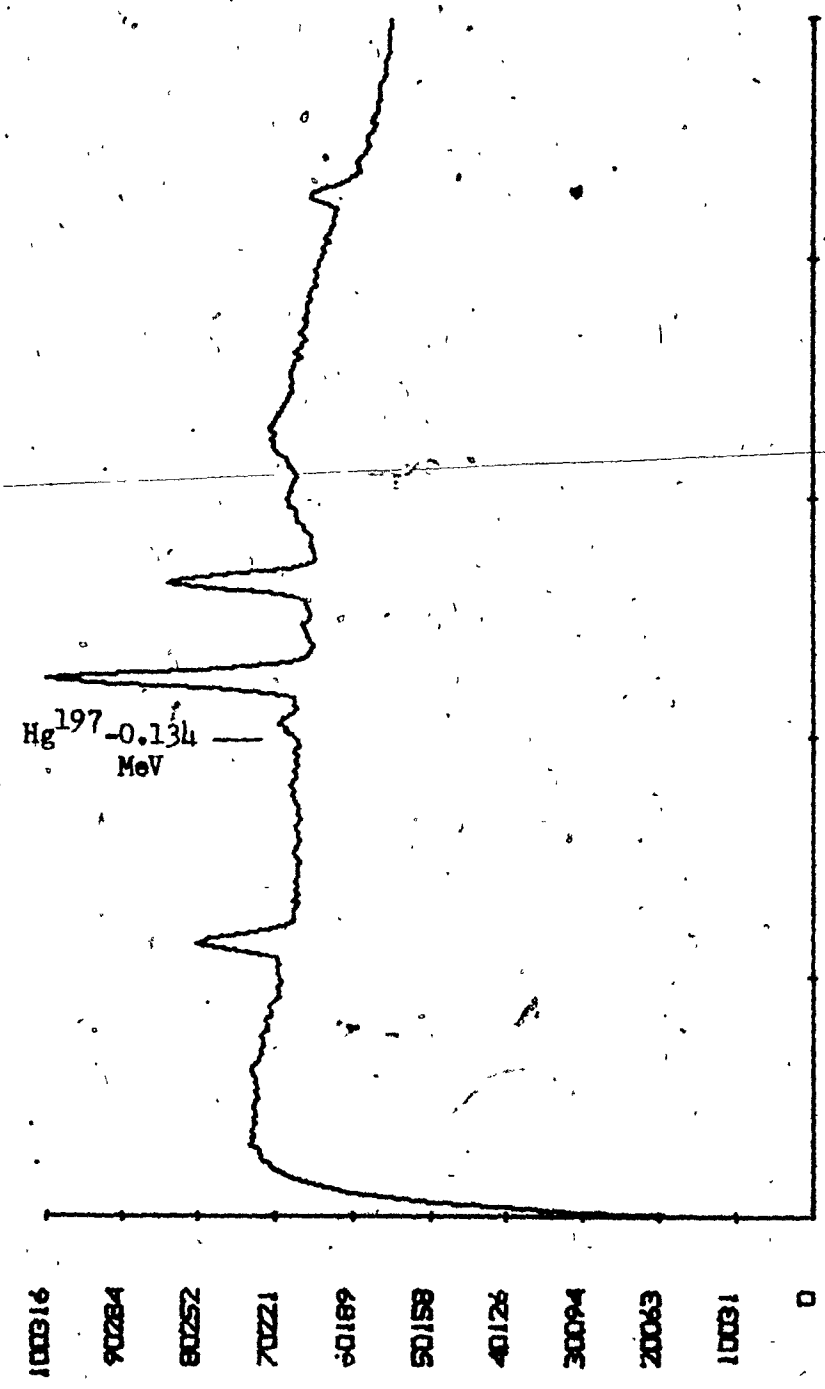

Figure 21a. (Figure 21, expanded).

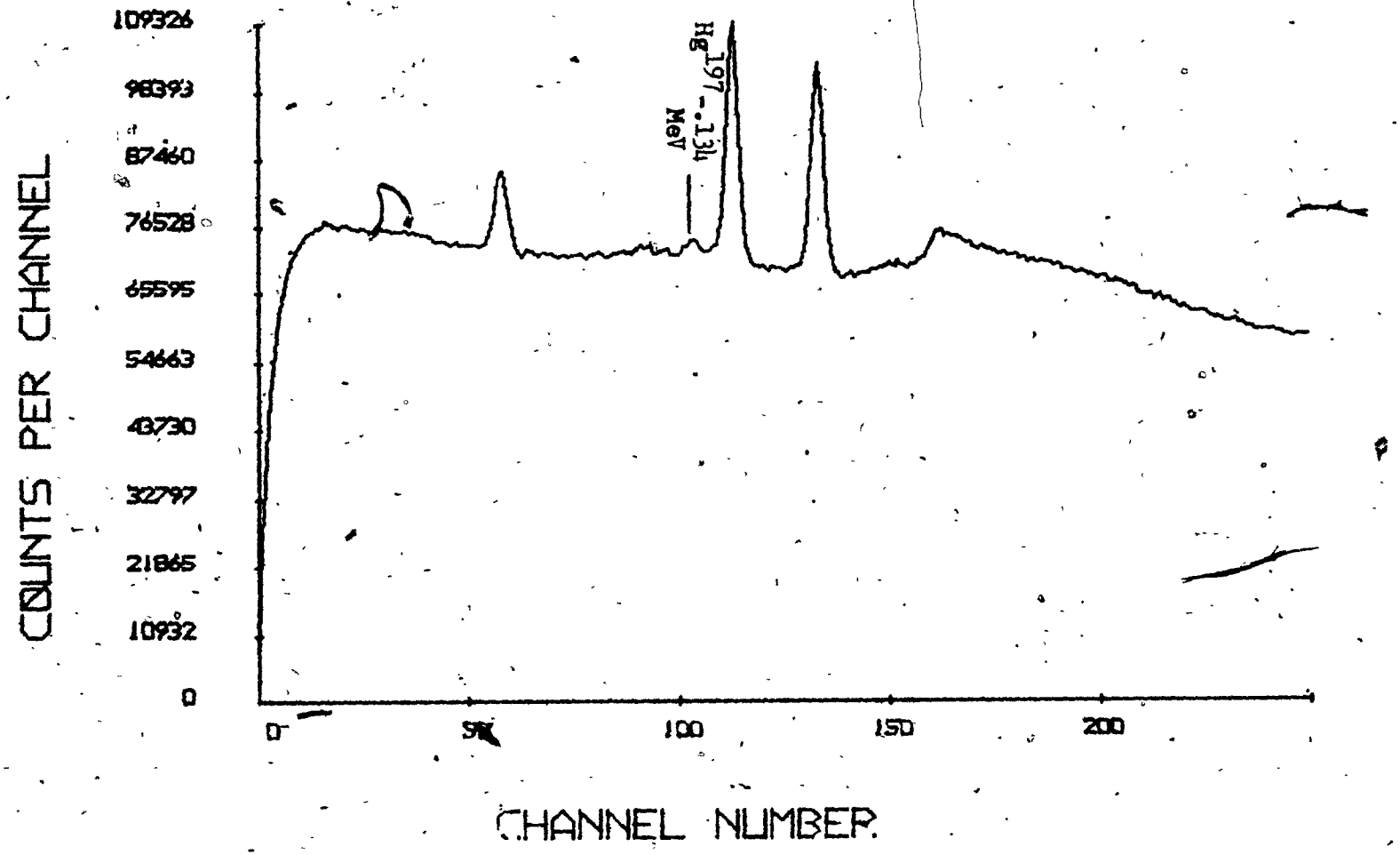

Figure 22a. (figure 22, expanded).

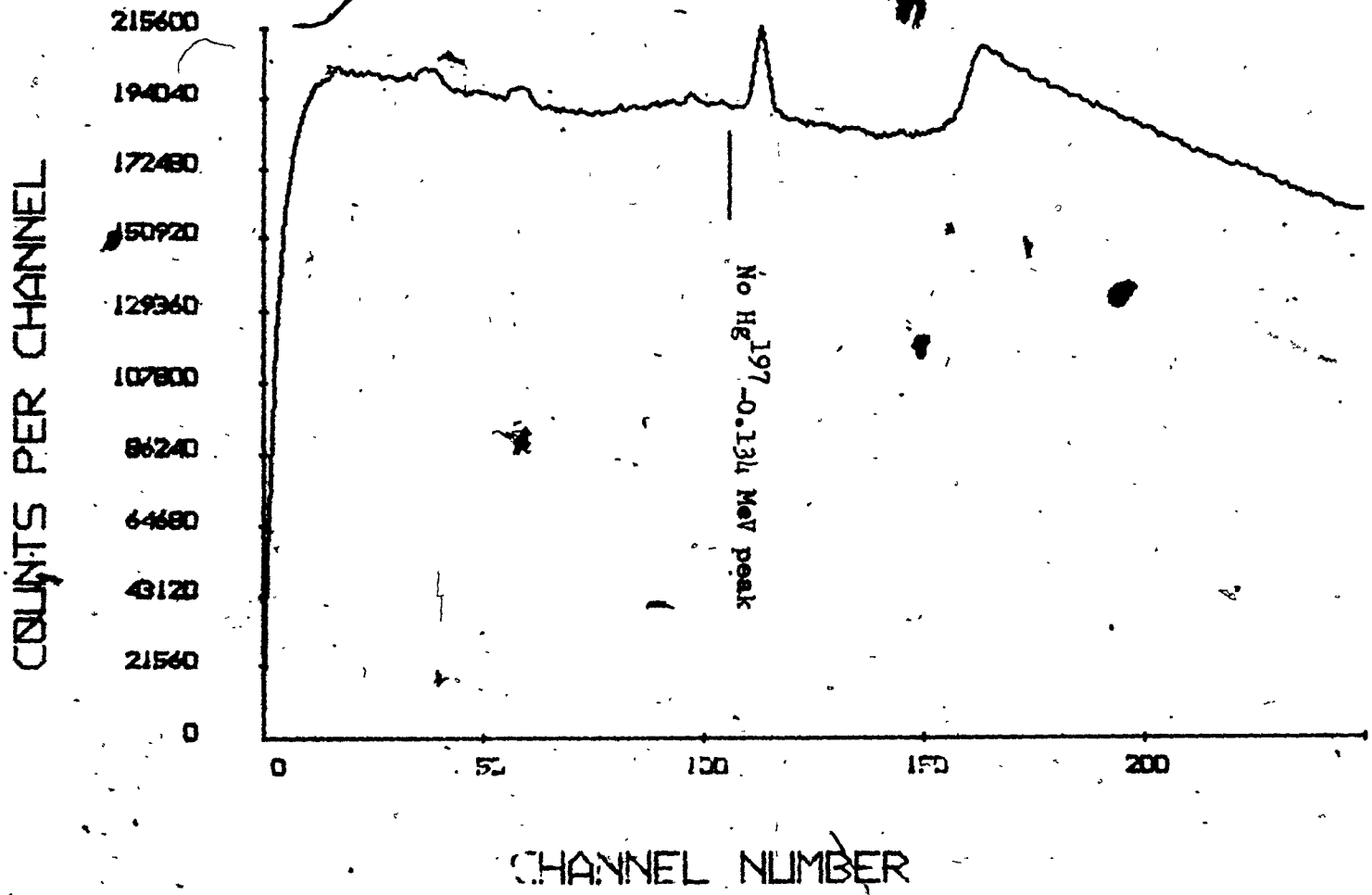

Figure 23a. (figure 23, expanded).

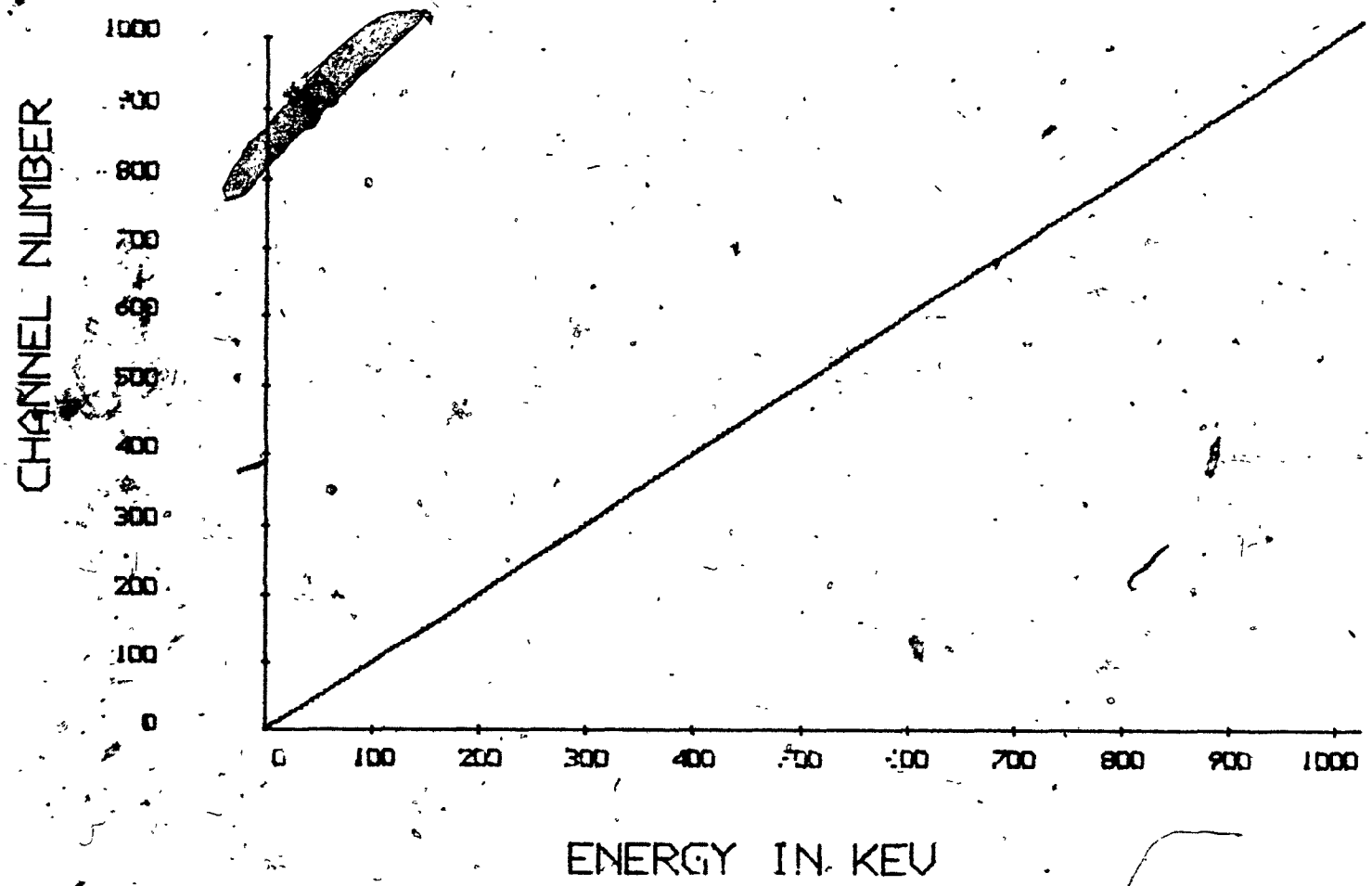

Figure 24. Calibration curve for Au-spectrum.

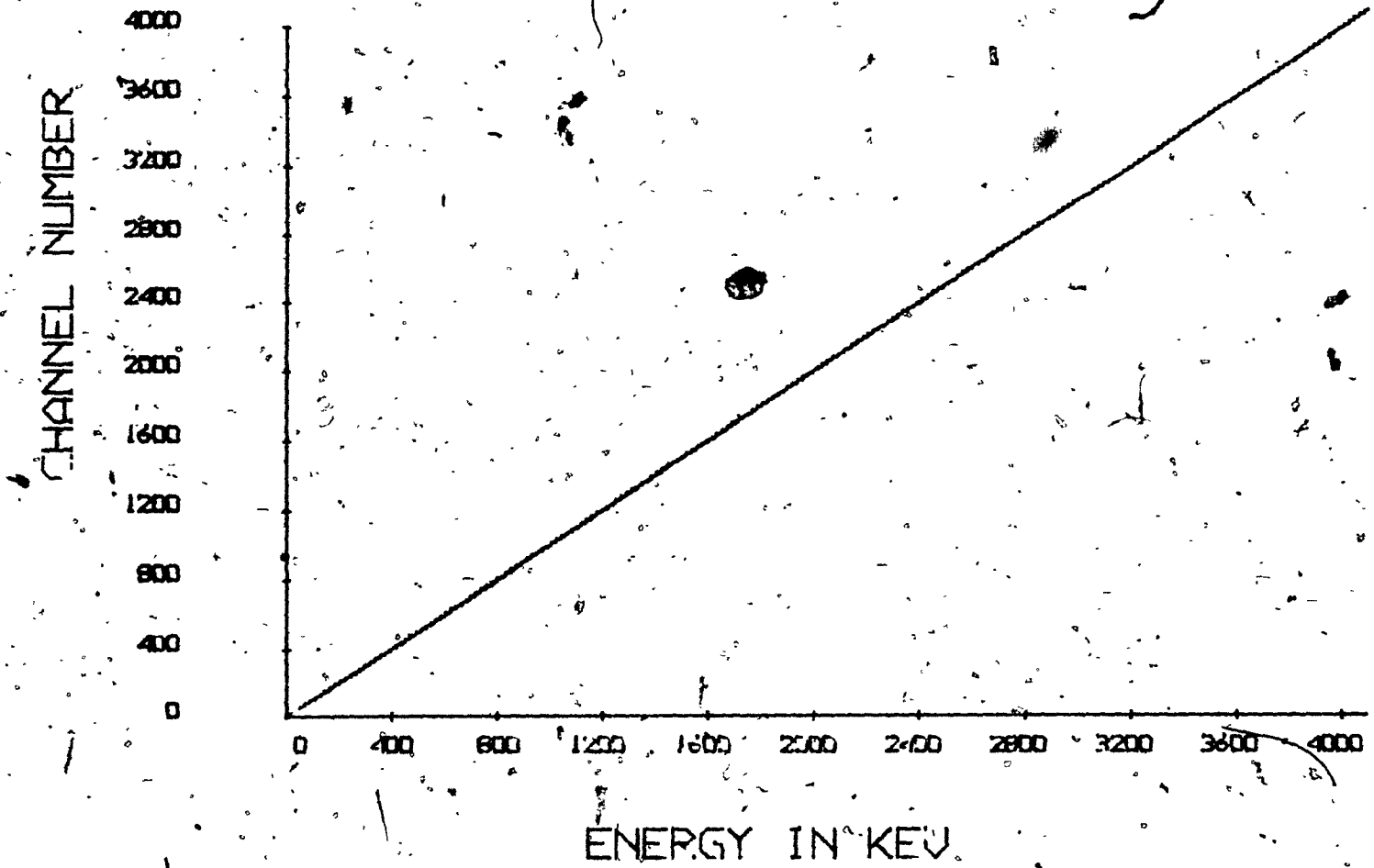

Figure 25. Calibration curve for (sand+gold)-spectrum.

CHAPTER V

RESULTS AND DISCUSSION

V.1 The Activation of Quartz and Sand

The first spectrum of quartz (SiO_2) is of no help in identifying peaks of various elements. It was anticipated. The quartz crystals are composed of mainly Silicon and Oxygen. Both silicon and oxygen have three naturally occuring isotopes in the following abundances:

Si^{28}	92.21%	O^{16}	99.759%
Si^{29}	4.70%	O^{17}	0.037%
Si^{30}	3.09%	O^{18}	0.204%

The (p,n), (p,2n), (p,d) reactions on all of the isotopes of Si give P^{30}, P^{29}, P^{28}, and Si^{27}. All of these radioactive isotopes have half-lives in milliseconds, with the exception of P^{30} (half-life 2.5 minutes). Hence the "cooling-off" period of a few minutes shows no peaks from Si.

Similarly, (p,n), (p,2n), (p,d), etc. reactions on oxygen isotopes yield flourine isotopes of half-lives in seconds, except F^{18} (half-life 109.8 minutes), which is not a gamma emitter.

However, F^{18} is one of the main contributors to the 0.511 MeV peak (annihilation radiation) through positron emission. Besides the 0.511 MeV peak, no other peaks are observed due to oxygen. Therefore, all

the peaks in the pure quartz spectrum are due to the following four sources:

(i) Trace elements or impurities in quartz.

(ii) Impurities in the aluminum sample holder.

(iii) Contamination (while handling the sample or the sample holder)

(iv) Background radiation.

Trace elements present in quartz are Fe, Mg, Al, Ti, Na, B, Ga, Ge, Mn, Zn. It is very difficult to determine the source of an element definitely. It can be present in quartz, or in the sample holder, or in the form of contamination while handling them. At any rate, there were no peaks of reasonably high counts, except the 0.511 MeV, the Compton edge, and the back-scatter of 0.511 MeV, see figure 1.

The next thing was to change the proton energy from 13 MeV to 25 MeV, in order to investigate other reactions which have a higher cross-section at 25 MeV. But again, there are no peaks besides the 0.511 MeV which is stronger this time. See figure 2.

After being certain that from pure quartz there were no peaks of high counts, a sample of sandy loam was irradiated with protons of 25 MeV for a period of 20 minutes. The sample was cooled for three minutes and then counted with a standard Eu^{154} source. The "hot" sand sample was kept 8cm away from the Ge(Li) detector while Eu^{154} was 35cm away. The highest peak was 0.511 MeV due to positron emission and the rest of the peaks were from the standard Eu^{154}, see figure 3. This figure should be compared to the next one, i.e., figure 4 which consists of two

standard sources, namely; Eu^{154} and Co^{60}. As again it was expected, the sand spectrum was not basicly different from the quartz spectrum. See Chapter III for the composition of sand.

The following are the elements which produce 0.511 MeV by emitting positrons: Ga^{63}, Mn^{50m}, Co^{54}, K^{38m}, Sc^{42}, Ti^{43}, Ca^{39}, Ne^{19}, F^{18}, O^{15}, N^{13}, C^{11}, Cl^{34}, B^{8}. At very high energies, i.e. 10-50 MeV, the following nuclear reactions take place: (p,2n), (p,n), (p,p) inelastic, (p,np), (p,2p), (p,α), (p,3n) and (p,t). These reactions are listed in the order of reaction cross-section.

The (p,d) reaction has fairly high cross-section at very high energies. Therefore, there is high probability that $Ca^{40}_{97\%}$ (p,d) Ca^{39}, $O^{16}_{99.7\%}$ (p,d) O^{15}, $N^{14}_{99.6\%}$ (p,d) N^{13}, $C^{12}_{98.89\%}$ (p,d) C^{11} and $Cl^{35}_{75\%}$ (p,d) Cl^{34}. We know that all these elements are present in sand. Therefore, the above reactions are the cause of the high counts from 0.511 MeV peak.

The half-lives of the above positron emitters are as follows:

Radionuclide	Half-life
Ca^{39}	87 sec.
O^{15}	122 sec.
N^{13}	10 min.
C^{11}	20 min.
Cl^{34}	1.53 sec.

But F^{18} has a half-life of 109 minutes. Hence, it is the main positron emitter after a few hours of cooling off period.

V.2 Identification of Peaks from the Spectrum of the (p,xn) Reactions of Au^{197}

It was necessary to irradiate gold and identify the peaks to facilitate recognition of the peaks due to the nuclear reaction of gold. Figures 5 , 6 , 7 , 8 and 9 all belong to one spectrum of nuclear reactions caused by irradiating pure gold (99.99%) with protons of 20 MeV for 5 minutes.

The reaction Au^{197} (p,2n) Hg^{196} does not give gammas because Hg^{196} is stable. The reaction Au^{197} has half-lives: 64.1 hours and 23.8 hours (meta-stable). There is delayed radiation of 0.077 MeV and over-laps with X-rays due to the Au $K_{\beta 1}$. From meta-stable Hg^{197} there is gamma radiation of .1339 MeV (isomeric transition). The third radiation of highest abundance is .279 MeV. Hg^{197} decays back to Au^{197}.

The reaction Au^{197} (p,d) Au^{196} gives a set of gamma radiations. Au^{196} has a half-life of 6.18 days and a meta-stable state which has a half-life of 9.7 hours. Au^{196} gives three clear peaks for energies 0.356 MeV; 0.333 MeV and 0.426 MeV and decays to Pt^{196}. The gamma emission is not the only mode of decay of the 9.7 hour meta-stable state. It also decays by emitting positrons and capturing electrons. The Pt^{196} X-rays ($K_{\alpha 1}$) of .0668 MeV can be seen in figure 5 .

The third reaction is a combination of two competing reactions, namely; Au^{197} (p,3n) Hg^{195} (Hg^{195} decays to Au^{195}) and Au^{197} (p,t) Au^{195}. Hg^{195} has a half-life of 9.5 hours and also it has an isomeric state which has a half-life of 40 hours. Through a (p,3n) reaction of Au^{197},

we get Hg^{195} which, after the emission of characteristic gamma-rays, decays to Au^{195} (half-life 184 days). But through a (p,t) reaction, we again get Au^{195} but (it has an isomeric state of half-life of 30.5 seconds) this time it can decay to Pt^{195}.
Pt^{195} characteristic X-rays $K_{\alpha 1}$ and $K_{\beta 1}$ can be seen in figure 5.

It is interesting to take notice of the fact that Au^{197} (p,3n) Hg^{195} and Au^{197} (p,t) Au^{195} reactions are observed using protons of only 20 MeV. The threshold for this reaction is $E_{th} = (1 - \frac{M_p}{M_{Au197}}) \cdot |Q|$, where the Q-value (the mass difference of the reactants multiplied by c^2) is -6.265 MeV. A greater yield of (p,3n) and (p,t) reactions could be realized at higher proton energies, but it was desired to keep the spectra as simple as possible.

A summary of these reactions would be appropriate. There are no other gold isotopes which are stable in nature except Au^{197}.

Reaction	Q-value [13] in MeV
(i) Au^{197} (p,2n) Hg^{196}	-8.178
(ii) Au^{197} (p,n) Hg^{197}	-1.197
(iii) Au^{197} (p,p) Au^{197}	0.00
(iv) Au^{197} (p,d) Au^{196}	-5.855
(v) Au^{197} (p,2p) Pt^{196}	-5.815
(vi) Au^{197} (p,α) Pt^{194}	8.437
(vii) Au^{197} (p,3n) Hg^{195}	-16.930
(viii) Au^{197} (p,t) Au^{195}	-6.265

A (p,4n) is not possible as the Q-value for the reaction is -23.984 MeV.

Therefore, while irradiation is going on, the reactions are producing Au^{197}, Hg^{196}, Pt^{196}, Pt^{195} and Pt^{194}. If this process continued for a long time, all of the gold will be transmuted into Mercury and Platinum.

V.3 The Irradiation of Sand

Figures 10, 11, 12, 13 and 14 show the spectrum of sand doped with gold, irradiated with protons of 20 MeV for 10 minutes. After 5 minutes of "cooling-off" period, it was counted. There is hardly anything but the 0.511 MeV peak and associated with it, the Compton edge and the back-scatter.

The same sample was taken out of the aluminum tubing and after 26 hours of "cooling-off", it was recounted. Figures 10a and 12a show the spectrum where many more peaks have appeared and the 0.511 MeV peak has a very low count.

The second sand sample was irradiated similarly to the first one, but was allowed to "cool-off" for 25 minutes and then counted for 25 minutes. This is an interesting spectrum. Many elements are identified here. Also a peak of .134 MeV can be seen which is due to Au^{197} (p,n) Hg^{197} reaction. See figures 15, 16, 17, 18 and 19. Many of the peaks are sum-peaks, single escape, and double escape peaks.

The most easily detected elements were iron, calcium, copper, gold (which was added), and nickel.

V.4 The Final Run

As mentioned before, in Chapter IV, the first run was made with three samples of sand doped with gold of different concentrations. They were all irradiated with the same energy and for the same time. The sample with the highest concentration was counted first. Very soon there was a peak of 0.134 MeV. The next highest concentrated sample was counted for 3 hours and there was a peak which was reasonably Gaussian. The third sample was counted after a "cooling-off" period of 26 hours. This was the least concentrated of the samples and also the activity had gone down. 26 hours of "cooling-off" is more than one half-life of Hg^{197} (23.8 hours).

The three spectra are shown in figure 21 (4000 ppm), figure 22 (400 ppm), and 23 (40 ppm). Due to the high counts from the 0.511 MeV peak, the Hg^{197} peak cannot be seen in these plots. Therefore, the regions which contain 0.134 MeV peaks were expanded and now they can be clearly identified. See figures 21a, 22a, and 23a.

It is interesting to notice the relationship between the 0.511 MeV peak and the Cs^{137} - 0.662 MeV peak. Cs^{137} peak height remained the same whereas 0.511 MeV went down. Similarly, other peaks of shorter half-lives show less activity. These facts noted on the computer outputs (SPEC) can be easily checked and confirmed from the plots of the spectra.

CHAPTER VI

CONCLUSION

The activation technique used in this project can be improved and applied in many fields.

A few important suggestions are made to determine the sensitivity of the system of gamma-ray spectroscopy by activation of gold in a sand matrix:

(i) the proton energy should be reduced to 15 MeV to enhance the yield of Hg^{197}. As it can be seen that with protons of 20 MeV (p,3n) reaction is taking place. The Q-value for (p,3n reaction is approximately -17 MeV. Therefore, the protons of 15 MeV cannot produce Hg^{195}.

(ii) The irradiation time should be increased greatly. Activity generated is:

$$At = \frac{N_A m}{M_A} f \sigma \Theta \left(1 - e^{-\lambda t}\right) \quad \text{counts per second.}$$

where N_A = Avogadro's number

m = sample mass

M_A = atomic weight of sample

f = irradiation flux (number/m^2/sec)

σ = cross-section

Θ = isotopic abundance

λ = decay constant

t = irradiation time

Since $\lambda = \frac{0.693}{T}$, T is the half-life of the radionuclide;

in case of Hg^{197}, T approximately 24 hours.

Ideally the irradiation time should be about 12 hours. But irradiation for 1 hour would greatly increase the activity.

(iii) A longer cooling-off time should be allowed, so that the counts from short lived radionuclides could be decreased.

(iv) The sample should be taken out of the aluminum tubing. It has two-fold advantages; one, the counts from the irradiated impurities in the aluminum tubing would be diminished and two, fewer positrons will be annihilated. In consequence the counts in the (peak) 0.511 MeV will be much less.

(v) The counting time should be considerably increased.

If these suggestions are followed, it can be expected that as little as 0.01 ppm gold can be detected.

The same technique can be used in many situations; for example: to detect arsenic in fish or mercury in lakes and fish. The only requirement is that the sample be dried, to prevent catastrophic effects due to beam heating of the sample.

It has many obvious geological, agricultural applications as well.

REFERENCES

(1) Hevesy, von G., and Levi, H., Kgl. Danske Vidensk. Selskab. Math. Fys. Medd. 14 (5), (1936); 15 (11), (1938).

(2) Rommel, H., Schade, H., Sobbi, A., and Marimer, P., Kerenergie 5, 859 (1962).

(3) Pierce, T.B., Peck, P.F., and Henry, W.M., The Analyst 90,339 (1965).

(4) Lederer, C.M., Hollander, J.M., and Perlman, I., Table of Isotopes, 6th ed., John Wiley, New York, 1967.

(4a) Bowman, W.W., and Macmurdo, K.W., Radioactive-decay Ordered by Energy and Nuclide. Atomic Data and Nuclear Data Tables 13, 2-3, 1974.

(5) Rose, M.E., Internal Conversion Coefficients, North Holland Amsterdam, 1958.

(6) Milner, W.T., Nuclear Physics 74,281 (1965).

(7) Murray, G., Nuclear Physics 63, 353, (1965).

(8) Friedlander, G., Kennedy, J.W. and Miller, J.M., Nuclear and Radiochemistry, John Wiley & Sons, Inc.

(9) Ricci, E. and Hahn, R.L., Analytical Chemistry, 40, 54.

(10) Grodstein, G.W., Nat. Bur. Stand., 1003 (1954).

(11) Condon, E.U. and Odishaw, H., Handbook of Physics, McGraw Hill.

(12) Velenfkee, D.G., Pouvovedenee, Moscow, 1957. Israel Program for Scientific Translation, 1957.

(13) Grove, N.B., and Wapstra, A.H., Q-values, Nuclear Data Tables, Vol. 11, nos. 2 and 3, Nov. 1972.

BIBLIOGRAPHY

(1) Siegbahon, Kai, Alpha-, Beta- and Gamma-ray Spectroscopy, Vol. 1 and Vol. 2, North-Holland Publishing Company, Amsterdam.

(2) Lenihan, J. M. A., Thomson, S. J., Advances in Activation Analysis, Vol. 1 and Vol. 2, Academic Press, London and New York.

(3) Fremlin, J. H., Applications of Nuclear Physics, Hart Publishing Company, Inc., New York City.

(4) Quittner, P., Gamma-ray Spectroscopy, Adam Hilger Ltd., London.

(5) Lyon, William S., Guide to Activation Analysis.

(6) Crouthamel, C. E., Adams, F. and Dams, R., Applied Gamma-ray Spectroscopy, Pergamon Press.

(7) Condon, E. U. and Odishaw, Hugh, Handbook of Physics, McGraw-Hill Book Company, Inc.

(8) Hoste, J., Op de Beeck, J., Gijbels, R., Adams, F., van den Winkel, P. and de Soete, D., Activation Analysis, London, Butterworth's.

APPENDIX

The following computer programs were used for data transferring, analysis and spectra plotting:

(1) MCGILL

(2) REFORM

(3) SPEC

(4) PLOTAK

(5) CALIB

```
REQUEST,TAPE8,F=B,C=800. INPUT 24283 EDDY FOR MCGILL TAPE..
REWIND AND SAVE MCGILL DATA UNDER SOME FNAME.
XFOR,OLD,REFORM FOR PROGRAM TO REFORMAT DATA IN FNAME.
GET,TAPE1=FNAME AND RNH.
AT "READY" REWIND AND SAVE TAPE2= ? .
OLD,MCGILL AND GET,TAPE2= ? AND RNH.
DATA IN FORMAT(1017) WILL BE IN TAPE3=MCGIOUT.

PROGRAM MCGILL(TAPE2,TAPE3,OUTPUT)
DIMENSION IY(1024)
100 FORMAT(1018)
150 FORMAT(1017)
N=1024
READ(2,100)(IY(I),I=1,N)
WRITE(3,150)(IY(I),I=1,N)
ENDFILE 3
REWIND 3
CALL REPLACE(5HTAPE3,7HMCGIOUT,0,0)
END

READY.
```

```
PROGRAM REFORM(TAPE1,TAPE2)
DIMENSION L(8)
REWIND 1
REWIND 2
10 CALL CREADW(5LTAPE1,L,8,IS,IC)
IF(IS.EQ.-3)GOTO 99
IF(IS.EQ.-2)GOTO 99
IF(IS.EQ.-1)GOTO 10
WRITE(2,100)L
100 FORMAT(8A10)
GOTO 10
99 ENDFILE 2
END
```

READY.

```
"RNH" IMMEDIATELY.  SPEC OBTAINS PROGRAM DATA FROM "DATA".
FOR PLOT2, DELETE LINE 2550 TO SUPPRESS COMPARISON OUTPUT.

      PROGRAM SPEC(INPUT,TAPE1,TAPE2,TAPE3,OUTPUT)
      DIMENSION X(2048),Y(2048),YC(2048),PX(2048),XC(300)
      DIMENSION XFWHM(300),XCHI-SQ(300),XXMUO(300),XCO(300)
      DIMENSION XA(300),XVARI(300),AR(300),XB(300),N0(300)
      DIMENSION IY(2049),PU(2048),R(2048)
  100 FORMAT(/6X,F4.1,I5)
  101 FORMAT(3A10)
  102 FORMAT(A7,I1)
  105 FORMAT(*DURATION*2X16,1X*SEC*)
  114 FORMAT(*SKIPPED*I3* LINE(S) OF SPECTRUM*)
  115 FORMAT(*ENTER SPECTRUM "NAME,ISKIP,XNI". ISKIP=# LINES TO
     * SKIPPED IN SPECTRUM FILE.*/*  ISKIP=2 IF TIMING IN CHANNEL
     *' XNI=  #.CHANNELS TO BE ADDED TO XMUO.*/)
  116 FORMAT(/*ANALYSIS OF *A7*GOES INTO SPECOUT*)
  120 FORMAT(10I7)
  125 FORMAT(//1X,*TOTAL COUNTS*,F15.)
  150 FORMAT(10F7.0)
  151 FORMAT(* TOTAL PEAKS FITTED*,I5)
  152 FORMAT(1X*PEAKS DROPPED*5XI5)
  153 FORMAT(1X*NET PEAKS LISTED*2XI5)
  154 FORMAT(2E8.1)
  155 FORMAT(F4.0,F7.0,2F10.3)
  156 FORMAT(19X,F13.3,11X,F13.3)
  157 FORMAT(/1X*X(I)*2X*Y(I)*4X*PU(I)*4X*R(I)*)
  160 FORMAT(2X,*YC =*,F11.3,* + *,F11.3,* X*)
  575 FORMAT(9(/6XI4))
  800 FORMAT(//2X,*N0*,8X,*FWHM*,6X,*CHISQ/VARI*,6X,*XMUO*,3X,
     *COUNTS/AREA*,8X,*CO*)
  810 FORMAT(/I4,F13.3,F13.8,3F13.3)
      CALL GET(5HTAPE1,4HDATA,0,0)
      READ(1,100) SIGMAO,N
      SIGI=SIGMAO
      NM1=N+1
      NM2=N-1
      READ(1,575)NL1,NL2,NP1,NP,NP2,NR1,NR2,N1,N2
      SUMY=0.
      K=0
      L=0
      MQ=1
       PRINT 115
      READ,FNAME,ISKIP,XNI
       NI=XNI
       CALL GET(5HTAPE2,FNAME,0,0)
      PRINT 116,FNAME
      PRINT 114,ISKIP
       IF(ISKIP.EQ.1)GO TO 22
```

```
      IF(ISKIP.EQ.0)GO TO 39
      READ(2,120)(IY(I),I=1,NM1)
      PRINT 120,(IY(I),I=1,NM1,100)
      REWIND 2
      WRITE(2,105)IY(1)
      DO 10 J=2,NM1
      K=K+1
      IF(J.EQ.1025)GO TO 19
      IY(K)=IY(J)
      GO TO 10
   19 K=K-1
   10 CONTINUE
      WRITE(2,120)(IY(K),K=1,NM2)
      DO 28 I=1,NM2
      Y(I)=IY(I)
   28 CONTINUE
      ENDFILE 2
      REWIND 2
      CALL REPLACE(5HTAPE2,FNAME,0,0)
      GO TO 90
   22 READ(2,101)
   39 READ(2,150)(Y(I),I=1,NM2)
   90 DO 30 I=NL1,NM2
      X(I)=I
      SUMY=SUMY+Y(I)
   30 CONTINUE
      WRITE(3,125)SUMY
      M=NL2-NL1+NR2-NR1+2
   83 XSUM1=0.
      DO 40 I=NL1,NL2
      XSUM1=XSUM1+X(I)
   40 CONTINUE
      XSUM2 =0.
      DO 41 I=NR1,NR2
      XSUM2=XSUM2+X(I)
   41 CONTINUE
      XSUM=XSUM1+XSUM2
      YSUM1=0.
      DO 42 I=NL1,NL2
      YSUM1=YSUM1+Y(I)
   42 CONTINUE
      YSUM2=0.
      DO 43 I=NR1,NR2
      YSUM2=YSUM2+Y(I)
   43 CONTINUE
      YSUM=YSUM1+YSUM2
      XYSUM1=0.
      DO 44 I=NL1,NL2
      XYSUM1=XYSUM1+X(I)*Y(I)
   44 CONTINUE
```

```
      XYSUM2=0.
      DO 45 I=NR1,NR2
      XYSUM2=XYSUM2+X(I)*Y(I)
   45 CONTINUE
      XYSUM=XYSUM1+XYSUM2
      XXSUM1=0.
      DO 46 I=NL1,NL2
      XXSUM1=XXSUM1+X(I)**2
   46 CONTINUE
      XXSUM2=0.
      DO 47 I=NR1,NR2
      XXSUM2=XXSUM2+X(I)**2
   47 CONTINUE
      XXSUM=XXSUM1+XXSUM2
      B=(M*XYSUM-XSUM*YSUM)/(M*XXSUM-XSUM**2)
      A=(YSUM-B*XSUM)/M
      COUNTS=0.0
      DO 48 I=NL1,NR2
      YC(I)=Y(I)-A-B*X(I)
      IF(I.LT.NL2.OR.I.GT.NR1)GO TO 48
      COUNTS=COUNTS+YC(I)
   48 CONTINUE
      CO=YC(NP)
      XMUO=X(NP)
      SIGMAO=SIGI
      J=1
   15 B1=0.0
      B2=0.0
      B3=0.0
      A11=0.0
      A12=0.0
      A13=0.0
      A22=0.0
      A23=0.0
      A33=0.0
      DO 20 I=NP1,NP2
      XI=X(I)
      YCI=YC(I)
      ARG=(XI-XMUO)**2/(2.0*SIGMAO**2)
      AA=CO*(XI-XMUO)**2/SIGMAO**3
      BB=CO*(XI-XMUO)/SIGMAO**2
   18 DPDC=EXP(-ARG)
      DPDSIG=AA*EXP(-ARG)
      DPDMU=BB*EXP(-ARG)
      PXI=CO*EXP(-ARG)
      PX(I)=PXI
      RI=PXI-YCI
      A11=A11+DPDC**2
      A12=A12+DPDSIG*DPDC
      A13=A13+DPDMU*DPDC
```

```
      A22=A22+DPDSIG**2
      A23=A23+DPDMU*DPDSIG
      A33=A33+DPDMU**2
      B10=-RI*DPDC
      B20=-RI*DPDSIG
      B30=-RI*DPDMU
      B1=B1+B10
      B2=B2+B20
      B3=B3+B30
   20 CONTINUE
      A21=A12
      A31=A13
      A32=A23
      A111=A22*A33-A32*A23
      A222=A12*A33-A32*A13
      A333=A12*A23-A22*A13
      DELTA=A11*A111-A21*A222+A31*A333
      TEST=.00000001
      IF(DELTA.LT.TEST)GO TO 86
      DELC=-(B1*A111-B2*A222+B3*A333)/DELTA
      B111=B2*A33-B3*A23
      B222=B1*A33-B3*A13
      B333=B1*A23-B2*A13
      DELSIG=(A11*B111-A21*B222+A31*B333)/DELTA
      C111=A22*B3-A32*B2
      C222=A12*B3-A32*B1
      C333=A12*B2-A22*B1
      DELMU=(A11*C111-A21*C222+A31*C333)/DELTA
      IF(DELSIG)1,1,2
    1 DELTS=-DELSIG
      GO TO 3
    2 DELTS=DELSIG
    3 TEST=0.00001
      AXE=50.0
      IF(DELTS-AXE)31,86,86
   31 IF(DELTS-TEST)4,4,11
    4 IF(DELMU)6,6,7
    6 DELTM=-DELMU
      GO TO 8
    7 DELTM=DELMU
    8 TEST=0.00001
      IF(DELTM-TEST)9,9,11
    9 IF(DELC)12,12,13
   12 DELTC=-DELC
      IF(DELTC.GT.10**5) GO TO 5
      GO TO 14
   13 DELTC=DELC
   14 TEST=0.00001
      IF(DELTC-TEST)5,5,11
   11 SIGMA0=SIGMA0+DELSIG
```

```
      SIGTEST=ABS(SIGMAO)
      IF(SIGTEST.LT.0.4)SIGMAO=SIGI
   17 XMUO=XMUO+DELMU
      CO=CO+DELC
      IF(J-20)16,16,5
   16 J=J+1
      GO TO 15
    5 FWHM=ABS(2.35482*SIGMAO)
      IF(FWHM.GT.15.0.OR.FWHM.LT.1.0)GO TO 86
      AREA=2.50663*CO*SIGMAO
      DO 53 I=NL1,NR2
        ARG=(X(I)-XMUO)**2/(2.0*SIGMAO**2)
        PX(I)=CO*EXP(-ARG)
       R(I)=PX(I)-YC(I)
   53 CONTINUE
      CHISQ=VARI=0.
      DO 75 I=NP1,NP2
      IF(CO.LT.5.0)GO TO 86
      VARI=VARI+R(I)**2
      SET=2.*R(I)**2/((NP2-NP1+1)*CO**2)
      CHISQ=CHISQ+SET
      IF(CHISQ.GT.0.1)GO TO 86
   75 CONTINUE
      IF(XMUO-XXMUO(MQ-1)+XNI-4.0)21,21,25
   21 L=L+1
      IF(CHISQ-XCHISQ(MQ-1))23,24,24
   24 CHISQ=0.
       GO TO 25
   23 XCHISQ(MQ-1)=0.
   25 XFWHM(MQ)=FWHM
      XCHISQ(MQ)=CHISQ
      XXMUO(MQ)=XMUO+XNI
      XC(MQ)=COUNTS
      AR(MQ)=AREA
      XCO(MQ)=CO
      NQ(MQ)=NL1+NI
      XA(MQ)=A
      XB(MQ)=B
      XVARI(MQ)=VARI
      MQ=MQ+1
   86 NL1=NL1+1
      NL2=NL2+1
      NP1=NP1+1
      NP=NP+1
      NP2=NP2+1
      NR1=NR1+1
      NR2=NR2+1
      IF(NR2-NM2)83,82,82
   82 MQ=MQ-1
      NET=MQ-L
```

```
      WRITE(3,151)MQ
      WRITE(3,152)L
      WRITE(3,153)NET
      WRITE(3,800)
      DO 87 J=1,MQ
      IF(XCHISQ(J).EQ.0.)GO TO 87
      WRITE(3,810)N0(J),XFWHM(J),XCHISQ(J),XXMUQ(J),XC(J),XCO
      WRITE(3,156)XVARI(J),AR(J)
      WRITE(3,160)XA(J),XB(J)
      IF(N0(J).EQ.N1)GO TO 88
      GO TO 87
   88 WRITE(3,157)
      DO 32 I=N1,N2
      XI=I+NI
      ARG=(2.35482*(XI-XXMUQ(J)))**2/(2.0*XFWHM(J)**2)
      PX(I)=XCO(J)*EXP(-ARG)
      PU(I)=PX(I)+XA(J)+XB(J)*XI
      R(I)=PU(I)-Y(I)
      WRITE(3,155)X(I),Y(I),PU(I),R(I)
   32 CONTINUE
   87 CONTINUE
      ENDFILE 3
      REWIND 3
      CALL REPLACE(5HTAPE3,7HSPECOUT,0,0)
      END
```

"-END OF FILE-

?

```
AK IS PLOT1 WITH ALLOWANCE FOR UP TO 4096 CH.'S.
TAPE3=FNAME OF UNCORRECTED DATA.  1ST LINE NOT SKIPPED.
NSION FACTOR (EX) USED LIKE MCA DISPLAY (ENTIRE SPECTRUM EXP

PROGRAM PLOTAK(INPUT,TAPE1,TAPE2,TAPE3,OUTPUT)
DIMENSION Y(1024),KARAY(40),MARAY(11),NARAY(4096)
FORMAT(*DAMN*)
FORMAT(*OK*)
FORMAT(//*ENTER: 1ST CH., LAST CH., EXP., "LOG" AND "YES"*
 * OR "NO" FOR OVERLAP.*/*  FORMAT(2I4,F5.1,2(1XA3)):*).
FORMAT(/)
FORMAT(* YM = *,F12.4,* NXT = *,I3)
FORMAT(40HCOUNTS PER CHANNEL   CHANNEL NUMBER      )
FORMAT(F3.1)
FORMAT(F10.3)
FORMAT(10F7.0)
FORMAT(I4)
FORMAT(2I4,F5.1,2(1XA3))
FORMAT(* EXPANSION FACTOR =*,F6.1)
FORMAT(I7)
PRINT 100
READ 157,NI,NF,EX,LG,OVR
IF(NI.GT.3072)GO TO 3
IF(NI.GT.2048)GO TO 2
IF(NI.GT.1024)GO TO 1
GO TO 5
NI=NI-1024
NF=NF-1024
NP=1025
GO TO 4
NI=NI-2048
NF=NF-2048
NP=2049
GO TO 4
NI=NI-3072
NF=NF-3072
NP=3073
GO TO 4
NP=NI
PRINT 157,NI,NF,EX,LG,OVR
N=NF-NI+1
READ(3,150)(Y(I),I=1,1023)
IF(LG.NE.3HLOG)GO TO 13
DO 50 I=1,1023
IF(Y(I).EQ.0.)Y(I)=1.0
Y(I)=1000.*ALOG10(Y(I))
CONTINUE
YM=0.
DO 10 I=NI,NF
```

```
      IF(YM.LT.Y(I))YM=Y(I)
      CONTINUE
      IF(N.GT.1024)XT=200.
      IF(N.LE.1024.AND.N.GT.500)XT=100.
      IF(N.LE.500.AND.N.GT.249)XT=50.
      IF(N.LE.249.AND.N.GT.100)XT=25.
      IF(N.LE.100)XT=10.
      LX=8
      LY=5
      XL=1.30*N
      YL=1.25*YM
      XLO=-0.25*N
      YLO=-0.22*YM
      XC=0.
      YC=0.
      NXT=XT
      PRINT 120,YM,NXT
      YT=0.1*YM
      NYT=YT
      XLY=-0.20*N
      YLY=YT
      XLX=XT
      YLX=-0.2*YM
      XNX=-0.03*N
      YNX=-0.05*YM
      XMY=-0.15*N
      CALL SAXESX(1,LX,LY,XT,XL,YL,XLO,YLO,XC,YC)
      CALL PLOTXYX(XC,YC,0,0)
      XX=0.
      DO 60 K=NI,NF,NXT
      XX=XX+XT
      IF(XX.GT.N)GO TO 15
      CALL PLOTXYX(XX,YC,1,0)
      CALL PLOTXYX(XX,YC,1,29)
      CONTINUE
      XX=N
      CALL PLOTXYX(XX,YC,1,0)
      CALL PLOTXYX(XC,YC,0,0)
      YY=0.
      DO 70 K=1,10
      YY=YY+YT
      CALL PLOTXYX(XC,YY,1,0)
      CALL PLOTXYX(XC,YY,1,31)
      CONTINUE
      ATIVE PEAK HEIGHT"
      ENCODE(40,130,KARAY(1))
      CALL PLOTXYX(XLY,YLY,0,0)
      CALL LABELX(20,2,3,KARAY(1))
      NNEL NUMBER"
      CALL PLOTXYX(XLX,YLX,0,0)
```

```
      CALL LABELX(20,2,4,KARAY(3))
      NEL ID'S
      INC=NP
      IF(NP.EQ.1)INC=INC-1
      L=0
      DO 20 K=NI,NF,NXT
      L=L+1
      NARAY(L)=INC
      ENCODE(4,156,NARAY(L))NARAY(L)
      CALL PLOTXYX(XNX,YNX,0,0)
      CALL LABELX(4,1,4,NARAY(L))
      INC=INC+NXT
      XNX=XNX+XT
      CONTINUE
       PK. HEIGHT ID'S
      IF(LG.EQ.3HLOG)GO TO 14
      DO 30 K=1,11
      YMY=YM*(K-1)/10.
      IF(OVR.EQ.3HYES)YMY=YMY*EX
      MARAY(K)=YMY/EX
      PRINT 190,MARAY(K)
      ENCODE(7,190,MARAY(K))MARAY(K)
      CALL PLOTXYX(XMY,YMY,0,0)
      CALL LABELX(7,1,4,MARAY(K))
      CONTINUE
      GO TO 17
      DO 90 K=1,11
      YMY=YM*(K-1)/10.+1
      RPH=(K-1)/10.
      ENCODE(3,140,MARAY(K))RPH
      CALL PLOTXYX(XMY,YMY,0,0)
      CALL LABELX(3,1,4,MARAY(K))
      PRINT 141,YMY
      CONTINUE
      DATA. EX=EXPANSION FACTOR
      PRINT 158,EX
      IF(Y(NI).GT.YM)Y(NI)=Y(NI)/EX
      CALL PLOTXYX(0.,Y(NI),0,0)
      DO 40 J=NI,NF
      XJ=J-NI+1
      YJ=Y(J)*EX
      IF(EX.EQ.1.0)GO TO 12
      IF(YJ.LE.YM)GO TO 11
      IF(OVR.EQ.2HNO)GO TO 16
      YJ=YJ/EX
      GO TO 11.
      YJ=0.
      CALL PLOTXYX(XJ,YJ,0,0)
      GO TO 40
      CALL PLOTXYX(XJ,YJ,0,0)
```

```
      CALL PLOTXYX(XJ,YJ,1,0)
      CONTINUE
      CALL ENDPLTX
      PRINT 99
      STOP
      END
```

-END OF FILE-
?

```
      THIS PROGRAM WAS TAKEN FROM NUMERICAL METHODS AND FORTRAN
      PROGRAMMING .....MCCRACKEN
      JOHN WILEY.....
      PROGRAM CALIR(INPUT,TAPE1,TAPE2,OUTPUT)
      THIS PROGRAM WILL PERFORM A LEAST-SQUARES POLYNOMIAL CURVE
      FIT. THE PROGRAM IS TO BE ABLE TO FIT ANY POLYNOMIAL FROM
      FIRST TO TENTH DEGREE, WITH THE DEGREE SPECIFIED BY A HEADER
      CARD.
      ***************************************************************

      LIST OF PRINCIPAL VARIABLES & THEIR MEANING

      NUMBER : THE ACTUAL NUMBER OF X-Y DATA PAIRS; MAX 200
      M      : THE DEGREE OF THE POLYNOMIAL; MAX 10
      N      : THE NUMBER OF EQUATIONS (=M+1)
      X,Y    : ARRAYS FOR THE DATA PAIRS
      A      : ARRAY FOR THE SUMS, WHICH BECOME THE COEFFICIENTS
      OF THE UNKNOWNS IN THE SIMULTANEOUS EQUATIONS
      B      : ARRAY FOR THE CONSTANT TERMS IN THE SIMULTANEOUS
      EQUATIONS
      C      : ARRAY FOR THE UNKNOWNS, WHICH BECOME THE CO-
      EFFICIENTS IN THE POLYNOMIAL
      P      : ARRAY FOR THE POWERS OF THE X'S,FROM 1 TO 2M

      ***************************************************************

      READING THE DATA, FORMING THE POWERS OF X
      DIMENSION X(200),Y(200),A(11,11),B(11),C(11),P(20)
      DIMENSION YC(200),DY(200)
      DIMENSION CHISQ(200),XMU(200),E(200)


      M=3

      DO 11 I=1,201
      READ(1,10)X(I),Y(I)
      10 FORMAT(6X,2F8.3)
      IF(EOF,1)12,11
      11 CONTINUE
      12 NUMBER = I-1
      READ,CHI
      MX2 = M*2
      DO 13 I=1,MX2
      P(I) =0.0
      DO 13 J = 1,NUMBER
      13 P(I) = P(I) + X(J)**I
      DEVELOPING THE COEFFICIENTS AND THE CONSTANT TERMS OF THE
      NORMAL EQUATIONS
      N = M + 1
```

```
      DO 30 I = 1,N
      DO 30 J=1,N
      K = I + J - 2
      IF (K) 29,29,28
   28 A(I,J) = P(K)
      GO TO 30
   29 A( 1,1 ) = NUMBER
   30 CONTINUE
      B(1) = 0.0
      DO 21 J = 1,NUMBER
   21 B(1) = B(1) + Y(J)
      DO 22 I = 2,N
      B(I) =0.0
      DO 22 J=1,NUMBER
   22 B(I) =B(I) +Y(J)*(X(J)**(I-1))
      NM1 = N-1
      PIVOTAL CONDENSATION
      DO 300 K = 1,NM1
      KP1 =K+1
      L=K
      DO 400 I=KP1,N
      IF (ABSF(A(I,K))-ABSF(A(L,K))) 400,400,401
  401 L=I
  400 CONTINUE
      IF (L-K) 500,500,405
  405 DO 410 J=K,N
      TEMP = A(K,J)
      A(K,J) =A(L,J)
  410 A(L,J) = TEMP
      TEMP = B(K)
      B(K) =B(L)
      B(L) = TEMP
      ELIMINATION, BACK SOLUTION AND PRINTING RESULTS
  500 DO 300 I = KP1,N
      FACTOR = A(I,K)/A(K,K)
      A(I,K) = 0.0
      DO 301 J = KP1,N
  301 A(I,J)=A(I,J)-FACTOR*A(K,J)
  300 B(I) = B(I)-FACTOR*B(K)
      C(N) = B(N)/A(N,N)
      I = NM1
  710 IP1 = I+1
      SUM = 0.0
      DO 700 J = IP1,N
  700 SUM = SUM +A(I,J)*C(J)
      C(I) = (B(I)-SUM)/A(I,I)
      I = I-1
      IF (I) 900,900,710
  900 CONTINUE
      90) FORMAT(*YC=*,E13.7,* + *,E13.7,* X +*,E13.7,* X**2 + *
```

```
 ,E13.7,* X**3*)
904 FORMAT(//5X*Y(I)*6X*YC(I)*6X*DY(I)*)
DO 903 I=1,NUMBER
YC(I)=C(1)+C(2)*X(I)+C(3)*X(I)**2+C(4)*X(I)**3
DY(I)=Y(I)-YC(I)
902 FORMAT(F8.3,3X,F9.2,3X,F9.2)
903 CONTINUE
 CALL GET(5HTAPE2,7HSPECOUT,0,0)
1 READ(2,151)XYG
151 FORMAT(A7)
 IF(XYG.NE.7H      )GO TO 1
 READ(2,153)NET
 PRINT 153,NET
153 FORMAT(////19X15/)
810 FORMAT(///17X,F13.8,F13.3)
PRINT 179
179 FORMAT(//3X*XMU(I)*3X*E(I)(KEV)*)
 DO 87 I=1,NET
 IF(EOF,2)999,998
998 READ(2,810)CHISQ(I),XMU(I)
 IF(CHISQ(I).GT.CHI)GO TO 87
 E(I)=C(1)+C(2)*XMU(I)+C(3)*XMU(I)**2+C(4)*XMU(I)**3
 PRINT 180,XMU(I),E(I)
180 FORMAT(2F9.3)
87 CONTINUE
999 STOP
 END
```

-END OF FILE-